1

Types of Flame Retardants

COPYRIGHTED MATERIAL

Polymeric materials are generally subject to burn. Therefore, for safety reasons, flame retardants are added. A measure for the flammability is the limiting oxygen index (LOI). The LOI is the percentage of oxygen in the atmosphere that allows burning under standardized conditions (1, 2). Table 1.1 gives an idea about the flammability.

A series of flame retardants with different chemical structures exists and the mechanism of action is dependent on the nature of the particular compounds.

There are monographs dealing with flame retardant materials (3–6).

1.1 History of Organic Flame Retardants

The history of organic flame retardants has been detailed in an article (7) as follows:

Polychlorinated biphenyls were manufactured and used as flame retardants from the late 1920s until the mid-1980s, although polychlorinated biphenyls were also used in a multitude of other applications, particularly in electrical equipment. Other chlorinated compounds came into use as flame retardant, probably from the 1960s onwards, sometimes also including a phosphate group, such as the tris-(2,3-dichloropropyl) phosphate and tris-(1,3-dichloro-iso-propyl) phosphate (8).

Table 1.1 Limiting oxygen index of selected materials (9–11).

Material	LOI/[% Oxygen]
Poly(formaldehyde)	15
Poly(ethylene oxide)	15
Styrene-butadiene rubber	16.9
Poly(methyl methacrylate)	17
Poly(acrylonitrile)	18
Poly(ethylene)	18
Poly(propylene)	18
Acrylonitrile-butadiene-styrene	18.0 – 39
Cellulose acetate	18 – 27
Poly(butadiene)	18.5
Poly(styrene)	18.5
Poly(imide)	18.6
Cellulose butyrate	18.8 – 19.9
Cellulose	19
Styrene acrylonitrile copolymer	19.1
Poly(ethylene terephthalate)	21
Poly(vinyl alcohol)	22
Poly(amide) 66	23
Wool	25
Silicone rubber	25
Poly(carbonate)	27
Aramid	28.5
Poly(vinyl chloride)	42
Poly(vinylidene fluoride)	44
Isocyanurate foam	29
Phenol formaldehyde	35
Poly(benzimidazole)	38.0 – 43.0
Poly(vinylidene chloride)	60
Carbon	60
Poly(tetrafluoroethylene)	>95.0

The brominated analog of the former compound, tris-(2,3-dibromopropyl) phosphate made headlines in the 1970s due to its use in children's pajamas (12).

At the beginning of the 1970s, an increasing number of brominated flame retardants (BFrs), e.g., polybrominated biphenyls and polybrominated diphenyl ethers, came on the market. In 1997, the World Health Organization tried to list all major flame retardants, also including any inorganic chemicals used in that role (13).

The first review of BFrs appeared in 1995 (14), including what was known of their analysis, toxicity and environmental occurrence. Numerous other reviews and/or assessment documents have been published since then (15–19).

Among the most recent documents concerning BFrs are five published opinions from the European Food Safety Authority (EFSA) on polybrominated biphenyls (20), polybrominated diphenyl ethers (21), hexabromocyclododecanes (HBCDDs) (22), tetrabromobisphenol A and its derivatives (23), and also an opinion concerning other phenolic BFrs and their derivatives (24). EFSA is presently also preparing an opinion on emerging and novel BFrs for publication in 2012. In 2011, a book on BFrs was published which covered a multitude of issues relating to BFrs (25).

Other major reviews of BFrs from 2005 onwards are included in (26–29).

A review on phosphorus-containing flame retardants was published (30), while, among the chlorinated flame retardants, only the Dechloranes have been comprehensively reviewed (31).

The scientific literature of bromine-, chlorine- and phosphate-containing flame retardants was reviewed (7). The compounds mentioned are collected therein. Also, the trade names are given. The chemical names of these compounds are given in Table 1.2.

1.2 Commercially Available Flame Retardants

Some commercially available flame retardants are listed in Table 1.3.

Table 1.2 Bromine-, chlorine- and phosphate-containing flame retardants (7).

Compound name
2,4-Dibromophenol
Dibromostyrene
2,4,6-Tribromophenol
1,3,5-Tribromo-2-hydroxybenzene
2,4,6-Tribromophenyl allyl ether
1,2,4,5-Tetrabromo-3,6-dimethylbenzene
1,4-Dimethyltetrabromobenzene
2,3,5,6-Tetrabromo-1,4-dimethylbenzene
2,3,4,5-Tetrabromo-6-chlorotoluene
Tetrabromo-*o*-chlorotoluene
2,3,4,5-Tetrabromo-6-chloromethylbenzene
1,3-Isobenzofurandione
3,4,5,6-Tetrabromophthalic anhydride
4,5,6,7-Tetrabromobenzofuran-1,3-dione
Tetrabromophthalic acid anhydride
Tetrabromophthalic anhydride
1,2,3,4,5-Pentabromo-6-methylbenzene
2,3,4,5,6-Pentabromotoluene
Pentabromomethylbenzene
Pentabromophenol
Pentabromoethylbenzene
Pentabromobenzyl chloride
Pentabromophenol allyl ether
2,4,6-Tribromophenyl 2,3-dibromopropyl ether
2-Ethylhexyl-2,3,4,5-tetrabromobenzoate
Hexabromobenzene
2,3,4,5,6-Pentabromobenzyl acrylate
Pentabromobenzyl bromide
Di(2-ethylhexyl) tetrabromophthalate
3-(Tetrabromopentadecyl)-2,4,6-tribromophenol
Tetrabromobisphenol A
2,2-Bis(4-hydroxy-3,5-dibromophenyl)propane
2,2′,6,6′-Tetrabromobisphenol A
3,3′,5,5′-Tetrabromobisphenol A
3,5,3′,5′-Tetrabromobisphenol A
4,4′-(1-Methylethylidene)bis[2,6-dibromophenol]
4,4′-Isopropylidenebis[2,6-dibromophenol]
Tetrabromodiphenylolpropane

Table 1.2 (cont) Bromine-, chlorine- and phosphate-containing flame retardants (7).

Compound name
Tetrabromobisphenol A
Bis(3,5-dibromo-4-hydroxyphenyl) sulfone
Tetrabromobisphenol A dimethyl ether
Tetrabromobisphenol A methyl ether
(3,5-Dibromo-4-methoxyphenyl) sulfone
2,2-Bis(4-acetoxy-3,5-dibromophenyl)propane
2,2-Bis[3,5-dibromo-4-(2-hydroxyethoxy)phenyl]propane
2,2-Bis(3,5-dibromo-4-allyloxyphenyl)propane
2,2′,6,6′-Tetrabromobisphenol A diacrylate
2,2′,6,6′-Tetrabromobisphenol A diglycidyl ether
Tetrabromobisphenol A bispropanoate
1,2-Bis(2,4,6-tribromophenoxy)ethane
Tetrabromobisphenol A bis(2-hydroxyethyl)ether bisacrylate
Octabromotrimethylphenyl indane
4,5,6,7-Tetrabromo-1,1,3-trimethyl-3-(2,3,4,5-tetrabromophenyl)-2,3-dihydro-1H-indene
Tetrabromobisphenol A bis(2,3-dibromopropyl) ether
N,*N*′-Ethylenebis(tetrabromophthalimide)
4,4′-Bis(2,3-dibromopropoxy)-3,3′,5,5′-tetrabromodiphenyl sulfone
Decabromodiphenyl ethane
Decabromodibenzyl ether
Bis(pentabromophenoxy)benzene
5-(Tetrabromophenyl)-1,2,3,4,7,7-hexachloro-2-norbornene
1,2,5,6-Tetrabromocyclooctane
Hexabromocyclodecane
1,2,5,6,9,10-Hexabromocyclododecane
1,3-Bis(2,3-dibromopropyl)-5-allyl-1,3,5-triazine-2,4,6(1H,3H,5H)-trione
1,3,5-Tris(2,3-dibromopropyl)-1,3,5-triazine-2,4,6-trione
1,3,5-Tris(2,3-dibromopropyl) isocyanurate
1,3,5-Tris(2,3-dibromopropyl)-2,4,6-trioxohexahydrotriazine
Tris(2,4,6-tribromophenoxy)-s-triazine
Tris(tribromoneopentyl) phosphate
Tris(2,3-dibromopropyl) phosphate
Dibromoneopentyl glycol
Tribromoneopentyl alcohol

Table 1.3 Commercially available flame retardants (32).

Trade name	Supplier	Composition
Apyral 60CD	Nabaltec	Aluminum hydroxide
Sidistar T 120	Elkem	Amorphous silicon dioxide
UltraCarb LH15	LKAB Minerals	Huntite + hydromagnesite
Exolit AP 422	Clariant	Ammonium poly(phosphate)
Exolit OP 1230	Clariant	Aluminum diethylphosphinate
Exolit AP 750	Clariant	APP-based intumescent system
Aflammit PPN 978	Thor	APP-based multicomponent intumescent system, unmeltable
Aflammit PPN 923	Thor	APP-based intumescent multicomponent system, meltable
Aflammit PPN 903	Thor	P/N-based intumescent system
Masteret 15460 B2XF	Italmatch Chemicals	60% red phosphorus in PP
NORD-MIN 503	NRC	Expandable graphite
Safire 400	Floridienne Chimie	Melamine poly(zinc phosphate)
Uniplex FRX 44-94	Lanxess	Ethylenediamine-*o*-phosphate + melamine
Charex 44PSS	Nanops	Quaternary ammonium/siloxane treated montmorillonite
LS-8980	Shin-Etsu Silicone	Silicone
Charmax LS-MOM		Melamine octamolybdate

1.3 Chlorine-Containing Materials

1.3.1 HET Acid

HET acid is also known as chlorendic anhydride. In particular, chlorendic anhydride is the Diels-Alder adduct of hexachlorocyclopentadiene and maleic anhydride. HET acid is shown in Figure 1.1.

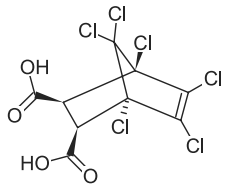

Figure 1.1 HET acid.

Chlorendic acid and chlorendic anhydride are used as reactive flame retardants, i.e., are built into the polymeric backbone, in polyester resins and as plasticizers for electrical systems and paints. Chlorendic acid is fairly persistent in soil. It has been found in landfill leachate in amounts up to 455 $mg\,l^{-1}$.

After oral and intravenous administration of radioactive labeled chlorendic acid to rats, the substance is rapidly distributed throughout the body and rapidly metabolized. Chlorendic acid has been reported to exert toxic effects on algae in concentrations of 250 $mg\,l^{-1}$.

In summary, these chemicals seem to have a low acute and subacute oral toxicity, although they are dermal, eye and respiratory irritants. From the results of long-term toxicity and carcinogenicity studies on rats and mice, it has been concluded that chlorendic acid induces tumors in rats and mice. Therefore, a carcinogenic potential is suspected. However, a full hazard assessment for humans and the environment cannot be made in view of the lack of data (33).

1.3.2 Dechlorane Plus

Dechlorane Plus is a highly chlorinated flame retardant (34). Dechlorane Plus is shown in Figure 1.2.

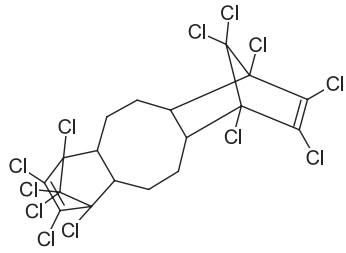

Figure 1.2 Dechlorane Plus.

Dechlorane Plus is a high production volume, chlorinated flame retardant (31). Despite its long production history, it has only recently been found in the environment. Although Dechlorane Plus has been used as a polychlorinated flame retardant for almost half a century, its detection in the environment was not reported until 2006 (35).

The first sightings of Dechlorane Plus were in the Great Lakes of North America, but subsequent work has indicated that it is a global contaminant (31).

For example, Dechlorane Plus has recently been detected along a pole-to-pole transect of the Atlantic Ocean. Although it was initially thought that Dechlorane Plus was produced only in North America, another Dechlorane Plus production plant has recently been identified in China. During the course of characterizing Dechlorane Plus in the environment, other *Dechlorane Plus-like* compounds were identified. These Dechlorane Plus analogs, some created from impurities contained in the starting materials during its synthesis, have also been detected globally.

Screening-level modeling data are in general agreement with available environmental measurements. These data suggest that Dechlorane Plus and its analogs may be persistent, bioaccumulative, and subject to long-range transport, and that these chemicals may be candidates for Annex D evaluation under the United Nations Stockholm Convention on Persistent Organic Pollutants. There is a need to obtain more monitoring, bioaccumulation, degradation rates, and toxicity information (31).

Three typical emission sources in the environment were cate-

gorized after introducing the measurement method of Dechlorane Plus (35). The temporal-spatial distribution was then evaluated on a global scale, which provides an integrated representation of the environmental occurrence of Dechlorane Plus and potential impact on human health and ecosystems. The variations of Dechlorane Plus isomer ratio in various matrices reinforce its source-related distribution and their stereoselective bioaccumulation.

The measurement methods for Dechlorane Plus have been described (36) and provide an integrated picture of its occurrence and behavior as an environmental contaminant. Dechlorane Plus in ambient air and sediments is characterized by strong source-related concentration elevations and temporal trends reflecting commercial use. Long-range atmospheric transportation of Dechlorane Plus has been observed in remote regions.

The change in the isomer ratio of Dechlorane Plus in various environmental matrices from commercial products indicates that the behavior of the two isomers is not the same in the environment or in biota (36).

The presence of significant amounts of several emerging Dechlorane flame retardants was reported in environmental and biota samples, principally from Canada and China, but also from Europe (37). Several molecules were identified, e.g., Dec 602, 603, 604, Dechlorane Plus, and Chlordene Plus. Gas chromatography (GC) coupled to electron ionization high-resolution mass spectrometry can be used for their measurement in various matrices based on hexachlorocyclopentadiene fragment ions.

Two luminous bacteria, *Vicia faba* and *Tetrahymena thermophila*, were chosen as testing organisms to investigate the acute toxicity and mutagenicity of Dechlorane Plus (38). The concentration gradient of Dechlorane Plus used in the study was chosen based on its environmental levels (Experiments of luminous bacteria: 0.591, 2.95, 14.8, 73.8, 369 $\mu g\, l^{-1}$; Micronucleus tests: 2.4, 12, 60, 300, 1500 $\mu g\, l^{-1}$; Comet assay: 2.4, 12, 60, 300, 1500 $\mu g\, l^{-1}$).

For luminous bacteria, the relative luminosities were around 100% in the treated groups, which suggested that there is no acute toxicity to luminous bacteria under the studied Dechlorane Plus concentrations. Also, the micronucleus test showed no significant difference between treatment and control groups, indicating no genotoxicity of Dechlorane Plus.

However, the comet assay conducted with *T. thermophila* was relatively sensitive as there was a significant increase in deoxyribonucleic acid damage when the concentrations of Dechlorane Plus increased from 300 to 1500 $\mu g\, l^{-1}$, while the lower concentrations failed to show any treatment-related differences. Therefore, Dechlorane Plus may pose a potential risk at concentrations ≥300 $\mu g\, l^{-1}$ (38).

1.3.3 Chlordene

Chlordene is another highly chlorinated flame retardant. Chlordene Plus is shown in Figure 1.3.

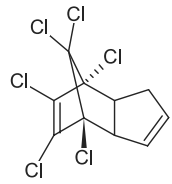

Figure 1.3 Chlordene.

1.3.4 Tris(1,3-dichloroisopropyl) phosphate

Foam samples collected from 101 commonly used baby products were analyzed (39). Eighty samples contained an identifiable flame retardant additive, and all but one of these was either chlorinated or brominated. The most common flame retardant detected was tris(1,3-dichloroisopropyl) phosphate with a detection frequency of 36%. This compound is shown in Figure 1.4.

This was followed by components which are typically found in the Firemaster 550 commercial mixture with a detection frequency of 17% (39).

Firemaster® 550 (FM550) is a chemical mixture that is used as an additive flame retardant in commercial products (40). It contains 2-ethylhexyl-2,3,4,5-tetrabromobenzoate, bis(2-ethylhexyl) tetrabromophthalate, triphenyl phosphate, and isopropylated triphenyl phosphate. These compounds are shown in Figure 1.5.

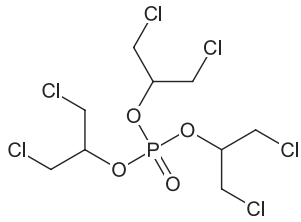

Figure 1.4 Tris(1,3-dichloroisopropyl) phosphate.

1.3.5 Tris(2-chloroethyl) phosphate

In baby products that were analyzed in poly(urethane) foams (39), a compound was also identified, which is commercially sold as V6 with a detection frequency of 15%, and it contained tris(2-chloroethyl) phosphate as an impurity. Tris(2-chloroethyl) phosphate is shown in Figure 1.6.

1.4 Bromine-Containing Materials

There is a monograph dealing with brominated flame retardants (25).

1.4.1 Brominated Diphenyl Ethers

Polybrominated diphenyl ethers have a large number of congeners, depending on the number and position of the bromine atoms on the two phenyl rings. Commercial brominated diphenyl ethers are produced by the bromination of diphenyl oxide. Brominated diphenyl ethers are used as flame retardants.

Since brominated diphenyl ethers are used by blending, they are referred to as additive flame retardants. These additive flame retardants are much more prone to leaching or escaping from the finished polymer product than the reactive flame retardants.

Examples of polymer types, principal applications, and final products have been compiled (41). Studies on potential risks have been conducted by industry. These studies do not reveal severe risks of the use of polybrominated diphenyl ethers.

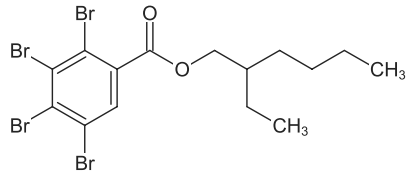

2-Ethylhexyl-2,3,4,5-tetrabromobenzoate

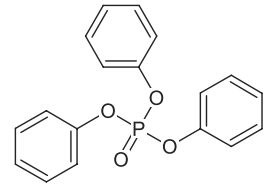

Triphenyl phosphate

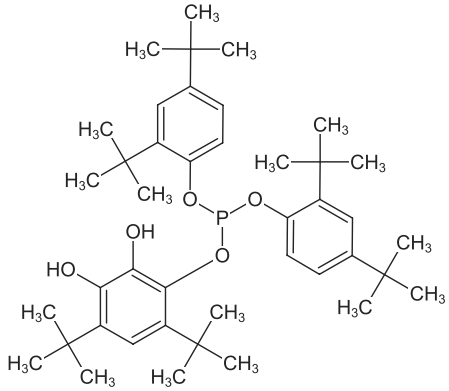

Isopropylated triphenyl phosphate

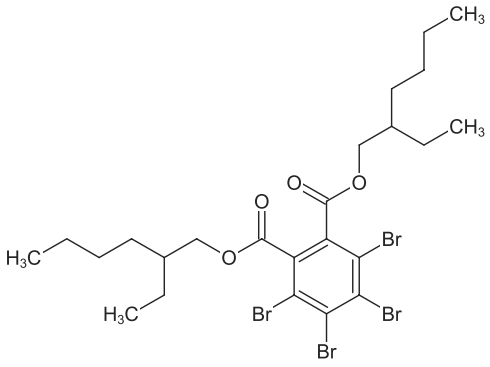

Bis(2-ethylhexyl) tetrabromophthalate

Figure 1.5 Components in Firemaster® (40).

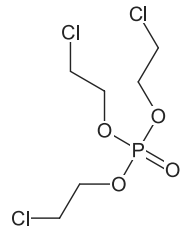

Figure 1.6 Tris(2-chloroethyl) phosphate.

1.4.2 1,2-Bis(2,4,6-tribromophenoxy)ethane

1,2-Bis(2,4,6-tribromophenoxy)ethane (BTBPE) is currently one of the most commonly applied novel brominated flame retardants (42). The mechanisms pertinent to its thermal decomposition in view of analogous experimental findings have been analyzed.

It could be shown that a 1,3-hydrogen shift, leading to 2,4,6-tribromophenol and 1,3,5-tribromo-2-(vinyloxy)benzene molecules, dominates direct scission of $-O-CH_2$ bonds up to a temperature of around 680 K. The reaction is shown in Figure 1.7.

Furthermore, hydrogen atom abstraction from the $-CH_2-$ sites, followed by a fission of a C–C bond, produce a 2,4,6-tribromophenoxy radical and a 1,3,5-tribromo-2-(vinyloxy)benzene molecule (42).

Bimolecular condensation reactions involving the above-mentioned molecules generate several congeners of brominated diphenyl ethers and their $-OH/-O-CH-CH_2$ substituents, which serve as direct precursors for the formation of polybrominated dibenzo-*p*-dioxins (42).

The release and transformation of BTBPE during the thermal treatment of acrylonitrile-butadiene-styrene (ABS) plastics was investigated (43). The maximum release rate of BTBPE was observed at 350°C. A release kinetic model was developed to explore the mechanism of BTBPE release while heating the ABS. Material-phase diffusion was found to be the rate-determining step during release.

According to the developed release model, it was estimated that 0.04–0.17% of the embedded BTBPE could be released to air during the industrial processing of ABS plastics. When

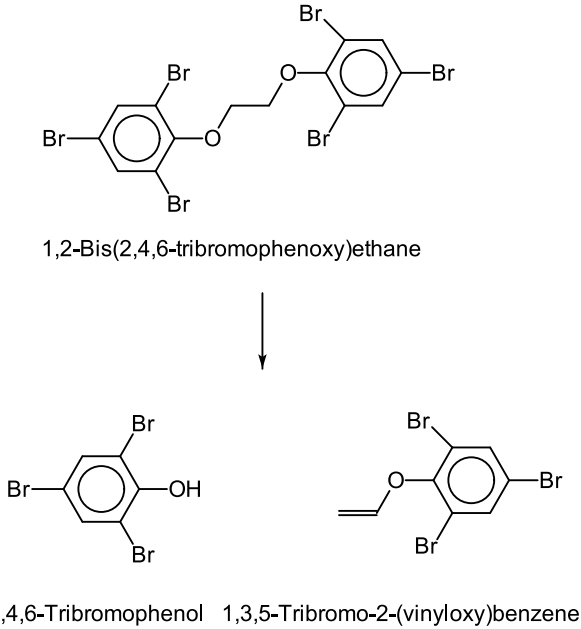

Figure 1.7 1,3-Hydrogen shift (42).

the heating temperature was 350°C, approximately 15–56% of the embedded BTBPE decomposed to bromophenols and 1,3,5-tribromo-2-(vinyloxy)benzene. This decomposition followed a first-order kinetics at 350°C.

Polybrominated dibenzo-*p*-dioxins and dibenzofurans were also significantly formed at 350°C from bromophenols and 1,3,5-tribromo-2-(vinyloxy)benzene via a precursor mechanism. A higher temperature of 450°C was favorable for the formation of polybrominated dibenzofurans (43).

1.4.3 Trioxohexahydrotriazine Compound

The 1,3,5-tris(2,3-dibromopropyl)-2,4,6-trioxohexahydrotriazine is shown in Figure 1.8.

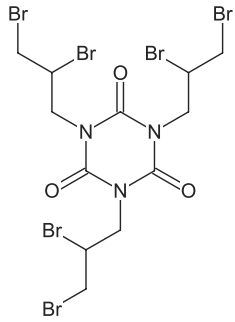

Figure 1.8 1,3,5-Tris(2,3-dibromopropyl)-2,4,6-trioxohexahydrotriazine.

The three structural 2,3-dibromopropyl groups in this compound contain two reactive carbons, i.e., the ones that are substituted with bromines. The reactivity of these groups has not yet been explored any further but may be both environmentally and biologically relevant (44).

1.4.4 2,4,6-Tris(2,4,6-tribromophenoxy)-1,3,5-triazine

A high molecular weight compound, 2,4,6-tris(2,4,6-tribromophenoxy)-1,3,5-triazine (TTBP-TAZ), was detected during the analysis of BFrs in dust samples collected from an electrical and electronic waste

(e-waste) recycling facility in Ontario, Canada (45). TTBP-TAZ is shown in Figure 1.9.

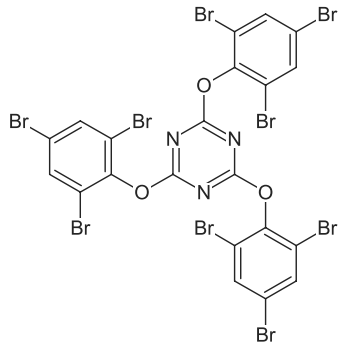

Figure 1.9 2,4,6-Tris(2,4,6-tribromophenoxy)-1,3,5-triazine.

Gas chromatography coupled with both high-resolution and low-resolution mass spectrometry (MS) was used to determine the chemical structure and concentrations. To date, 2,4,6-tris(2,4,6-tribromophenoxy)-1,3,5-triazine has only been detected in plastic casings of electrical and electronic equipment and house dust from The Netherlands.

The concentrations of 2,4,6-tris(2,4,6-tribromophenoxy)-1,3,5-triazine in selected samples from North America were reported. The sample types and the amounts detected are collected in Table 1.4.

Table 1.4 Sample types for analysis (45).

Sample type	Numbers	Concentrations	
E-waste dust	4	5540	$ng\,g^{-1}$
Air	4	5.75	$ng\,m^{-3}$
Residential dust	30	6.76	$ng\,g^{-1}$
Selected outdoor air	146		
Precipitation	19		
Sediment	11		
Water from the Great Lakes	2		

TTBP-TAZ was detected in all the e-waste dust and air samples, and in 70% of residential dust samples.

Also, the flame retardants 2,4,6-tribromophenol, tris(2,3-dibromopropyl) isocyanurate, and 3,3′,5,5′-tetrabromobisphenol A bis(2,3-dibromopropyl) ether were measured for comparison. None of these other flame retardants concentrations significantly correlated with those of TTBP-TAZ in any of the sample types, suggesting different sources.

TTBP-TAZ was not detected in any of the outdoor environmental samples, which may relate to its application history and physicochemical properties (45).

1.4.5 Pentabromodiphenyl ether

Because of the banning of pentabromodiphenyl ether in Europe and voluntary withdrawal of this product from the market in the US, the poly(urethane) (PU) industry is searching for a more environmentally acceptable low-scorch alternative (46). Pentabromodiphenyl ether is shown in Figure 1.10.

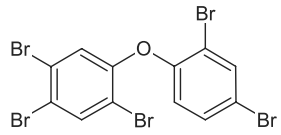

Figure 1.10 Pentabromodiphenyl ether.

Both halogenated and halogen-free solutions have been considered, but the PU industry seems to have a preference for the halogen-free products, generally containing phosphorus (46).

1.5 Phosphorus Flame Retardants

There has been a growing interest in halogen-free solutions, with the preponderance of the literature focusing on phosphorus-based flame retardants (46). Patents published on the flame retardance of poly(carbonate) (PC) and its blends significantly exceeded the number of patents on flame retardancy of any other polymer. Bridged aromatic diphenyl phosphates, especially resorcinol bis(diphenyl phosphate) and bisphenol A bis(diphenyl phosphate) (BDP) have

found a broad application because of their good thermal stability, high efficiency, and low volatility.

Another actively reported group of compounds are the metal salts of dialkylphosphonic acid as well as calcium hypophosphite, which have recently been found to be particularly effective in poly(butylene terephthalate) (PBT) and PC.

These products are synergistic with a number of phosphorus- and nitrogen-containing compounds, such as melamine salts, which seem to be very efficient and commercially useful in nylons.

Printed wiring boards comprise the largest market for flame retardant polymeric materials. Also, there has been a strong interest in halogen-free solutions in East Asia and Europe.

1.5.1 DOPO

A recent halogen-free compound is 9,10-dihydro-9-oxa-10-phosphaphenanthrene-10-oxide (DOPO), c.f. Figure 7.6, which can be reacted into epoxy resins (46). Another reactive product with some processing and property advantages is poly(*m*-phenylene methylphosphonate).

1.5.1.1 Modification of Cellulose

The inherent high flammability and poor processability characteristics of cellulosic materials result in dominant adverse impacts on their practical applications (47).

A robust strategy was proposed for converting highly flammable cellulose into an inherently flame retardant, halogen-free, anti-dripping and easy-to-process material, DOPO-cellulose acrylate, by introducing acrylate groups into the cellulose chains and later covalently immobilizing DOPO through an addition reaction between acrylate groups and DOPO. A small number of DOPO groups in DOPO-cellulose acrylate significantly reduce the heat release rate and total heat release, and promote the formation of dense and continuous char. Thus, the freestanding and transparent films of the resultant DOPO-cellulose acrylate self-extinguish instantly (<1 *s*) once removed from the flame.

Partial acrylate groups are deliberately retained to obtain UV light-crosslinkable DOPO-cellulose acrylate, which can form a

rigid three-dimensional crosslinked network, thereby inhibiting melt dripping. Benefitting from the excellent formability, the UV light-crosslinkable DOPO-cellulose acrylate can easily be processed into a flame retardant, anti-dripping and transparent coatings for protecting various flammable materials from fire, such as paper and wood. These compositions show promise for their use as functional bulk materials and coatings to protect books, buildings and furniture (47).

1.5.2 Resorcinol bis(diphenyl phosphate)

Resorcinol bis(diphenyl phosphate) is available from Supresta LLC under the trade name Fyrolflex® RDPO. This compound is shown in Figure 1.11.

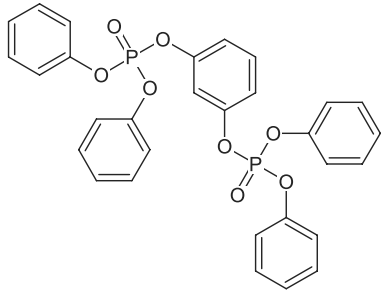

Figure 1.11 Resorcinol bis(diphenyl phosphate).

1.5.3 Resorcinol bis(di-2,6-xylyl phosphate)

Resorcinol bis(di-2,6-xylyl phosphate) is another diphosphate manufactured on a commercial scale.

Because of steric hindrance of the 2,6-xylyl groups, this product shows a higher hydrolytic stability than BDP. Its fire retardant efficiency is comparable to BDP, because it provides a V-0 rating in PC/ABS blends at a loading of 12% to 16% (48).

In contrast to BDP, resorcinol bis(di-2,6-xylyl phosphate) is a solid. This is sometimes considered as an advantage by compounders.

However, its relatively high cost retards a large-scale use of this product.

1.5.4 Phosphor Amides

Most phosphor amides are high melting solids, therefore it was concluded that they may retain the high heat distortion temperature of PC/ABS.

A series of bisphosphoramidates with a piperazine bridging unit have been described. Bisphosphoramidates such as *N*,*N*′-bis[di-(2,6-xylenoxy)phosphinyl]piperazine and *N*,*N*′-bis(neopentylenedioxy)phosphinyl)piperazine are effective flame retardant agents for thermoplastic polymers and blends thereof. In addition, the blends containing such bisphosphoramidates have excellent high temperature properties, as demonstrated by high heat deflection temperatures and a low tendency to decrease their glass transition temperature (49).

Sterically hindered phosphoramidates, e.g., *N*,*N*′-bis[di-(2,6-xylenoxy)phosphinyl]piperazine, can be prepared by the reaction of a sterically hindered diaryl chlorophosphate, such as di-(2,6-xylyl)chlorophosphate, with a basic nitrogen compound containing at least two basic N−H groups, preferably a heterocyclic compound such as piperazine, in the presence of calcium oxide as an acid acceptor (50, 51). The reaction is conducted in the presence of at least one dipolar aprotic solvent. The synthesis is shown in Figure 1.12.

1.5.5 Polyphosphate Ester Morpholides

Polyphosphate ester morpholides have been described for their use as flame retardants suitable for various synthetic resins. The synthesis of diphenyl morpholide monophosphate and dimorpholide phenyl monophosphate has been described (52). The preparation of a phosphoric acid ester morpholide compound runs as follows (52):

Preparation 1–1: First, 307 *g* (2 *mol*) of phosphorus oxychloride, 188 *g* (2 *mol*) of phenol, 174 *g* (2 *mol*) of morpholine, 4 *g* of aluminum chloride, and 900 *g* of triethylamine were charged into a four-necked flask equipped with a thermometer, condenser, stirrer and dropping instrument. After heating to a temperature of 140°C, the mixture was reacted for 2 *h* under

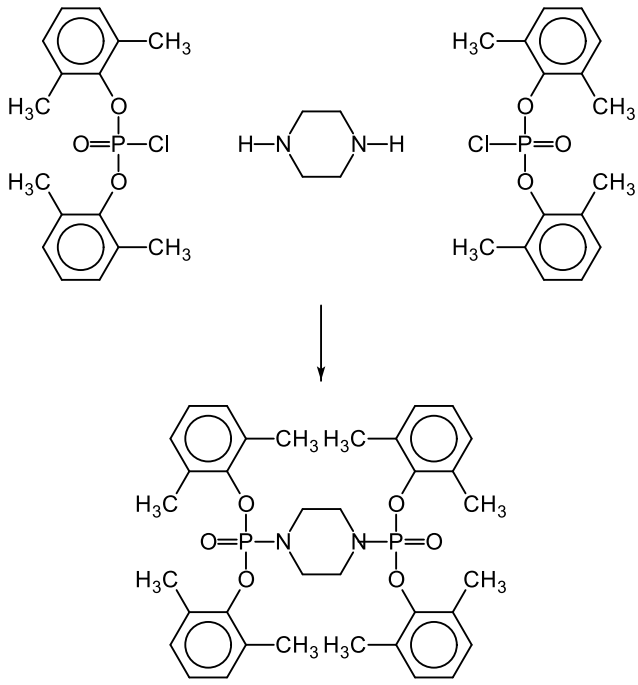

Figure 1.12 Synthesis of *N*,*N*′-Bis[di-(2,6-xylenoxy)phosphinyl]piperazine.

an atmosphere of nitrogen. Then, 110 *g* (1 *mol*) of resorcinol was further added, heated to a temperature of 160°C and reacted for 4 *h* under an atmosphere of nitrogen. The reaction was then washed with deionized water. Catalyst and other impurities were removed to obtain 510 *g* of phosphoric acid ester morpholide.

1.5.6 Cyclic Phosphazenes

Cyclic phenoxyphosphazenes are thermally stable phosphorus-nitrogen products. A blend consisting of mostly tri- and tetra-phosphazenes as well as some large rings was found to be effective in PC/ABS at 12% to 15% (53).

Specific examples of a phenoxyphosphazene which can be used are phenoxyphosphazene or methylphenoxyphosphazene. A phosphazene is generally synthesized by substituting a chlorophosphazene with a phenol compound.

Specific examples of cyclic phosphazene compounds substituted by both cyanophenoxy and phenoxy groups are summarized in Table 1.5.

Table 1.5 Cyclic phosphazene compounds (54).

Cyclic phosphazene compound
Dicyanophenoxytetraphenoxycyclotriphosphazene
Tricyanophenoxytriphenoxycyclotriphosphazene
Tetracyanophenoxydiphenoxycyclotriphosphazene
Pentacyanophenoxymonophenoxycyclotriphosphazene
Monocyanophenoxyheptaphenoxycyclotetraphosphazene
Dicyanophenoxyhexaphenoxycyclotetraphosphazene
Tricyanophenoxypentaphenoxycyclotetraphosphazene
Tetracyanophenoxytetraphenoxycyclotetraphosphazene
Pentacyanophenoxytriphenoxycyclotetraphosphazene
Hexacyanophenoxydiphenoxycyclotetraphosphazene
Heptacyanophenoxymonophenoxycyclotetraphosphazene

A flame retardant microcapsule with a shell containing a cyclic phosphazene molecule and a process for forming this material has been described (55). A flame retardant may be incorporated into the microcapsule by the addition of cyclic phosphazene molecules within the microcapsule shell. By incorporating cyclic phosphazene

molecules into the shell of the microcapsule, a number of additives needed to create the microcapsule may be reduced.

The synthesis of a cyclic phosphazene molecule has been detailed. The synthesis is shown in Figure 1.13.

Here, a strong base, such as sodium hydride (NaH), and tetrahydrofuran (THF) may be reacted with cyclic phosphazene molecule. Also, other bases, e.g., potassium hydride, lithium hydride, rubidium hydride, cesium hydride, or acids, may be used in place of the strong base NaH. Additionally, a molecule such as phenol molecule may be reacted with the cyclic phosphazene molecule, NaH, and THF to form the cyclic phosphazene molecule (55).

1.6 Boron Additives

Fire-resistant photocurable materials, such as phosphorus- or boron-containing photocurable coatings have been reviewed in a chapter of a monograph (56).

The fabrication of boron-containing compositions has been documented (57). Besides their use as flame retardants, these compositions may be used for a lot of other purposes, such as in (57):

1. Heavy clay bodies, glass and fiberglass,
2. Agriculture as wood preservatives and pesticides,
3. Polymers and rubbers,
4. Wood-plastic composites,
5. Paints and coatings,
6. Soaps and detergents,
7. Cosmetics,
8. Industrial fluids,
9. Steel slag,
10. Water treatment,
11. Gypsum wallboard, and
12. Glazes.

1.6.1 Zinc Borate

The effect of zinc borate, boric acid and boric oxide was studied on the flame retardant and thermal stability properties of an epoxy resin containing red phosphorus (58). The flame retardancy

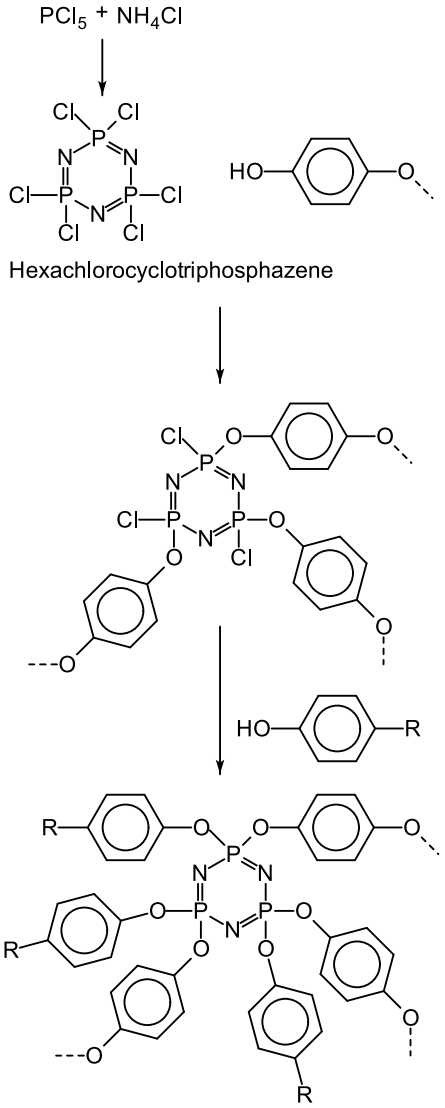

Figure 1.13 Synthesis of a cyclic phosphazene molecule (55).

of epoxy-based composites was investigated using LOI, the UL-94 standard, thermogravimetry (TG), and other methods.

The addition of 15% red phosphorus-based flame retardant additive increased the LOI value from 19.5 to 32.5 and a V-0 rating was obtained in the UL-94 test.

According to flammability properties, the maximum adjuvant effect was observed at a ratio of 9:1 of red phosphorus to boron compounds with the addition of zinc borate and boric acid and at a ratio of 7:3 with the addition of boric oxide. With the partial substitution of boron compounds for red phosphorus, a lower heat release rate and total heat evolved was obtained (58).

According to fire performances, zinc borate-containing composite showed lowest heat release rate and total heat evolved values. Also, the boron compounds showed a beneficial effect by increasing the char yield in the condensed phase (58).

Also, the synergistic effect of boron/phosphorus compounds in an epoxy resin was explored (59).

Three typical boron compounds, zinc borate, boron phosphate, and boron oxide, blended with the phosphaphenanthrene compound TAD were incorporated into the epoxy, respectively. The phosphaphenanthrene compound TAD is shown in Figure 1.14.

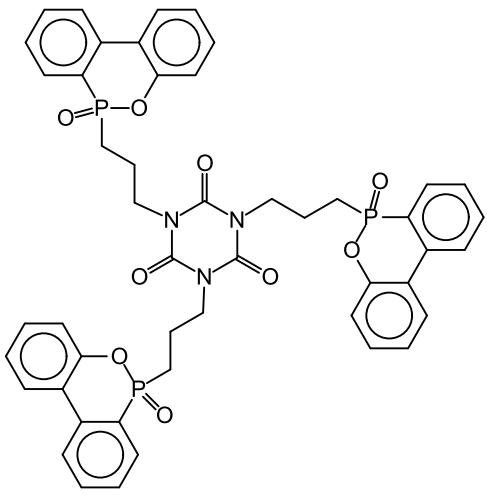

Figure 1.14 Phosphaphenanthrene compound (TAD).

All three boron/phosphorus compound systems inhibited the heat release and increased residue yields and exerted smoke suppression effect. Among the boron/phosphorus compound systems, boron oxide/TAD system showed the best flame retardant effect to epoxy thermosets in improving the UL-94 classification of epoxy composites and also reducing heat release most efficiently during combustion.

Boron oxide can interact with the epoxy matrix and enhance the charring quantity and quality, resulting in obvious condensed-phase flame retardant effect. The combination of condensed-phase flame retardant effect from boron oxide and the gaseous phase flame retardant effect from TAD effectively optimized the action distribution between gaseous and condensed phases (59).

In another report, a phosphorus, nitrogen-containing compound, poly(4,4′-diaminodiphenyl methane phenyl dichlorophosphate) (PDMPD) with high thermal stability was synthesized (60). The synthesis is shown in Figure 1.15.

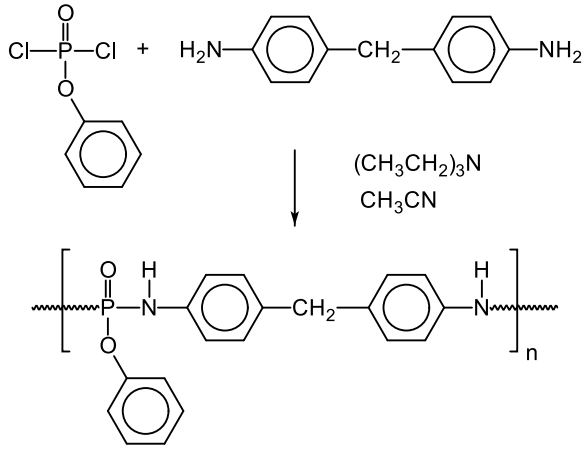

Figure 1.15 Synthesis of poly(4,4′-diaminodiphenyl methane phenyl dichlorophosphate) (PDMPD) (60).

The PDMPD was then incorporated into poly(styrene) (PS) to be used as halogen-free flame retardant. Moreover, small amounts of two boron-containing compounds, zinc borate and boron phosphate, were combined with PDMPD to explore effective flame retardant formulations for PS.

The flammability and the thermal properties of the composites were evaluated with a LOI test, a microscale combustion calorimeter, and TG. The char residues of the samples were investigated by scanning electron microscopy (SEM) and Fourier transform infrared spectroscopy (FTIR).

The incorporation of PDMPD does not significantly affect the composition of the gas phase in the course of a pyrolysis experiment. This occurs because the evolved gases of PDMPD during pyrolysis also consist of aromatic compounds.

Furthermore, it was shown that the incorporation of PDMPD can significantly decrease the flammability of virgin PS, and enhance the thermal stability at high temperature region, in both nitrogen and air atmosphere. A combination of PDMPD with small amounts of boron compounds can further decrease the flammability (60).

In order to develop an organic/inorganic synergistic flame retardant, organic phosphorus-nitrogen flame retardant 6,6-(((sulfonylbis(4,1-phenylene)) bis(azanediyl))bis(thiophen-2-ylmethylene)) bis(6H-dibenzo[c,e][1,2]oxaphosphinine-6-oxide (DOPO-N) and an inorganic boron flame retardant, i.e., zinc borate, were selected. This flame retardant is shown in Figure 1.16.

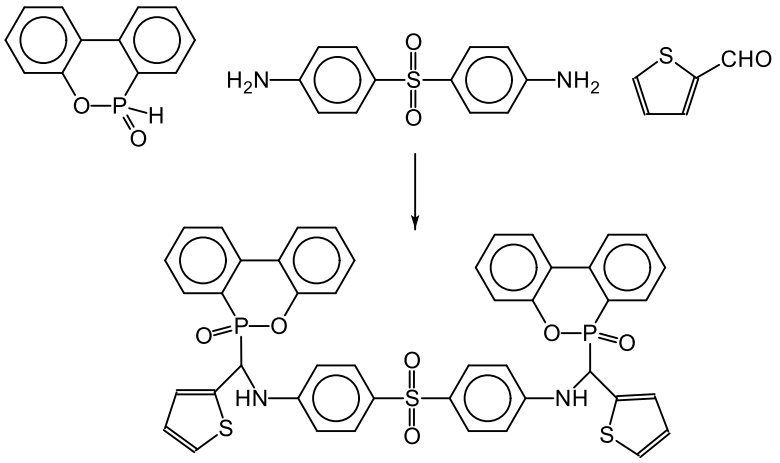

Figure 1.16 Synthesis of DOPO-N.

The flame retardant properties of poly(ethylene) (PE) that contained these compounds were investigated (61). A PE with 20% zinc

borate and 10% DOPO-N had a better thermal stability and flame retardant properties. The limiting oxygen index of this composition reached 24.6%, and an UL-94 V-0 rating was attained.

The peak heat release rate (PHRR), total heat release, average effective heat combustion, and fire growth index of this composition were lower than when zinc borate and DOPO-N were added separately (61).

The elemental analysis of the residual char of some compositions is shown in Table 1.6. The residual char was formed at 800°C.

Table 1.6 Elemental analysis of the residual char (61).

Composition	Elemental composition/[%]					
	C	O	P	Zn	B	S
PE	–	–	–	–	–	–
PE 30 % ZB	8.36	35.57	–	33.10	22.97	–
PE 30 % DOPO-N	62.19	26.02	7.30	–	–	4.50
PE 20 % ZB 10% DOPO-N	11.35	31.69	–	34.13	22.83	–

1.6.2 Boron Compounds and Magnesium Hydroxide

A synergistic flame retardant has been developed to reduce the dosage and cost of flame retardants (62). The synergistic flame retardant was made from hexakis(4-boronic acid-phenoxy)-cyclophosphazene and magnesium hydroxide. The compound is shown in Figure 1.30.

The flame retardant properties of this flame retardant in an epoxy resin were evaluated. These materials had better flame retardancy and heat resistance compared to epoxides with hexakis(4-boronic acid-phenoxy)-cyclophosphazene alone and epoxides with magnesium hydroxide (62).

With 3.0% hexakis(4-boronic acid-phenoxy)-cyclophosphazene and 0.5% magnesium hydroxide, an LOI of 31.9% and a V-0 vertical burning rating were achieved (62).

1.6.3 Boron Compounds and Aluminum Trihydroxide

The flame retardant properties of boron compounds with respect to aluminum trihydroxide were investigated in an epoxy sys-

tem based on bisphenol A, epichlorohydrin with a cycloaliphatic polyamine-based curing agent (63). Six different boron compounds, including colemanite, ulexite, boric acid, boric oxide, melamine borate and guanidinium nonaborate, were used as flame retardant additives.

The flame retardant properties of the epoxy-based composites were investigated using LOI, UL-94 standards both in vertical and horizontal position, cone calorimeter, TG, and SEM.

Boron compounds except for colemanite and ulexite showed better performance than aluminum trihydroxide. According to the LOI results, a sample with 40% boric acid had the highest LOI value of 28.5, while 30% melamine borate, 35% guanidinium nonaborate and 40% boric acid-containing samples had the highest UL-94 rating with V-0 (63).

According to the cone calorimeter test results, all boron-containing samples showed better fire performances than the aluminum trihydroxide-containing sample. A sample with 40% boric oxide showed the lowest PHRR, average heat release rate and total heat release values (63).

1.6.4 Boron/Phosphorus Polymer

A halogen-free flame retardant (DTB) containing phosphorus, nitrogen and boron was successfully synthesized (64). The synthesis is shown in Figure 1.17.

The DTB was then blended with the diglycidyl ether of bisphenol A to prepare flame retardant epoxy resins.

The thermal properties, flame retardancy and combustion behavior of the cured epoxy thermosets were investigated (64). The results of these studies indicated that DTB can significantly improve the flame retardancy as well as smoke inhibition performance of the prepared thermosets. Compared with the neat epoxy thermoset, the LOI was increased to 35.6% and the sample reached an UL-94 V-0 rating. The average of heat release rate, total heat release, and the total smoke production of the thermoset were decreased by 33.3%, 33.0% and 35.5%, respectively. The char yields of EP/DTB thermosets were increased by 45.1 to 72.8% compared with that of the neat epoxy thermoset (64).

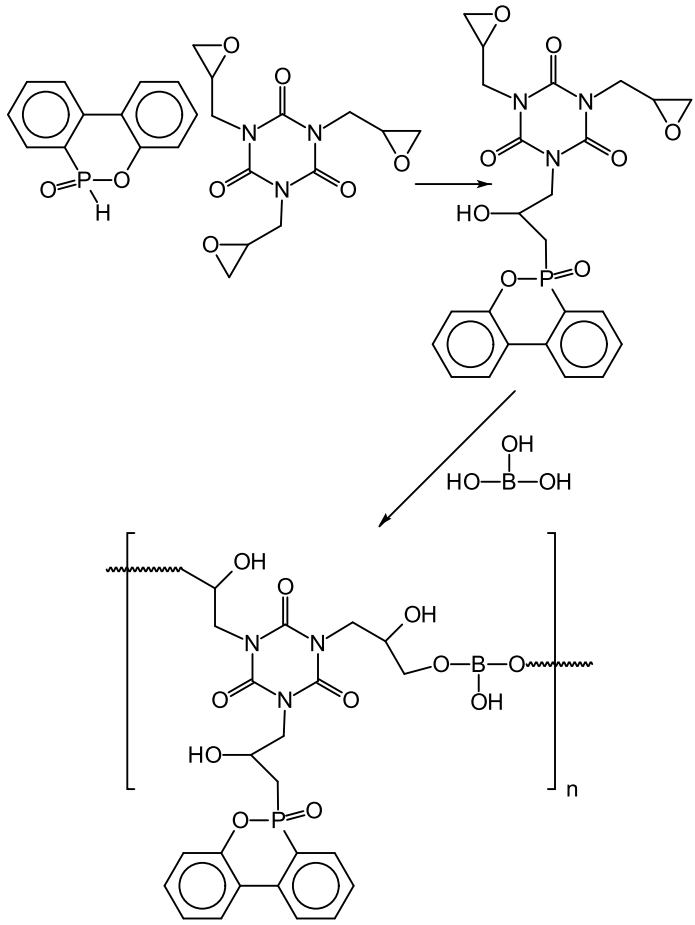

Figure 1.17 Synthesis of a halogen-free flame retardant (DTB) (64).

The DTB contributed to the formation of intumescent and glassy char layers and decomposed to generate free radicals with a quenching effect. Also, DTB was an effective radical trapper as well as efficient charring agent for epoxy resin (64).

1.6.5 Boron Phosphate

1.6.5.1 Boron Phosphate and Ammonium Poly(phosphate)

A microencapsulated ammonium poly(phosphate) with a PU resin was prepared by *in-situ* polymerization (65). The combination of microencapsulated ammonium poly(phosphate) and boron phosphate on the flammability properties of thermoplastic PU was studied by vertical burning (UL-94) tests, LOI tests, cone calorimetry, and microscale combustion calorimeter. The thermal stability was investigated by TG and real-time FTIR.

The results showed that a suitable substitution of the microencapsulated ammonium poly(phosphate) by boron phosphate could improve the flame retardancy of the composites. The cone calorimetry and microscale combustion calorimeter data showed synergistic effects between the boron phosphate and the microencapsulated ammonium poly(phosphate) in the composites (65).

1.6.5.2 Boron Phosphates with Different Acidities

Catalyzing the carbonization is an effective method to achieve flame retardancy in the condensed phase by adding a charring agent into the matrix, which facilitates the crosslinking of fragments produced during thermal pyrolysis and formation of compact char layers that inhibit the transfer of heat, oxygen, and combustible substances.

Boron phosphate is a white microcrystalline solid acid with the traits of insolubility in water and high thermal stability. There are plenty of Brønsted acid sites and Lewis acid sites in the three-dimensional structure of boron phosphate, which are formed by tetrahedral phosphorus-oxygen and tetrahedral boron-oxygen sharing oxygen atoms.

Boron phosphates with different acidities can be prepared by changing the molar ratio of the elements B and P (B/P value) or the calcination temperature (66).

It was shown that when the B/P value is 1.25, the ratio of Brønsted acid sites and Lewis acid sites (B/L value) on the surface of boron phosphates was comparatively high and the catalyzing flame retardant behavior was improved (67).

1.6.6 Boron-Containing Novolac Resins

Boron-containing novolac resins were prepared from novolac resins and bis(benzo-1,3,2-dioxa-borolanyl)oxide and bis(4,4,5,5-tetramethyl-1,3,2-dioxa-borolanyl)oxide (68, 69).

These compounds are shown in Figure 1.18.

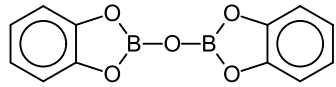

Bis(benzo-1,3,2-dioxa-borolanyl)oxide

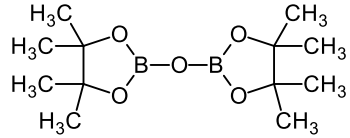

Bis(4,4,5,5-tetramethyl-1,3,2-dioxa-borolanyl)oxide

Figure 1.18 Dioxa borolanyl oxides.

These dioxa borolanyl oxides were prepared by the esterification of boric acid with catechol or pinacol (70). These compounds, which act as boron reagents, are very soluble in organic solvents such as toluene and dioxane, which makes the reaction with hydroxyl groups easier (68). On the other hand, boric acid and borate salts are insoluble in organic solvents and yield partially crosslinked compounds when they react with polyhydroxylic compounds.

The reaction of the model compound 2,6-dimethylphenol with these organoborates was complete but when the novolac resin was reacted, the degree of modification was only moderate, even when there was an excess of the boron compounds. The thermal degradation was investigated by TG and pyrolysis. The volatiles were investigated by GC-mass spectroscopy analysis.

The thermal degradation under air showed that the presence of boron is significant in the residue at high temperature. High LOI values were found. Correlations between the high char yields and the LOI values mean that the flame retardancy of the novolac resins improves when they are modified with bis(benzo-1,3,2-dioxa-borolanyl)oxide (68).

In another study, novolac resins were crosslinked with the diglycidyl ether of bisphenol A, and their thermal and flame retardant properties were evaluated (71). The boron-containing novolac resins were less thermally stable than the unmodified novolac resin. Their modification degree and the content of the diglycidyl ether of bisphenol A could be related to the crosslinking density of the materials.

The boron-containing novolac resins generated boric acid at high temperatures and gave an intumescent char that slowed down the degradation and prevented it from being total. They also showed good flame retardant properties (71).

1.6.7 Spirocyclic Boron Compounds

Spirocyclic boron compounds have been described for their use as a flame retardant additive for various plastics such as PU resins, epoxide resins and polyesters (72).

Examples for the manufacture of such compounds have been described. The synthesis may run as follows (72):

Preparation 1–2: First. 212.8 parts of tetrabromopyrocatechol in a mixture consisting of 586 parts of methanol and 147.26 parts of a 25% strength by weight methanolic tetraethylammonium hydroxide solution are brought to the reflux temperature in a stirred apparatus with reflux cooling. On heating the mixture, the tetrabromopyrocatechol dissolves completely.

Then, a hot solution consisting of 100 parts of water and 15.45 parts of boric acid is added to this solution at the reflux temperature in one operation. After some minutes, the reaction product starts to precipitate. The solution is kept at the reflux temperature for an additional 1 *h*. The solution is then cooled and the reaction product is filtered off, resulting in 224.87 parts of tetraethylammonium bis-(tetrabromopyrocatecholato)-borate.

Tetraethylammonium bis-(tetrabromopyrocatecholato)-borate is shown in Figure 1.19

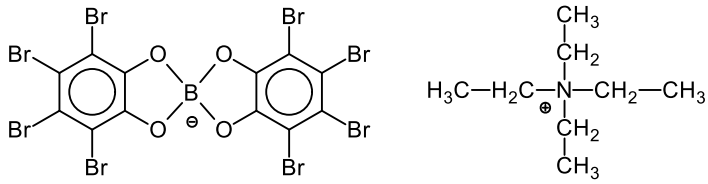

Figure 1.19 Tetraethylammonium bis-(tetrabromopyrocatecholato)-borate.

1.6.8 Boron Triazine

1.6.8.1 Thiophene Compounds

An organic boronic acid derivative containing a triazine ring, i.e., 2,4,6-tris(4-boronic-2-thiophene)-1,3,5-triazine, was synthesized (73). 2,4,6-Tris(4-boronic-2-thiophene)-1,3,5-triazine is shown in Figure 1.20.

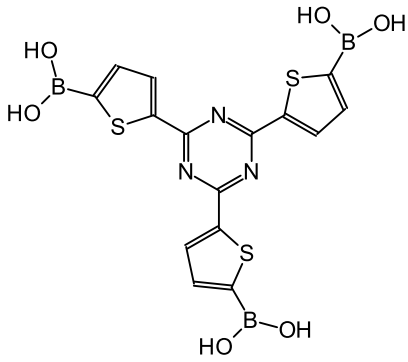

Figure 1.20 2,4,6-Tris(4-boronic-2-thiophene)-1,3,5-triazine.

The thermal properties of this compound and its corresponding intermediate products were investigated by TG. The results showed that this compound has a high char yield of 56.9%. The flame retardant properties of epoxy resin with the flame retardant were investigated by cone calorimeter, LOI test, and vertical burning test (UL-94). The LOI of EP with 20% 2,4,6-tris(4-boronic-2-thiophene)-1,3,5-triazine is 31.2% and

the UL-94 V-0 rating is achieved for an epoxide with 20% 2,4,6-tris(4-boronic-2-thiophene)-1,3,5-triazine (73).

1.6.8.2 Boronphenoxy Triazine

A halogen-free, organic boron/nitrogen compound, 2,4,6-tris-(4-boronphenoxy)-(1,3,5)-triazine (TNB), was synthesized (74). The synthesis is shown in Figure 1.21.

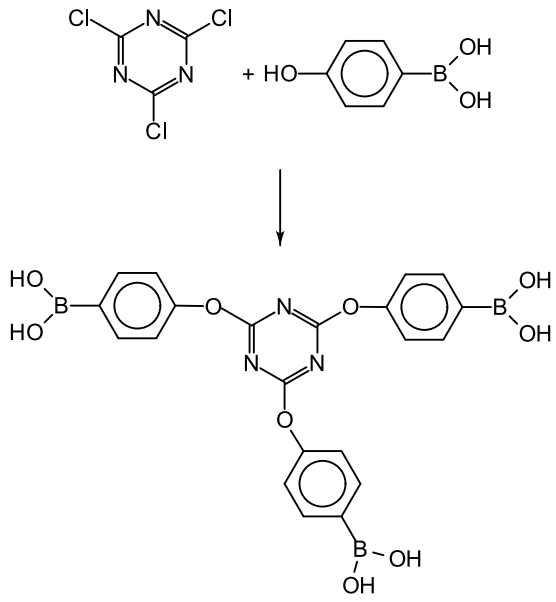

Figure 1.21 Synthesis of 2,4,6-tris-(4-boronphenoxy)-(1,3,5)-triazine (74).

In detail, the synthesis runs as follows (74):

Preparation 1–3: First, 15.5 *mmol* of 4-hydroxyphenylboronic acid and 31 *mmol* of sodium hydroxide were dissolved in 120 *ml* tetrahydrofuran in a three-necked flask, and the mixture was stirred at room temperature for 2 *h* under a nitrogen atmosphere. Next, 5 *mmol* of cyanuric chloride dissolved in 30 *ml* tetrahydrofuran was added dropwise to the flask, continuously and slowly, under a nitrogen atmosphere at room temperature. The reaction mixture was heated slowly to the reflux temperature, and then stirred vigorously for 16 *h*.

Then, the mixture was cooled to room temperature and the precipitate was separated by filtration. The precipitate was dissolved in 200 *ml*

water and hydrolyzed with acid for 1 *h* at a pH < 2. The pale-red precipitate was collected by filtration, purified on a silica-gel column using dichloromethane/ethanol (20:1 v/v), and dried at 70°C for 8 *h*. The obtained yield was 86.5%.

The thermal and flame retardant properties of epoxy resins containing the TNB compound were investigated using TG, limiting oxygen index LOI, vertical burning (UL-94) and cone calorimeter tests. The thermogravimetric curve of TNB is shown in Figure 1.22.

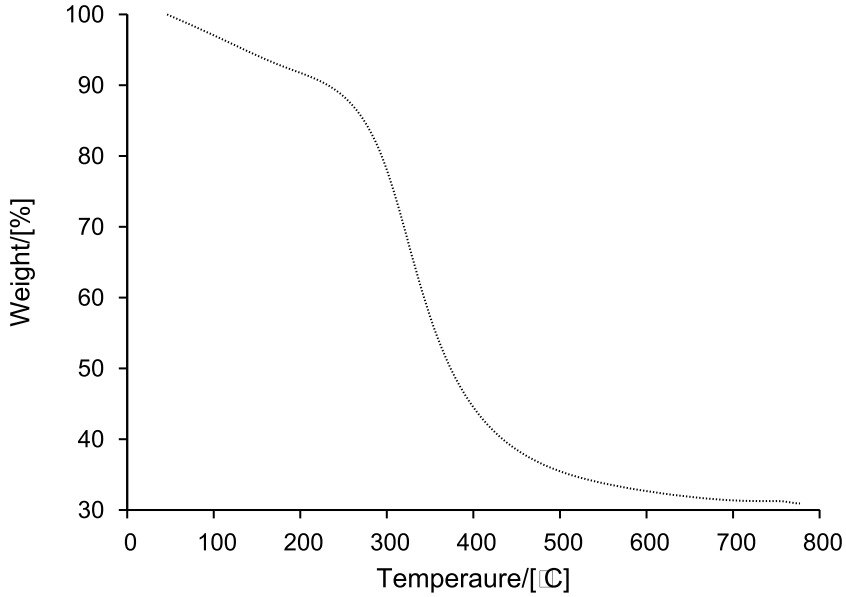

Figure 1.22 Thermogravimetric curve of 2,4,6-tris-(4-boronphenoxy)-(1,3,5)-triazine.

The residual char yield of TNB at 800°C was 30.6%. The TNB started to decompose at 127.4°C and thermal degradation occurred in two stages. The peak in the first stage at 175.3°C corresponds mainly to the conversion of the boronic acid group into boroxine. The second degradation stage occurred at 327.3°C. This is attributed to the degradation of boroxine to form a B–O–C char.

It was shown that the residual char of the epoxy resin increased in the presence of TNB. By adding 20% TNB, the LOI reached 31.2% and an UL-94 V-0 rating was achieved.

The PHRR and total heat release of this composition reduced to 305.3 $kW\,m^{-2}$ and 58.0 $MJ\,m^{-2}$, respectively (74).

1.6.9 Boron Nitride

1.6.9.1 Zinc Ferrite

A flame retardant and super paramagnetic zinc ferrite was adopted to decorate a boron nitride nanosheet through a typical solvothermal method so as to afford a zinc ferrite-boron nitride nanosheet nanofiller with improved flame retardant performance (75).

The resultant zinc ferrite-boron nitride nanosheet nanofiller was filled in an epoxy resin and exposed to a weak magnetic field of 0.05 *T* in order to achieve an ordered orientation in the epoxy resin matrix and to improve the flame retardant performance of the epoxy resin matrix composites.

It was shown that the weak magnetic field accommodates the ordered alignment of zinc ferrite-boron nitride nanosheet nanofiller in the epoxy resin matrix, and the well-ordered zinc ferrite-boron nitride nanosheet nanofiller is superior to the randomly distributed one in enhancing the fire resistance of epoxy resin (75).

The well-ordered zinc ferrite-boron nitride nanosheet nanofiller is able to reduce the PHRR, peak smoke production release and CO production of epoxy resin matrix nanocomposite by 48.5%, 46.0%, and 66.6% respectively. This occurs because the zinc ferrite-boron nitride nanosheet nanofiller can increase the char yield of epoxy resin at elevated temperatures, while layered-ordered boron nitride nanosheet and zinc ferrite exhibit a synergistic flame retardant effect.

The well-aligned boron nitride nanosheet may act as a strong physical barrier to retard the release and diffusion of thermally decomposed products via the so-called *tortuous path* effect, and zinc ferrite may act as the catalyst to promote the carbonization and char layer formation.

As a result, the density and strength of the carbon layers are increased in association with enhanced insulation shield effect to heat flux, oxygen and combustible pyrolysis products as well as their suppressed release and transfer during combustion. Moreover, zinc ferrite-boron nitride nanosheet/epoxy resin nanocomposites exhibit higher tensile strength and storage modulus than pure epoxy resin and boron nitride nanosheet/epoxy resin, which is due to the incorporation of zinc ferrite-boron nitride nanosheet nanofiller with a good dispersion in the epoxy resin matrix (75).

1.6.9.2 Phosphorus-Free Compositions

Resins with a high thermal conductivity and a greatly improved flame retardancy were developed through building phosphorus-free crosslinked network with three-dimensional porous framework based on a boron nitride skeleton and a bismaleimide resin. The preparation of a boron nitride skeleton runs basically as follows (76):

Preparation 1–4: An appropriate amount of boron nitride powder (3.0, 5.0, 7.0, 9.0 or 11.0 *g*) was dispersed in 25 *ml* deionized water with the aid of sonication to get a boron nitride suspension. Then, 1.178 *g* 1,4-butanediol diglycidyl ether and 0.4492 *g* triethylenetetramine were mixed in 25 *ml* iced deionized water with stirring for 10 *min* to get a 1,4-butanediol diglycidyl ether-triethylenetetramine solution; after that, the boron nitride suspension was quickly added into the 1,4-butanediol diglycidyl ether-triethylenetetramine solution with 60 *s* vigorous magnetic stirring. The resulting mixture was poured into 304 stainless-steel frame molds and then placed horizontally in a low-temperature (−70°C) environment for 24 *h*. After freeze-drying at a low temperature of −52°C and a pressure of 9.8 *Pa* for 24 *h*, the boron nitride skeleton with different boron nitride loadings was finally obtained through thermal curing at 150°C for 4 *h* to get a three-dimensional porous framework.

With the same loading of boron nitride, the composition with a boron nitride skeleton showed a much higher thermal conductivity than a composite based on boron nitride powders and a bismaleimide resin (76).

The thermal conductivities are shown in Figure 1.23 and the LOI values are shown in Figure 1.24.

A phosphorus-free hybrid was synthesized through chemically grafting cerium oxide on the surface of exfoliated boron nitride nanosheet with the aids of γ-aminopropyl triethoxy silane and poly(dopamine) coating, which was then embedded into a bisphenol A cyanate ester resin (77).

Compared to a bisphenol A cyanate resin, this composite with 4% of the phosphorus-free hybrid not only has delayed the initial ignition time by 23 *s*, but also shows 58.1% lower smoke production rate, 44.4% lower total heat release, and 23.1% lower PHRR (77).

The improved heat resistance and flame retardancy arises from boron nitride as physical barrier and cerium oxide as free-radical

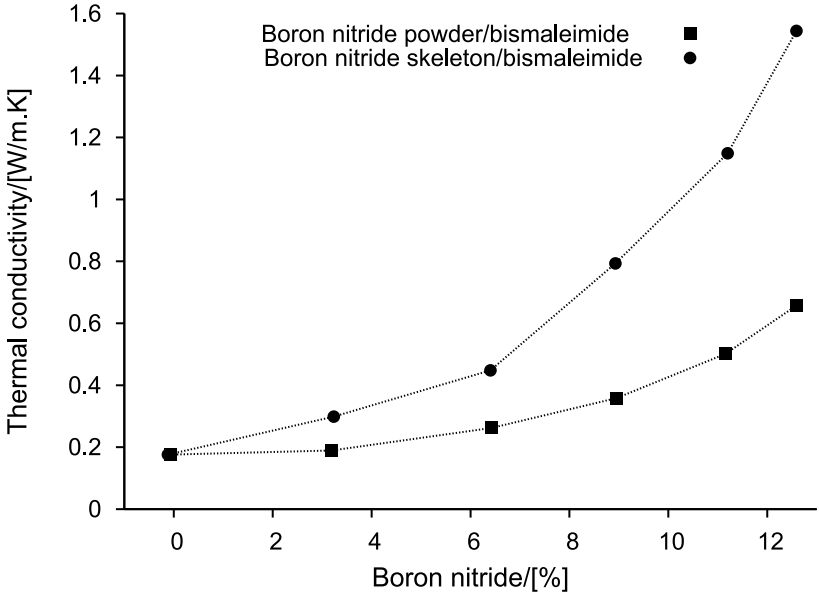

Figure 1.23 Thermal conductivity viz. temperature (76).

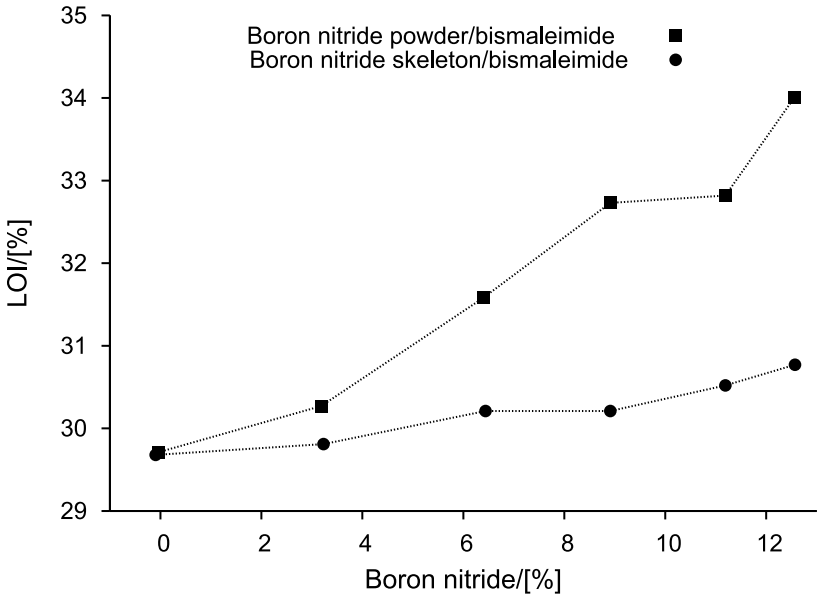

Figure 1.24 LOI values viz. temperature (76).

trapping and catalytic char layer formation. Also, a synergistic effect of boron nitride and cerium oxide occurs (77).

1.6.9.3 Boron Nitride Nanomaterials

The synthesis of boron nitride nanosheets containing phosphorus, nitrogen and silicon coexisting elements as high-performance nanofillers in an unsaturated polyester (UP) resin have been reported (78).

After incorporating 3% into the UP matrix, the combustion behavior of the UP nanocomposites was investigated by cone calorimeter. Here, a reduction of 28.2% in the PHRR and 38.0% of the total release rate was observed (78).

Hydroxyl-functionalized boron nitride nanoplatelets could be synthesized through a novel two-step method involving a simple ball milling of bulk boron nitride powders in the assistance of sodium hydroxide, which combine the synergetic effect of mechanical shear forces and chemical peeling, followed by annealing under air condition (79).

The so obtained boron nitride nanoplatelets have a high solubility and can form stable dispersions in water or various organic solvents. A boron nitride nanoplatelet was used as platform for embedding a supermolecular aggregate via ionic bonding and the electrostatic interaction between dicyandiamide and multivalent anions of phytic acid connected with cobalt ions. Phytic acid is shown in Figure 1.25.

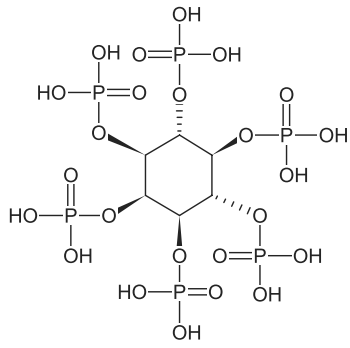

Figure 1.25 Phytic acid.

The introduction of nanohybrids significantly improves the flame retardancy of epoxy acrylate, i.e., 42.7% and 48.3% reductions in PHRR and total heat release, respectively (79).

Hexagonal boron nitride is a potential prospect in polymer composite fields; however, an undesirable interfacial interaction with the polymer matrix that generates a serious aggregation of nanomaterials has suppressed its enhancement effect (80). Moreover, the chemically inert surface of hexagonal boron nitride also makes the commonly used approach that improves the interfacial interaction between nanofillers and polymeric matrix invalid.

Using a high-performance composite of poly(amide) (PA) 6 with hexagonal boron nitride, a flame retardant was prepared via twin screw extrusion, followed by injection molding. The heat dissipation of this composite was significantly improved by incorporating 40 vol% hexagonal boron nitride (81).

In a study, the functionalized modification of chemically inert hexagonal boron nitride was successfully fabricated by the adsorption of cetyl-trimethylammonium bromide, with electrostatic interactions (80).

The so obtained hexagonal boron nitride (cetyl-trimethylammonium bromide-boron nitride) was characterized by systematic tests and then added into a thermoplastic PU matrix. The inclusion of functionalized hexagonal boron nitride can dramatically improve thermal stability, flame retardant, and mechanical properties of the thermoplastic PU composites (80).

With the incorporation of only 4.0% nanofillers, maximal value of heat release rate and total heat release of TPU were reduced by 57.5% and 17.8%, compared with those of pure thermoplastic PU, respectively. The tensile strength of a thermoplastic PU composite with a loading of 2.0% was increased by 79.3% in comparison with that of neat PU. So, the facile functionalized approach of chemically inert hexagonal boron nitride paves the way for promising applications of hexagonal boron nitride in the development of flame retardant polymer materials (80).

Also, a hexagonal boron nitride nanosheet filled flame retardant coating on the surface of flexible PU foams has been prepared by a layer-by-layer assembly method to improve the fire safety of the flexible PU foams (82).

The microstructures and compositions of the coatings could be well tailored by the alteration of the concentrations of the hexagonal boron nitride dispersions. This resulted in obvious improvements in the thermal stability and the flame retardant properties for the flexible PU foams under optimal conditions. In particular, cone calorimetry testing confirmed that the flexible PU foams coated with a proper amount of hexagonal boron nitride nanosheets effectively reduced the peak of the heat release rate to 50.1% and CO production to 53.8% of the flexible PU foams, which demonstrated excellent flame retardant performance (82).

These excellent flame retardant properties were attributed to the physical barrier and tortuous-path effects and anisotropic thermal conductivity of the hexagonal boron nitride nanosheets. These retarded the transfer and diffusion of heat toward the polymer matrix (82).

Boron nitride nanosheets decorated with bismuth ferrite nanoparticles (83) or decorated with cobalt ferrite nanoparticles (84) were prepared via a hydrothermal route.

The nanohybrids were incorporated into an epoxy resin with the introduction of a weak rotary magnetic field to achieve order orientation, in order to reduce the fire risk and toxic hazards using enhanced shielding effect of the boron nitride nanosheet upon combustion (84).

It was demonstrated that the nanohybrids are composed of cobalt ferrite nanoparticles uniformly dispersed on the nanosheet surface. The nanofiller among the epoxy matrix contributes to improving the char residues and mechanical properties of epoxy resin and reducing its fire risk as well as toxic hazards; the ordered one is especially advantageous over the disordered one in reducing the fire risk and toxic hazard (84).

The orderly aligned boron nitride nanosheets as the physical barrier can more effectively prevent the transfer and diffusion of oxygen and heat. On the other hand, the cobalt ferrite can catalyze the degradation of epoxide to afford excessive chars on polymer surface (84).

Boron nitride nanosheets were prepared by molten hydroxide-assisted liquid exfoliation from a hexagonal boron nitride powder with an effectively high yield, and then modified with hexachlorocyclotriphosphazene (85). These compounds were used to pre-

pare flame retardant cotton fabrics with the impregnation-drying method. Hexachlorocyclotriphosphazene is shown in Figure 1.13

A successful treatment was confirmed by SEM. The combustion performance of the as-prepared cotton fabrics was tested and evaluated. The combustion rate of the fabric is reduced under both vertical and horizontal combustion conditions and the LOI value of the cotton fabric increases to 24.1 (85).

1.6.10 Azo-Boron Compounds

An azo-boron compound and poly(dopamine) were synthesized and incorporated into poly(lactic acid) (PLA) using the solvent approach and hot compression molding (86). The synthesis runs as follows:

Preparation 1–5: First, 5.89 *g* (0.038 *mol*) of 3-aminophenylboronic acid monohydrate was dissolved in 6.39 *ml* (0.076 *mol*) HCl and 20 *ml* distilled water; 2.63 *g* (0.038 *mol*) of sodium nitrite was also dissolved in 10 *ml* water and cooled in an ice bath at 0°C – 5°C. Then the cooled sodium nitrite solution was added slowly drop by drop to the 3-aminophenylboronic acid monohydrate solution under stirring to form diazotized phenylboronic acid.

Meanwhile, 4.22 *g* (0.019 *mol*) of 2,2-bis(4-hydroxyphenyl)propane was dissolved in 1.54 *g* (0.038 *mol*) of NaOH and 30 *ml* distilled water and cooled in an ice bath at 0°C – 5°C. The cooled 2,2-bis(4-hydroxyphenyl)propane solution was added slowly to the diazotized phenylboronic acid and stirred for 2 *h* after which 0.076 *mol* HCl was added to precipitate the azo compound. The reaction was allowed to continue for 5 *h* under stirring at room temperature to obtain a brownish precipitate. The precipitate was filtered and washed with distilled water to remove the acid until a pH of 6–7 was attained. The final product was dried at 60°C for 12 *h*.

The synthesis of the azo-boron compound is shown in Figure 1.26.

The flame retardant properties of these compounds were investigated (86). TG analysis showed that the flame retardant was generally more efficient in reducing the degradation rate of PLA and gave appreciably much higher char residue compared to the individual components. Also, a V-0 rating was achieved with a LOI value of 23.7% at a 10% loading in the ratio 1:1 whereas the individual flame retardant components could only give a V-2 rating (86).

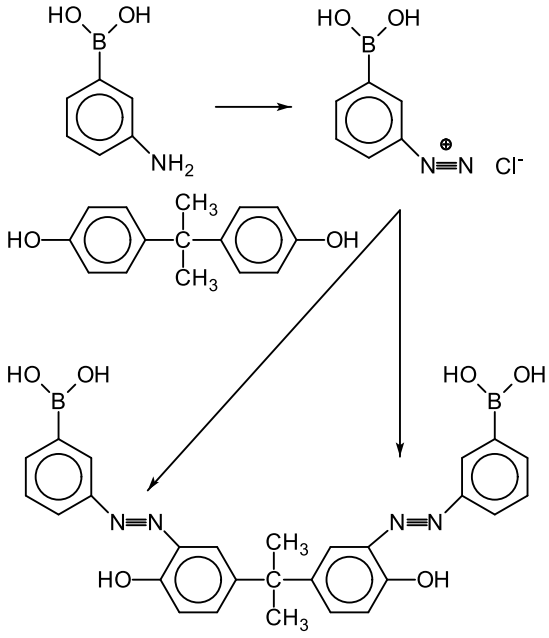

Figure 1.26 Synthesis of an azo-boron compound (86).

In another study, an efficient flame retardant for PLA biocomposites based on azo-boron coupled with 4,4′-sulfonyldiphenol-(((1E,1′E)-(sulfonylbis(6-hydroxy-3,1-phenylene)) bis(diazene-2,1-diyl))bis(3,1-phenylene))diboronic acid (SBDA) was synthesized (87). The synthesis of this compound is shown in Figure 1.27. The synthesis is quite similar to the synthesis shown in Figure 1.26.

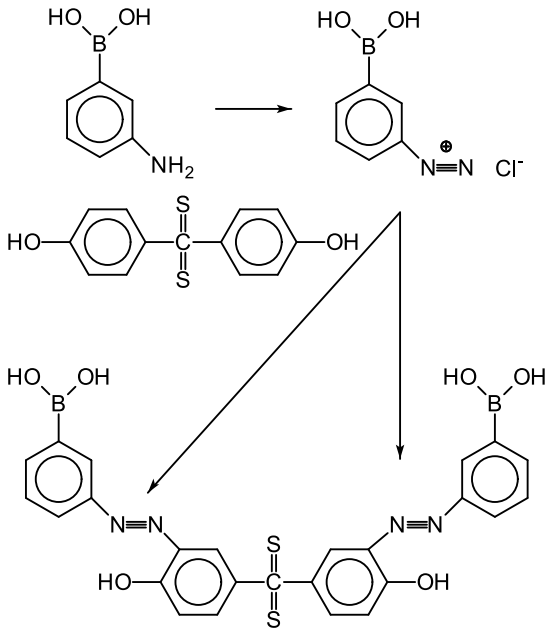

Figure 1.27 Synthesis of an azo-boron compound (87).

SBDA was combined with calcium lignosulfonate and compounded with PLA (BioPlus 6201D from NatureWorks, USA).

Calcium lignosulfonate is shown in Figure 1.28.

The addition of 10% calcium lignosulfonate and 5% SBDA into PLA led to important reductions in the PHRR of 54%, a total heat release of approximately 28.6%, and the average effective heat of combustion of approximately 29.4%. The fire performance index and fire growth index were improved by approximately 56.4% and 33.1%, respectively. A V-0 rating (vertical burning test) and a limiting oxygen index value of 28.8% were achieved for these biocomposites (87).

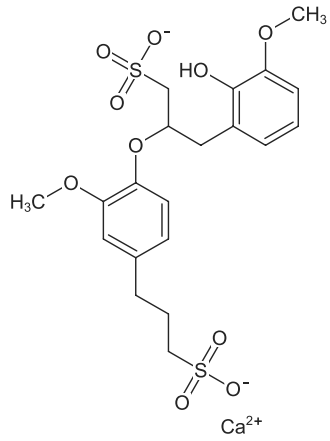

Figure 1.28 Calcium lignosulfonate.

1.6.11 Isosorbide-Derived Boron and Phosphorus Materials

An attempt to induce the inherent flame retardancy to the epoxy resin by incorporation of phosphorus and boron atoms in the polymer backbone through the curing agents has been presented (88).

Phosphorus- and boron-containing precursors were synthesized and incorporated into a commercial epoxy and hardener system with different molar ratios. The synthesis is shown in Figure 1.29.

TG and differential scanning calorimetry indicated an increased thermal stability and char yield along with the glass transition temperatures due to the incorporation of these phosphorus- and boron-containing compounds in the coating films.

The highest LOI of 29 was obtained for a formulation with equal amounts of phosphorus and boron compounds. The UL-94 showed a self-extinguishing behavior within 10 *s* after ignition (88).

1.6.12 Boron Cyclophosphazene Derivatives

Hexakis(4-boronic acid-phenoxy)-cyclophosphazene was synthesized and characterized (89). This compound contains phosphorus, nitrogen, and boron. The synthesis is shown in Figure 1.30.

Its flame retardant properties in an epoxy resin were investigated.

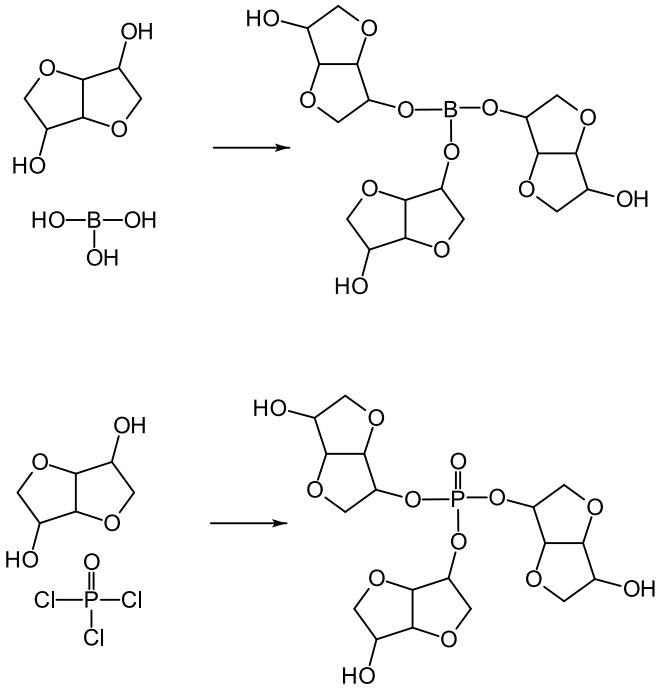

Figure 1.29 Synthesis of phosphorus- and boron-containing isosorbides (88).

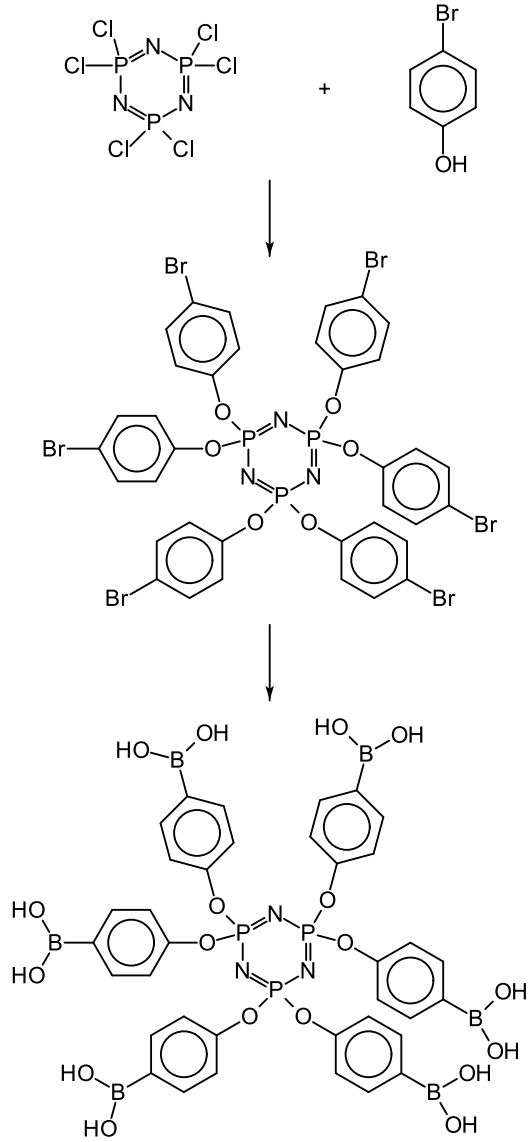

Figure 1.30 Synthesis of hexakis(4-boronic acid-phenoxy)-cyclophosphazene (89).

It was shown that the LOI value with 7% of this compound in the epoxy resin reached 32.3% and a UL-94 V-0 rating was attained (89).

A decomposition model based on spectroscopic data was developed (89). During the combustion process, the boric acid first forms boroxine (73, 90–92), which continues to decompose to generate free radicals and ions.

Finally, metaphosphoric acid, phosphoric acid and boric acid were produced. The resulting metaphosphoric acid could promote EP dehydration and carbonization. Phosphoric acid and boric acid formed BPO_4 at high temperature (93).

1.6.13 Cardanol DOPO and Boron-Doped Graphene

A bio-based phosphorus-containing a cardanol-based benzoxazine (CBz) monomer was successfully synthesized through the reaction between cardanol and a DOPO-based diamine. The synthesis of a 6-(1,1-bis(4-aminophenyl)ethyl)-6H-dibenzo[c,e][1,2] oxaphosphinine 6-oxide (BA-DOPO) is shown in Figure 1.31.

In order to simultaneously improve the toughness and flame retardancy of the epoxy resin, various contents of CBz in combination with boron-doped graphene nanosheets were incorporated into the resin to obtain boron-doped graphene/cardanol-derived benzoxazine-epoxy composites.

Also, cardanol-derived benzoxazine-epoxy co-polymers (EP/CBz) were fabricated (94). The results showed that the addition of the as-prepared CBz into epoxy resin not only endowed an epoxy resin with an excellent flame retardancy, but also improved the glass transition temperature and the impact strength.

The PHRR of the epoxy composite with 13% CBz and 2% boron-doped graphene decreased by 48% compared to that of a neat epoxy resin, accompanied by an increase of impact strength of 22%. These properties of the composites are attributed to the unique structure of CBz and the high resistance to thermal decomposition of the boron-doped graphene (94).

1.6.14 Boron Crosslinked Cellulose Nanofibrils

Low-flammability freeze-dried cellulose nanofibril/sodium montmorillonite (MMT) aerogels with improved mechanical properties

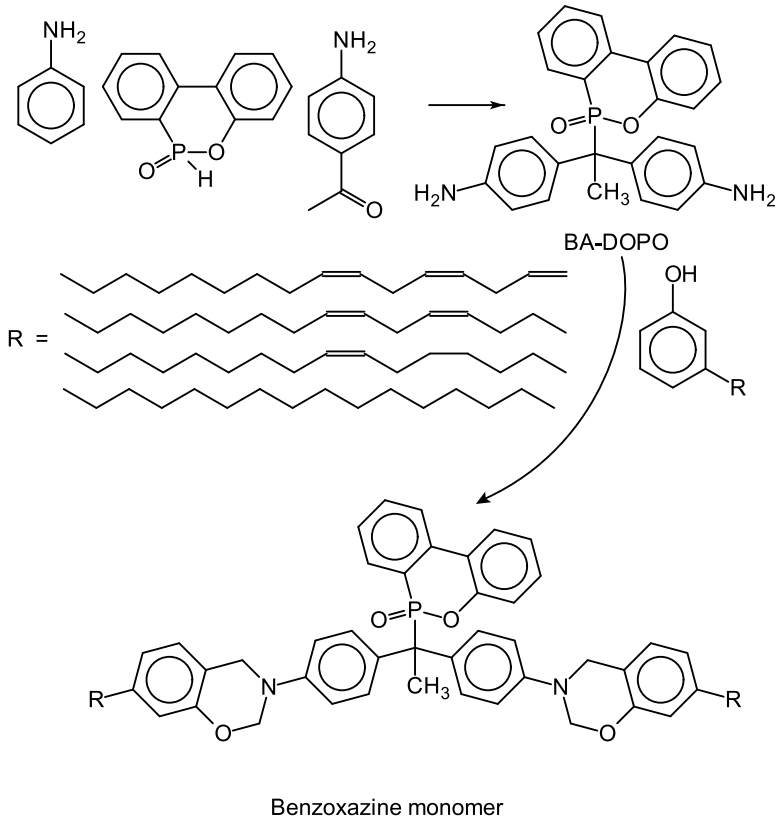

Figure 1.31 Synthetic routes of a DOPO-based diamine and a cardanol-based benzoxazine monomer (CBz) (94).

were fabricated via a facile crosslinking of boric acid and melamine-formaldehyde resins (95). SEM analysis showed that the crosslinking with boric acid reduced the interspacing of the layered cellulose nanofibril/MMT aerogels, whereas the introduction of melamine-formaldehyde formed polymeric fibrils that connected the layers.

These changes in the microstructures resulted in an improvement of the compressive mechanical properties of the crosslinked aerogels. Moreover, the boron-nitrogen-containing flame retardant crosslinkers greatly increased the limiting oxygen index values that could reach 85% and leveled the UL-94 rating from no rating to V-0.

Furthermore, cone calorimetric studies suggested that boric acid and melamine-formaldehyde induced a synergistic effect on the flame retardant properties of the cellulose nanofibril/MMT aerogels. The thermal conductivity was only little affected because the pore structure and the size were not substantially modified (95).

1.7 Silicones

Some recent studies about the flame retardation of silicone elastomers and applications of silicones as flame retardant agents in other polymers have been reviewed (96, 97).

1.7.1 Hydroxy Silicone Oil

The effects of hydroxy silicone oil as a synergistic agent on the flame retardancy of intumescent flame retardant (IFR) poly(propylene) (PP) composites were studied (98). The IFR system mainly consisted of ammonium poly(phosphate) and pentaerythritol.

The UL-94 test, TG, cone calorimeter, digital photography and X-ray photoelectron spectroscopy (XPS) were used to evaluate the synergistic effects of the hydroxy silicone oil. It was found that the PP composite that contained only ammonium poly(phosphate) and pentaerythritol does not show a good flame retardancy at an additive level of 30%. However, hydroxy silicone oil could promote the formation of a homogeneous and compact intumescent char layer. Thus, a suitable amount of hydroxy silicone oil has a synergistic effect in the flame retardancy (98).

A synergistic effect on flame retardancy was found when hydroxy silicone oil was incorporated into an ethylene vinyl acetate

(EVA)/aluminum hydroxide composite (99). The fire performance of EVA and EVA composites was studied by using LOI, UL-94, and a cone calorimeter test.

Compared with the EVA/aluminum hydroxide binary composite, the LOI values of the EVA/aluminum hydroxide/HSO ternary composites at the same additive loading are all decreased. The cone calorimeter test data indicated that the addition of the hydroxy silicone oil in EVA/aluminum hydroxide system not only reduced the heat release rate, but also prolonged the ignition time of the composite. TG revealed that aluminum hydroxide accelerated the loss of acetic acid, but hydroxy silicone oil assisted in reducing the accelerating effect of aluminum hydroxide (99).

Microencapsulated ammonium poly(phosphate) was prepared using hydroxyl silicone oil by *in-situ* polymerization (100). The microencapsulation gives the microencapsulated ammonium poly(phosphate) a better water resistance and flame retardance in comparison to an ordinary ammonium poly(phosphate) in thermoplastic poly(urethane) (TPU).

The thermal stability and the fire resistance behavior have been analyzed and compared (100). The LOI value of the TPU/microencapsulated ammonium poly(phosphate) composite is higher than that of the TPU/ammonium poly(phosphate) composite. The UL-94 rating of the this composite is V-0 with 20% of additive, whereas a TPU/ammonium poly(phosphate) gives a V-2 rating at the same loading level.

The results of cone calorimeter and microscale combustion calorimeter experiments showed that microencapsulated ammonium poly(phosphate) is a more effective flame retardant in TPU compared with ordinary ammonium poly(phosphate) (100).

A novel flame retardant (HSPCTP) was successfully designed and incorporated into a PC matrix. The synthesis is shown in Figure 1.32. In detail, the method of synthesis runs as follows (101):

Preparation 1–6: First, 3.0 *g* (8.63 *mmol*) hexachlorocyclotriphosphazene (HCCP), 16.40 *g* (8.63 *mmol*) bihydroxypropyl silicone oil and 10 *ml* dry THF were added at 25°C to a 250 *ml* four-necked flask equipped with a mechanical stirrer, a reflux condenser and a nitrogen inlet. Then, the reaction temperature was raised to 70°C, and 1.75 *g* (17.26 *mmol*) triethylamine was slowly added to the four-necked flask under a nitrogen atmosphere. After completion of the dropwise addition, the reaction continued for another 24

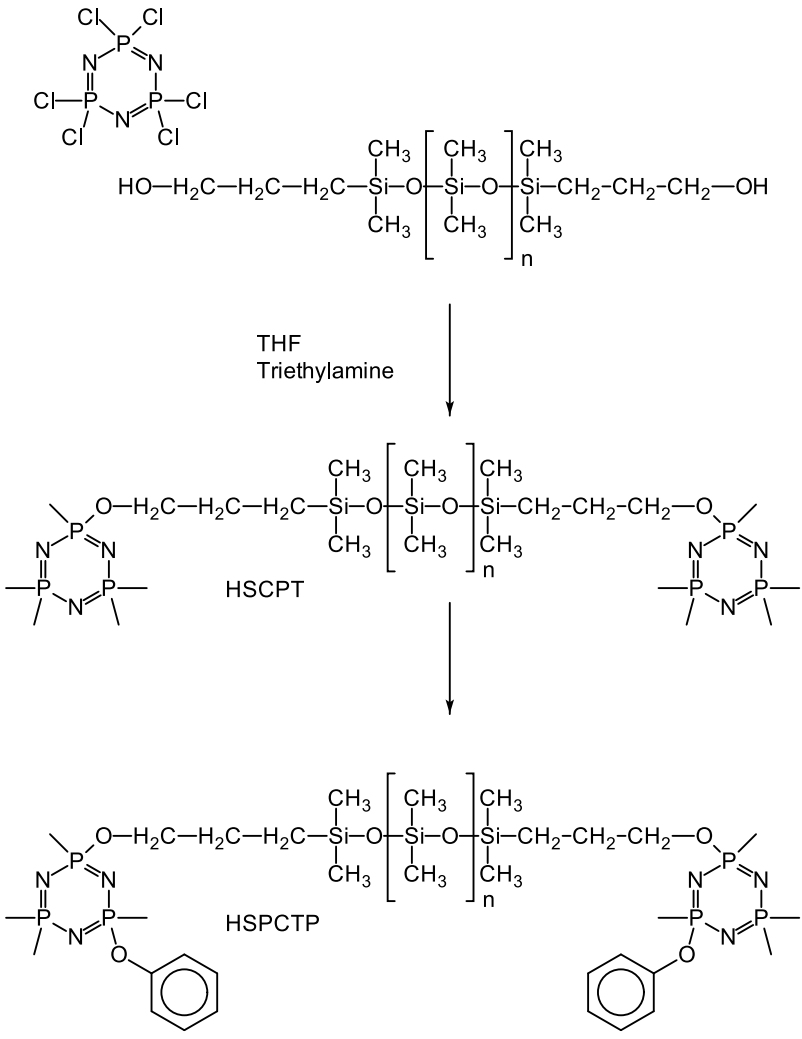

Figure 1.32 Synthesis of HSPCTP (101).

h to obtain a yellow oily product, and was then filtered under reduced pressure to remove triethylamine salt. Finally, the lower liquid was separated and then the solvent was removed by rotary evaporation. An amount of 15.93 *g* HSCPT was obtained with a yield of 84.82%. Anhydrous THF (20 *ml*) and 1.19 *g* (51.7 *mmol*) of sodium swarf were placed in a three-necked flask, and 4.87 *g* (51.7 *mmol*) of phenol was slowly added at room temperature. The reaction continued for 5–6 *h*. The sodium phenolate solution was successfully prepared. The obtained intermediate product HSCPT and 10 *ml* dry THF were added to a four-necked flask equipped with a mechanical stirrer, a reflux condenser and a nitrogen inlet. Afterwards, the HSCPT was completely dissolved in dry THF and stirred. The reaction temperature was raised to 70°C and the prepared sodium phenolate solution (5.00 *g*, 43.15 *mmol*) was slowly added to the four-necked flask under a nitrogen atmosphere. After completion of the addition, the reaction continued for 24 *h* to obtain a pale yellow viscous liquid product. The reaction mixture was concentrated by rotary evaporation to remove excess solvent and achieve a thick liquid. Then, the liquid was dissolved with the proper amount of methylene chloride and washed with plenty of deionized water 3–4 times until the water layer became clear. Afterwards, the lower liquid was separated and the solvent was removed by rotary evaporation. The liquid product was placed in a vacuum oven at 60°C for 12 *h*. An amount of 17.35 *g* HSPCTP was obtained, with a yield of 84.65%.

These composites passed UL-94 V-0 rating testing with an additive content of only 3%, and the LOI value increased from 25.0% to 28.4% (101).

The findings showed that HSPCTP exhibits both gas-phase and solid-phase flame retardant effects. Furthermore, the incorporation of HSPCTP into PC could suppress the release of smoke. The flame retardant mechanism is discussed in depth (101).

1.7.2 Hydrogen-Containing Silicone Oil

A silicone-containing flame retardant was synthesized from a hydrogen-containing silicone oil and bisphenol A. Here the Si−H groups in the silicone oil react with the −OH groups of the bisphenol A. The process runs as follows (102):

Preparation 1–7: Mixtures of hydrogen-containing silicone oil and bisphenol A with a certain molar ratio of Si−H in silicon oil to hydroxyl groups in bisphenol A of 1:1 were added to a 250 *ml*, three-necked round-bottom flask fitted with a mechanical stirrer and a reflux condenser. The condensation reaction between them was catalyzed by stannous octoate (stannous

octoate:silicon oil = 51/10,000 by weight). The temperature was held at 85°C for 6 *h*. No solution was used in this reaction, which will effectively simplify the prepared processing and purification steps. The resulting product was obtained as a white powder after washing with diethyl ether to remove the raw material in a yield of 92%.

This material was incorporated into a PC matrix to study effects on the flame retardancy. The LOI value of the composites is 31.7 and the UL-94 rating reaches V-0 when the content of the flame retardant is 3% (102).

1.7.3 Red Phosphorus and Alumina Trihydrate

The synergistic effects between the flame retardant's red phosphorus and alumina trihydrate were evaluated in silicone rubber composites (103). The properties were measured with LOI, UL-94 rating, cone calorimeter, TG and digital photography.

It has been found that a silicone rubber composite that contains only alumina trihydrate does not show a good flame retardancy at a loading of 39% (103).

Cone calorimeter experiments showed that the heat release rate, mass loss rate, mass and total heat release of silicone rubber/alumina trihydrate/red phosphorus composites decrease greatly in comparison with the silicone rubber/alumina trihydrate composites. The digital photographs demonstrated that 1% of red phosphorus could promote the formation of a homogeneous and compact char layer. Thus, a suitable amount of red phosphorus has a synergistic effect with alumina trihydrate in a flame retardant silicone rubber composite system (103).

1.7.4 Aluminum Hypophosphite and Expandable Graphite

The synergistic effect of expandable graphite and aluminum hypophosphite (AHP) was investigated on the flame retardancy of silicone rubbers (104). The synergistic effects of these materials in halogen-free flame retardant silicone rubber composites were studied by a cone calorimeter test, TG, and TG/infrared spectrometry.

The results of the cone calorimeter test showed that AHP and expandable graphite can effectively reduce the flammable properties, including PHRR, total heat release, smoke production rate,

total smoke release, and smoke factor. Also, an improvement of the thermal stability of silicone rubber/AHP/expandable graphite was observed (104).

Experimental observations from digital photographs showed positive evidence of the synergistic effects between AHP with expandable graphite. The TG results revealed that silicone rubber/AHP/expandable graphite samples show a slower thermal degradation rate and a higher thermal stability at high temperature than a pure silicone rubber sample.

The addition of AHP and expandable graphite also significantly decreased the combustible gaseous products such as hydrocarbons (104).

1.7.5 Phosphaphenanthrene Compound

An intrinsic flame retardant silicone rubber containing phosphaphenanthrene structure was synthesized (105). The synthesis is shown in Figure 1.33.

The synthesis procedure is as follows (105):

Preparation 1–8: First, 54.00 *g* DOPO powder and 118.13 *g* 3-glycidyloxypropyltrimethoxysiloxane were mixed at 120°C until the DOPO was dissolved completely in 3-glycidyloxypropyltrimethoxysiloxane, and then the reagents were poured into a three-necked flask equipped with an oil-bath pot, a mechanical stirrer and a reflux condenser. The reaction temperature was maintained at 170°C for 8 *h* under the atmosphere of nitrogen. After cooling to room temperature, adding 26.9 *g* deionized water, the reaction mixture was stirred at 65°C for 2 *h*, then the volatiles were removed at low boiling points with rotary evaporation (110°C, -0.1 *MPa*) to obtain the oily prepolymer. The prepolymer were poured into a mold, and then cured at 110°C for 24 *h*. Finally, alcohol was added to wash the products repeatedly for removing the unreacted substance.

A series of characterizations showed that this silicone rubber possessed much quicker self-extinguishment, lower heat release rate, higher LOI and higher thermal stability, as well as better charring capacity compared with unmodified silicone rubber.

An analysis of the char residues of these materials revealed the interactions between the phosphaphenanthrene group and siloxane in the condensed phase (105).

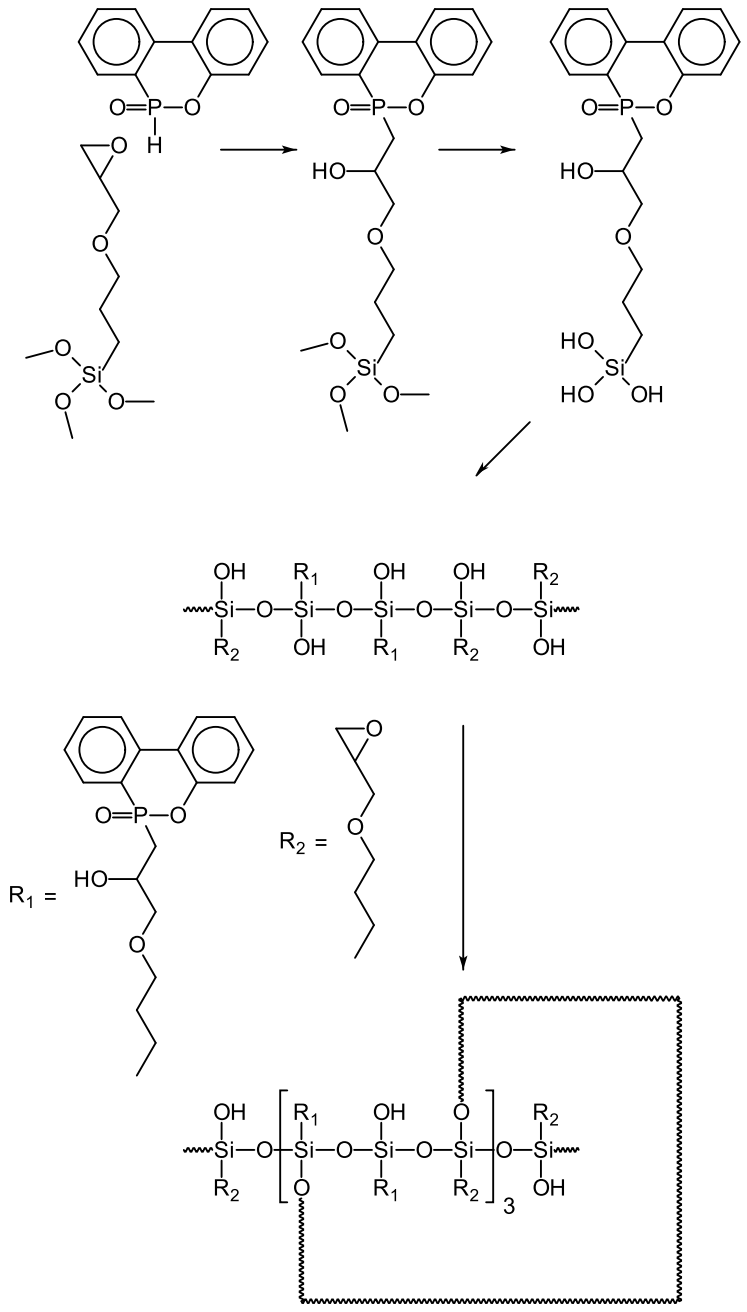

Figure 1.33 Synthesis of a phosphaphenanthrene-based flame retardant (105).

1.7.6 Phosphorus-Silicone-Nitrogen Ternary Flame Retardant

A phosphorus-silicone-nitrogen ternary flame retardant, [(1,1,3,3-tetramethyl-1,3-disilazanediyl)di-2,1-ethanediyl]bis(diphenylphosphine oxide) was synthesized with high yield via a one-step procedure by the reaction of diphenylphosphine oxide and vinyl-terminated silazane with triethylborane as the catalyst (106). The synthesis is shown in Figure 1.34.

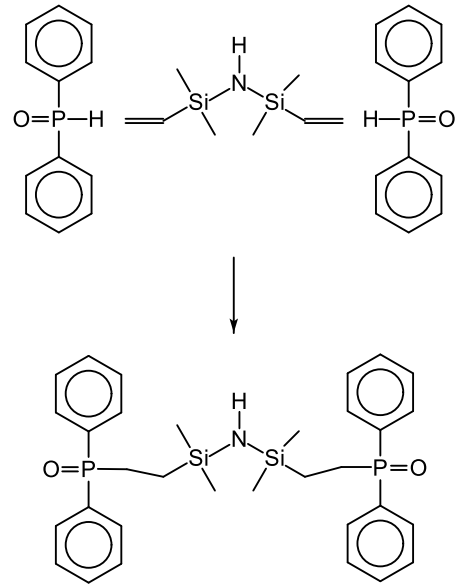

Figure 1.34 Synthesis of [(1,1,3,3-tetramethyl-1,3-disilazanediyl)di-2,1-ethanediyl]bis(diphenylphosphine oxide) (106).

The flame retardant was used in an *o*-cresol novolac epoxy/phenolic novolac hardener system (106). It was shown that the addition of [(1,1,3,3-tetramethyl-1,3-disilazanediyl)di-2,1-ethanediyl]bis(diphenylphosphine oxide) improved the flowability of the *o*-cresol novolac epoxy/phenolic novolac systems, while the thermal stability of the epoxy thermosets was maintained.

Also, the incorporation of the compound was in favor of the formation of char during the thermal degradation process of the epoxy thermosets. The limited oxygen index of the epoxy system increased along with the content of flame retardant. An UL-94

V-0 FR rating was achieved when the weight content of the flame retardant in the epoxy composites reached 20% (106).

1.7.7 Calcium and Aluminium-Based Fillers

Silicone composites with enhanced thermal behavior were tested for cable applications. Calcium and aluminium-based fillers introduced into silicone formulations were classified according to three categories (107):

1. Non-hydrated fillers such as $CaCO_3$ (precipitated calcium carbonate and natural calcite) and wollastonite,
2. Water-releasing fillers such as calcium hydroxide, aluminum trihydrate, boehmite, and
3. Hydroxyl-functionalized fillers including alumina and mica.

Calcium carbonates improve the final residue of silicone composites, surely because of *in-situ* co-crystallization phenomena between the CaO matter produced by $CaCO_3$ fillers and the matrix at high temperature (107).

A smaller particle size of a water-releasing filler led to a lower residue. This is correlated to a larger surface area that increases the surface contact between filler-matrix and therefore enhances the water release impact to promote thermal degradation of silicone. Composites that contain rhombohedral fillers show more synergistic effect on final residue than acicular fillers due to their capacity to induce a barrier effect.

The presence of hydroxyl groups on the surface of alumina and mica induced an early thermal degradation of the silicone composite due to the catalytic activity of the hydroxyl groups on the filler surface. Consequently, alumina with smaller particle size and bigger surface area degrades more silicone chains than bigger particles of mica. On the other hand, the heat barrier built by platelet mica particles at higher temperature is more effective at slowing down the degradation of corresponding composites (107).

The fire reaction of precipitated calcium carbonate, calcite, calcium hydroxide, aluminum trihydrate, boehmite and alumina-based composites could be correlated mainly with their thermal stability, while for mica and wollastonite-based composites, a barrier effect

was also evidenced (108). The endothermic effect was not established as an efficient flame retardancy mechanism for the silicone composites containing hydrated fillers. The mica composite exhibited the best flame retardancy, in terms of a depressed heat release rate, among all investigated formulations (108).

1.7.8 Macromolecular Charring Agent

A silicone-containing macromolecular charring agent was synthesized via polycondensation. The synthesis of the charring agent is shown in Figure 1.35. This compound was combined with ammo-

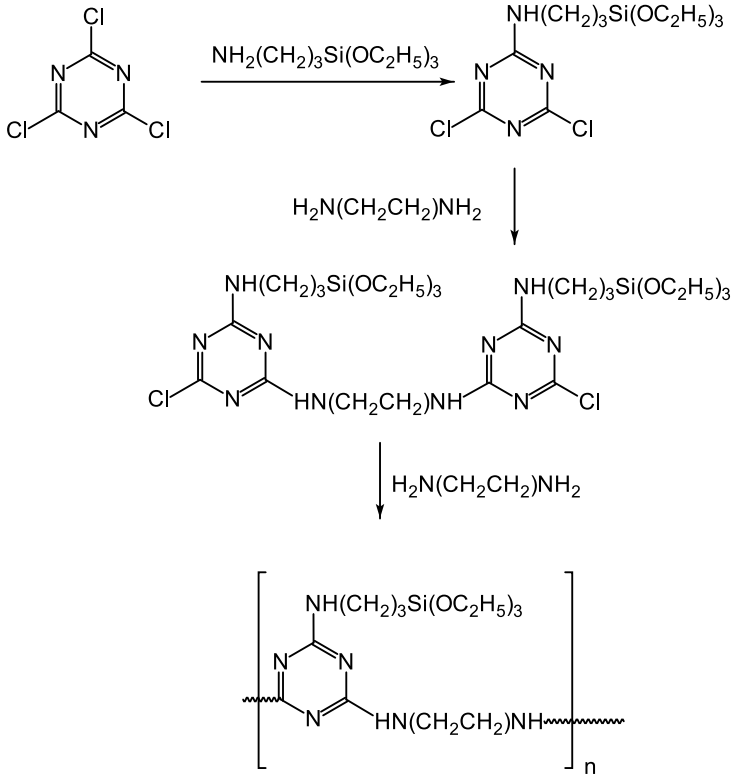

Figure 1.35 Synthesis of a macromolecular charring agent (109).

nium poly(phosphate) as flame retardant for PP (109).

The charring agent exhibited a good synergistic effect with ammonium poly(phosphate). When the content of ammonium poly(phosphate) was 18.7% and the content of the charring agent was 6.3%, the LOI value of this composite was 33.5%, and the UL-94 test showed a V-0 rating.

The PHRR, total heat release, average mass loss rate, and total smoke production of the composite were also decreased significantly. Moreover, the composite showed an outstanding water resistance (109). After soaking in 70°C water for 168 *h*, the composite could still reach a UL-94 V-0 rating at a loading of the IFR of 20.0%.

1.7.9 Intumescent Flame Retardants

1.7.9.1 Phosphorus Acid, Melamine, and Pentaerythritol

Organic Nano Montmorillonite. The flammability of room temperature vulcanized silicone rubber composites filled with melamine phosphate, c.f. Figure 7.10, as intumescent flame retardant additive was investigated by LOI, UL-94 test, and cone calorimeter. In addition, the thermal degradation of the composites was studied with TG (110).

Furthermore, in order to relate to actual application requirements, the comprehensive performance of the temperature vulcanized silicone rubber/melamine phosphate composites was optimized by adding organic nano montmorillonite (MMT) as a partial substitute for the melamine phosphate (110).

The so-prepared intumescent flame retardant nanocomposites were characterized by LOI, UL-94 test, TG, cone calorimetry, SEM, and mechanical tests. The residue morphology formed after the burning of the nanocomposites was analyzed by SEM and digital photographs. The results showed that the flame retardant nanocomposites filled with 10 *phr* organic nano MMT and 35 *phr* melamine phosphate displayed the best comprehensive performance with regard to flame retardancy, mechanical properties, and heat stability at low cost (110).

Iron Oxide. The feasibility of an IFR, based on phosphorus acid, melamine, and pentaerythritol, as a flame retardant and Fe_2O_3 as a

smoke suppression agent has been examined in silicone rubber composites. The smoke suppression of Fe_2O_3 in intumescent flame retardant silicone rubber composites was investigated using a smoke density test and a cone calorimeter test. The flammability of silicone rubber composites was characterized using a cone calorimeter test at an incident heat flux of 50 $kW\,m^{-2}$.

The test results revealed that Fe_2O_3 could increase the smoke suppression efficiency and the thermal degradation temperature. Furthermore, Fe_2O_3 can promote an early crosslinking of polymer during the decomposition to increase char formation.

The silica ash layer integrity governs the efficiency of diffusion barrier that restricts the diffusion of fuels into combustion zone and access of oxygen to the unburned fuels (111).

Zinc Oxide. The synergistic effects of zinc oxide with an IFR based on phosphorus acid, melamine and pentaerythritol in silicone rubber composites were studied (112).

A 2.0% loading of ZnO in the composites could greatly reduce the peak values of heat release rate and the smoke production rate. Also, a compact char layer is formed on the surface of the sample (112).

1.7.9.2 Phosphorus, Nitrogen, and Silicone

DTT. An IFR (DTT) based on silicone, phosphorus, and nitrogen was successfully synthesized from DOPO, aminopropyl triethoxy silane (KH550), and 1,4-phthalaldehyde. The flame retardant was used to improve the flame retardancy of a methyl ethyl silicone rubber. The synthesis is shown in Figure 1.36.

When the content of the flame retardant was increased, the LOI of methyl ethyl silicone rubber composite increased gradually, which was 29.8% when 25% DTT was added. A flame-retarded methyl ethyl silicone rubber composite obtained UL-94 V-0 rating. In addition, the combustion time was reduced by 50.96%, which went from 520 s to 255 s. Furthermore, the total heat release was reduced by 26.25%, which went from 53.53 $MJ\,m^{-2}$ to 39.48 $MJ\,m^{-2}$.

TG results indicated that the pure methyl ethyl silicone rubber composite had excellent thermal stability and the DTT decomposed ahead of the methyl ethyl silicone rubber matrix to perform the flame-retarding effect better (113).

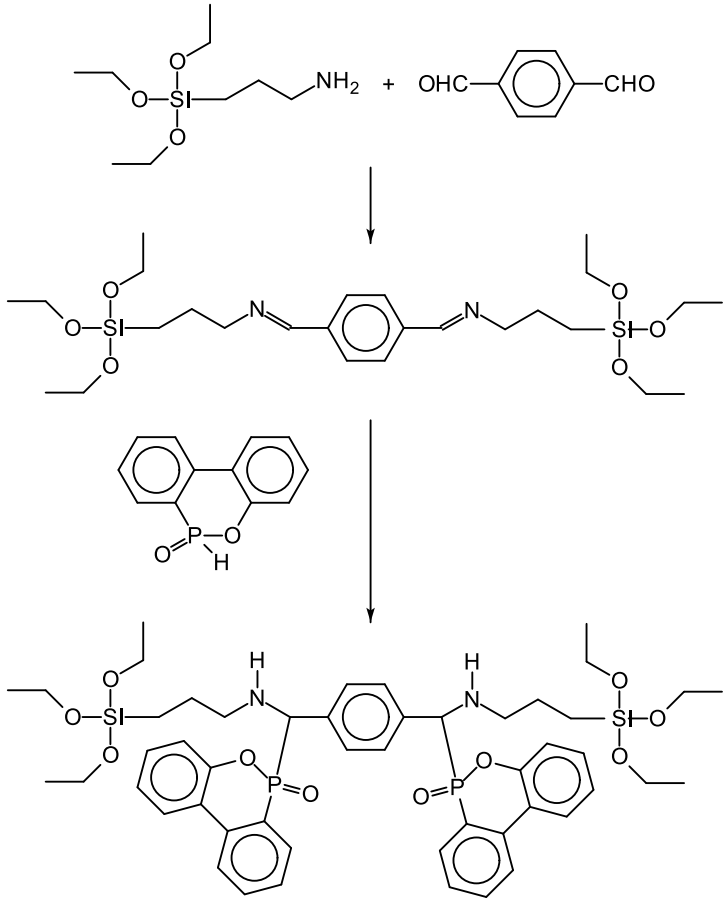

Figure 1.36 Synthesis of an intumescent flame retardant (113).

Hexophenoxy cyclotriphosphazene. To improve the flame retardancy of a methyl ethyl silicone rubber, the synergistic effect of an IFR system consisting of hexaphenoxycyclotriphosphazene and ammonium poly(phosphate) was investigated. Hexaphenoxycyclotriphosphazene is shown in Figure 1.37.

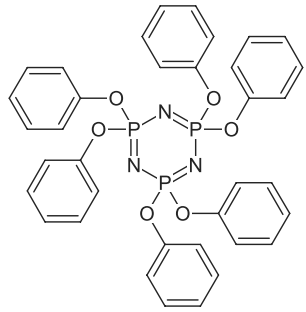

Figure 1.37 Hexaphenoxycyclotriphosphazene.

The results of the study showed that with a total loading of 30% of the IFR, the flame-retarded silicone rubber composite showed the highest LOI of 30.6% and a UL-94 rating of V-0 at a mass ratio of hexaphenoxycyclotriphosphazene and ammonium poly(phosphate) of 1:1 (114).

1.7.9.3 β-Cyclodextrin

The effects of β-cyclodextrin containing a silicone oligomer, as a synergistic agent, on the flame retardancy of PP polypropylene composites were studied. β-Cyclodextrin is shown in Figure 1.38.

The LOI values and UL-94 rating of several composites are shown in Table 1.7.

It was found that after a small amount of β-cyclodextrin containing a silicone oligomer partially replaced a charring-foaming agent in flame retardant, the LOI values of the composites were enhanced and they obtained a UL-94 V-0 rating. The system containing 6.25% of β-cyclodextrin containing a silicone oligomer presented the best flame retardancy in PP.

Also, the experimental results indicated that the combination of β-cyclodextrin and charring-foaming agent show synergistic effects

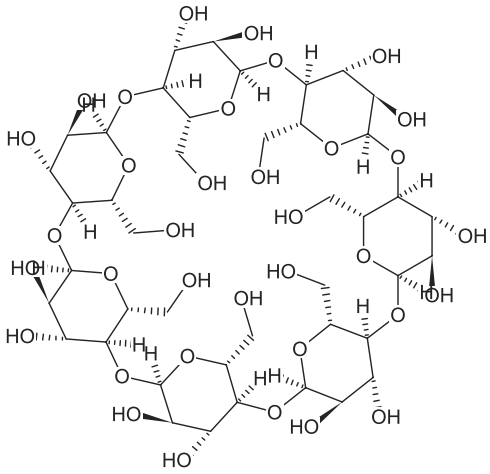

Figure 1.38 β-Cyclodextrin.

Table 1.7 LOI values and UL-94 rating of the composites (115).

IFR/[%]			LOI/[%]	UL-94/[%]
CDS	CFA	APP		
0	0	0	17.5	-
0.00	25.00	75	32.3	V-0
5.00	20.00	75	32.7	V-0
6.25	18.75	75	35.0	V-0
8.25	16.75	75	33.4	V-0
12.50	12.50	75	33.1	V-0
16.75	8.25	75	32.9	V-1
18.75	6.25	75	32.6	V-1
20.00	5.00	75	32.0	V-1

IFR: Intumescent flame retardant
CDS: β-Cyclodextrin containing a silicone oligomer
CFA: Charring-foaming agent, a triazine polymer
APP: Ammonium poly(phosphate)

in flame retardancy, char formation, and the mechanical properties of the composites (115).

1.7.9.4 Functionalized Expandable Graphite

Expandable graphite is typical of halogen-free IFR, which is an intrinsic graphite intercalation compound. It is a layered crystal consisting of sheets of carbon atoms tightly bound to each other.

An organic-inorganic hybrid IFR, i.e., functionalized expandable graphite, was synthesized (116). This material was used in silicone rubber composites.

The functionalized expandable graphite was prepared according to a process described in the literature (117):

Preparation 1–9: First, 20.0 *g* of expandable graphite, 6.2 *ml* $POCl_3$, and 500 *ml* 1,4-dioxane were put into a reactor equipped with a stirrer and condenser, and the reactor was then heated to 60°C and remained at that temperature for 3 *h*. Subsequently, 9.2 *g* pentaerythritol was charged into the reactor, followed by heating the reactor to 100°C. Then the reactor was maintained at 100°C for 6 *h* to obtain the crude product. After filtration and washing with 1,4-dioxane several times, the resultant product was dried under reduced pressure at 80°C for 12 *h* to get the functionalized expandable graphite.

It was shown that the functionalized expandable graphite can effectively reduce the flammable properties, including PHRR, total heat release, smoke production rate, total smoke release, and smoke factor (116). Compared with expandable graphite, functionalized expandable graphite can further enhance the flammable properties.

1.7.9.5 Phosphorus-Nitrogen-Silicone Grafted Graphene Oxide

Due to the poor dispersion in polymer matrix, graphene can hardly be used alone as a flame retardant additive for polymers (118, 119). A ternary graft product of silsesquioxane, graphene oxide and DOPO, c.f. Figure 7.6, with a structure of graphene oxide layers modified with the synergistic flame retardant multiple elements of phosphorus, nitrogen and silicon was synthesized (119).

This composite was used in combination with a traditional IFR to enhance the flame retardancy of PP. The experimental results show that the thermal and flame retardant properties of flame retardant

PP composites are significantly improved by introducing 5% of the composite as well as 20% IFR. The PHRR and total heat release of the flame retardant PP composite are reduced by 61.5% and 40.2%, respectively, compared to neat PP (119).

Based on the char layer observation and thermal analysis, the enhancement in flame retardancy was mainly attributed to the outstanding intumescent char layers with high strength and thermal stability formed under the synergistic effect of composite and the IFR. Besides, the introduced phosphorus, nitrogen and silicon hydrophilic groups do not show the negative effects on the surface hydrophobicity of flame retardant PP materials, which could broaden its scope of application (119).

1.7.10 Chitosan-Based Nanocoatings

Two types of low-cost and eco-friendly nanocoatings, i.e., chitosan/ammonium poly(phosphate) and chitosan/montmorillonite, were fabricated on silicone foams through a layer-by-layer assembly (120).

With seven bi-layers of chitosan/ammonium poly(phosphate) coatings, the LOI increases from 20.2% to 23.8%, the PHRR decreases by 27.6%, and the total smoke production decreases by 42%. In contrast, the fire hazard and the smoke release of chitosan/montmorillonite coated silicone foams were monotonously reduced (120).

1.7.11 Lignin-Based Silicone

The use of lignin as a filler for polymers to give composites provides both economic advantages and, in some cases, improved mechanical performance. The presence of lignin can also introduce certain advanced properties, including biodegradability, antimicrobial and antioxidant activity (121).

When lignin is compounded with hydride-functionalized silicones to give elastomeric and foam materials with improved thermal insulation, thermal stability, and flame retardancy are obtained (121).

In the absence of any additional inorganic flame retardant agent, a V-1 rating could be reached in the UL-94 test after a chemical post-treatment of the materials with NH_3 vapor to remove excess

SiH groups (which were identified as a culprit for excessive flammability). Furthermore, the fire resistance was improved to a V-0 rating by applying an additional thermal post-treatment at 220°C in air (121).

1.7.12 Silicone-Based Adhesive

A silicone-based elastomer filled with vinyl-silane treated aluminum hydroxide was used to replace a conventional PU-based adhesive to provide a flame retardant adhesive for plywood (122).

The shear strength and fire performance of such a silicone-based adhesive glued plywood were investigated and compared to those of the PU-based adhesive glued plywood. The shear strength of the silicone/plywood was about 63% lower than that of the PU/plywood at room temperature, but it was less sensitive to water. A 62% reduction was observed for the PU/plywood and a 30% reduction for the silcone/plywood after hot-water immersion at 63°C for 3 *h*.

The fire performance of plywood was assessed by a simulated match-flame ignition test (Mydrin test), lateral ignition and flame spread test, cone calorimetry, and thermocouple measurements (122). The Mydrin test (123) is a simulated match-flame ignition test that uses a butane burner compliant with a British Standard (BS 5438) (124).

With a higher burn-though resistance and thermal barrier efficiency, and lower flame spread and heat release rate, the silicone/plywood exhibited a superior fire resistance and reaction-to-fire performance and improved fire resistance as compared to the PU/plywood. The silicone adhesive generated an inorganic protective layer on the sample surface that visibly suppressed glowing and smoldering of the plywood during combustion.

The silicone adhesive was also combined and reinforced with cellulosic fabric or glass fabric to prepare plywood composites with improved fire performance. The use of cellulosic fabric or glass fabric in the composites, suppressed the delamination and the cracking of the composite plywood and promoted the formation of an effective thermal barrier during smoldering and flaming combustion. The silicone/glass fabric/plywood composite exhibited the most effective fire barrier with no crack formation, and the lowest heat release rate (122).

1.7.13 Nanofillers

The effects of three different nanofillers on the viscosity properties and fire behavior of a halogen-free flame retardant system were studied (125). These nanofillers are montmorillonite, sepiolite, and polyhedral oligomeric silsesquioxane. The original system, based on ethylene-acrylate copolymer, calcium carbonate, and a silicone elastomer, shows good flame retardant properties.

One of the nanofillers, MMT, significantly increases the viscosity above 250°C, resulting in reduced dripping and decreased heat release rate. The ash residue, however, is very brittle, indicating poor interactions between the MMT and other components of the system (125).

The second nanofiller, sepiolite, showed no improvement on the flame retardant properties of the system.

A reduced dripping is observed when a small amount of the third nanofiller, polyhedral oligomeric silsesquioxane (POSS), is incorporated into the system. In this case, high silica content on the surface indicates char formation originating from the POSS. However, an increased heat release is observed when POSS is used in the system (125).

1.8 Molybdenum Compounds

Graphene and molybdenum disulfide (MoS_2) are two well-known quasi-two-dimensional materials. A comparative survey of the complementary lattice dynamical and mechanical properties of graphene and MoS_2 has been presented in a review (126). This facilitates the study of graphene/MoS_2 heterostructures. Such hybrid heterostructures are expected to mitigate the negative properties of each individual constituent and have attracted intense academic and industrial research interest.

Sandwich-like melamine cyanurate/MoS_2 sheets as the hybrid flame retardants for poly(amide) 6 (PA6) have been described (126). The introduction of MoS_2 sheets function not only as a template to induce the formation of two-dimensional melamine cyanurate capping layers but also as a synergist to generate an integrated flame-retarding effect of hybrid sheets, as well as a high-performance smoke suppressor to reduce fire hazards of PA6 materials (126).

Also, a fire-blocking coating consisting of chitosan and molybdenum disulfide (MoS_2) could be deposited onto a flexible poly(urethane) foam by the layer-by-layer assembly technique (127).

MoS_2 and graphene sheets (GNS) were used as nanofillers to prepare PS composites by masterbatch melt blending (128).

The effect of MoS_2 and graphene sheets on the thermal stability, fire resistance and smoke suppression properties of the PS composites were studied. Cone test results indicated the PS/graphene sheets composites exhibited superior flame retardance over PS/MoS_2 composites. The results from TG showed that the addition of MoS_2 improved the thermal stability and char residues of the PS composites.

The main decomposition products of PS/MoS_2 and PS/graphene sheets composites were found to be aromatic compounds and alkenyl units which are similar to those of pure PS. However, less flammable gas products were released relative to pure PS, which further leads to the inhibition of smoke (128).

1.9 Graphenes

Graphene is an allotrope of carbon in the form of a single layer of atoms in a two-dimensional hexagonal lattice, in which one atom forms each vertex (129). It is the basic structural element of other allotropes, including graphite, charcoal, carbon nanotubes and fullerenes. It can also be considered as an indefinitely large aromatic molecule, the ultimate case of the family of flat polycyclic aromatic hydrocarbons.

The role of graphene in flame retardancy of polymeric materials has been reviewed (130, 131). Also, the properties of graphene-based nanomaterials have been reviewed with regard to cryo-mechanical properties, ballistic impact resistance, thermal conductivity, deicing/anti-icing behavior, self-cleaning, sensing properties, and flame retardant properties (132, 133).

1.9.1 Synergist for Intumescent Flame Retardants

The feasibility of using graphene as an effective synergist for IFR has been investigated (118).

The incorporation of graphene results in different responses of flame retardant/PP composites to small fire tests and burning under forced flaming conditions. The addition of graphene weakens the reaction of flame retardant PP to small flame. A lower loading of graphene is observed to improve the swelling of char, resulting in a better insulation of the char and a decrease in heat and smoke release (118).

Ammonium poly(phosphate) was modified by a cation exchange reaction with piperazine (134). Then, reduced graphene oxide nanosheets were attached to the surface of a modified flame retardant via hydrogen bonding interactions. Reduced graphene oxide is a form of graphene oxide that is processed by chemical, thermal and other methods in order to reduce the oxygen content. Methods of the reduction of graphene oxide have been detailed (135).

In a PP matrix, a good dispersion of graphene was observed (134). The dispersion state of the graphene showed an abnormal effect on the flammability results under small flame and fire behavior under forced flaming condition of IFR composites.

The well-dispersed graphene results in a significantly deteriorated LOI and UL-94 rating. The graphene with a good dispersion is adverse to flammability results, which is contrary to the widely-acknowledged flame retardant mechanisms. A low content of well-dispersed graphene exhibits a higher reduction effect on the heat release than that of a poorly dispersed counterpart (134).

A halogen-free intumescent flame retardant EVA copolymer system containing organic MMT and graphene nanosheets was fabricated (136). Ammonium poly(phosphate) was used as intumescent flame retardant. In order to improve the compatibility between the intumescent flame retardant and the EVA matrix, TPU was chosen as carbonization agent. This system showed a good dispersion structure and an enhanced thermal-oxidative resistance at high temperature.

In a sample with 100 g EVA, 19 g ammonium poly(phosphate), 6.5 g TPU, and 1 g graphene nanosheets, the amount of residual char is increased to 12.7% at 700°C, as was shown with TG. This composite exhibited the best flame retardancy with the lowest PHRR value of 529.58 $kW\,m^{-2}$, and the highest LOI value of 24.8%. This property is attributed to the formation of complete and compact protective char layer (136).

Tannic acid, a natural phenolic compound abundant in many plants, exhibits low flammability and good absorbility because of its multidentate properties (137). Tannic acid is shown in Figure 1.39.

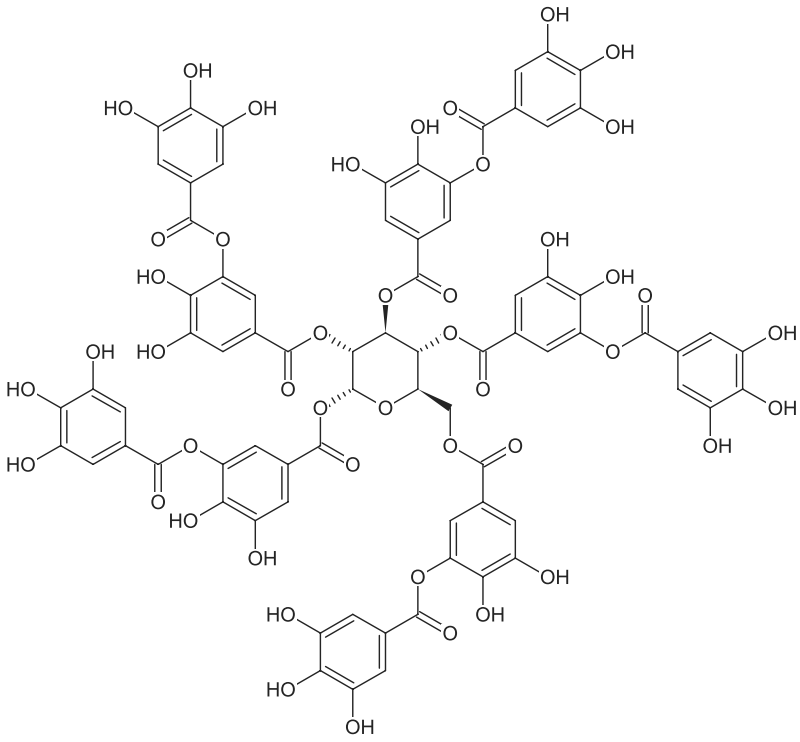

Figure 1.39 Tannic acid.

An IFR system was developed consisting of ammonium poly(phosphate) tannic acid functionalized graphene. This is a synergistic flame retardant and smoke suppressant for natural rubber due to the dual flame retardant functions of each component. The properties of such compositions are shown in Table 1.8.

This system is of interest to a variety of fields because of its distinct flame retardant and relatively good mechanical properties in comparison to a traditional IFR system (137).

Table 1.8 Properties of tannic acid compositions (137).

NR	APP /[*phr*]	GE	TA	LOI /[%]	UL-94
100	–	–	–	19.5	NC
100	20	–	–	20.5	NC
100	14.5	3.67	1.83	21.5	NC
100	40	–	–	24.5	V-2
100	29.1	7.27	3.63	25.1	V-1
100	60	–	–	30.5	V-0
100	43.6	10.93	5.47	32.1	V-0

NR: Natural rubber
APP: Ammonium poly(phosphate)
GE: Graphene
TA: Tannic acid

1.9.2 Electrochemical Preparation

A multifunctional flame retardant with phosphazene rings has been designed to simultaneously exfoliate and functionalize graphene (138). Due to the antioxidant function of flame retardant, the electrochemically exfoliated graphene sheets exhibit high quality and low defect (C/O=10.4).

The electrochemical exfoliation can acquire large quantities of graphene sheets with a high yield of more than 85% and a higher quality (C/O ratio of 17.2) than those of reduced graphene oxide prepared by a chemical method (139).

Hex(4-carboxylphenoxy)cyclotriphosphazene was used as flame retardant. The synthesis of this compound has been detailed (140). Hex(4-carboxylphenoxy)cyclotriphosphazene is shown in Figure 1.40.

The preparation of electrochemically functionalized graphene runs as follows (138):

Preparation 1–10: Graphene sheets were exfoliated from a graphite slice in an anode with voltage of 10 V. A copper rod as a cathode was placed at 1 cm spacing and kept parallel with graphite slice. The electrolyte was prepared by dissolving 0.5 g hex(4-carboxylphenoxy)cyclotriphosphazene in 100 ml of deionized water and the pH value was adjusted to 8 by 1 M NaOH solution. The exfoliation was conducted for 6 h

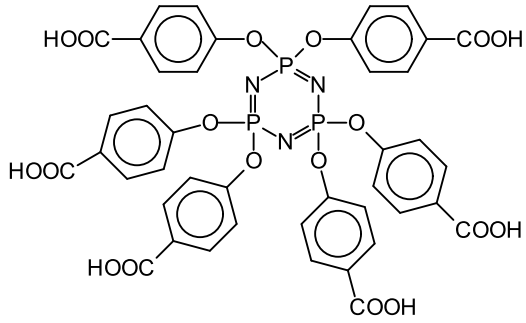

Figure 1.40 Hex(4-carboxylphenoxy)cyclotriphosphazene.

under ice. The suspension was collected through vacuum filtration and thoroughly washed with deionized water to remove unadsorbed hex(4-carboxylphenoxy)cyclotriphosphazene. The filter cakes were redispersed in deionized water by a mild sonication for 30 *min* and then centrifuged at 1200 *rpm* for 10 *min*. The obtained suspension solution was collected by vacuum filtration and designated as FGNS.

The obtained graphene was noncovalently modified to form flame retardant functionalized graphene sheets. Then, the functionalized graphene sheets were applied to improve the fire safety and the mechanical performance of TPU. Compared to pure sample, the PHRR and total heat release of TPU composites with the addition of 4 *wt*% functionalized graphene sheets are significantly decreased by 46.3% and 20.2%, respectively (138).

The elongation at break and tensile strength of TPU are enhanced by 11.6% and 59.9%, respectively, with the addition of 2.0% functionalized graphene sheets. The significant enhancement in fire safety is due to the conjunct effects of functionalized graphene sheets and the flame retardant.

Lower defect of graphene provides more stable layer structure, thus functionalized graphene sheets play a remarkable barrier action to confine the escape of degradation products. The coated flame retardant is conducive to form compact and robust char residue by reacting with degradation products. In addition, the flame retardant facilitates the load transfer to the robust graphene sheets with improved interface interaction. Through the electrochemical

route, designing a multifunctional flame retardant to simultaneously exfoliate and modify graphene provides a new possibility for the industrialized application of graphene (138).

1.9.3 Phosphaphenanthrene Graphene Hybrid Flame Retardant

A hybrid flame retardant was synthesized by combining graphene oxide with a long-chain phosphaphenanthrene, DOPO-*g*-(2,3-epoxypropoxy) propyltrimethoxysilane (141). This material was fabricated via surface grafting and was used in an epoxy resin laminate.

The phosphaphenanthrene greatly decreased the release rate of decomposed volatiles from the resin, as well as minimized the release of oxygen and the heat of combustion.

So, such a hybrid flame retardant can overcome the shortcomings of early acid-catalyzed degradation effects caused by conventional flame retardants that contain phosphorus. A satisfactory flame retardance was achieved with a UL-94 V-0 rating with only 4% addition of the hybrid flame retardant to the epoxy resin laminate.

Due to the long-chain and bulky phosphaphenanthrene groups, the interlayer attractive forces of the modified graphene oxide were effectively weakened, thus favoring the exfoliation and the dispersion of the graphene sheets.

The incorporation of the flame retardant slightly enhanced the mechanical properties of the polymer composites, rather than deteriorating them (141).

1.9.4 Phosphaphenanthrene Graphene Copolymer

A copolymer containing a methacryloisobutyl polyhedral oligomeric silsesquioxane, glycidyl methacrylate, bis-9,10-dihydro-9-oxa-10-phosphaphenanthrene-10-oxide methacrylate and a functionalized graphene oxide was synthesized by a one-step grafting reaction to create a hybrid flame retardant (142). The synthesis of this material is shown in Figure 1.41.

Flame retardant epoxy resin composites were prepared by adding various amounts of this composite to the thermal curing epoxy resin of diglycidyl ether of bisphenol A. The thermal properties of the epoxy composites were remarkably enhanced by adding this flame

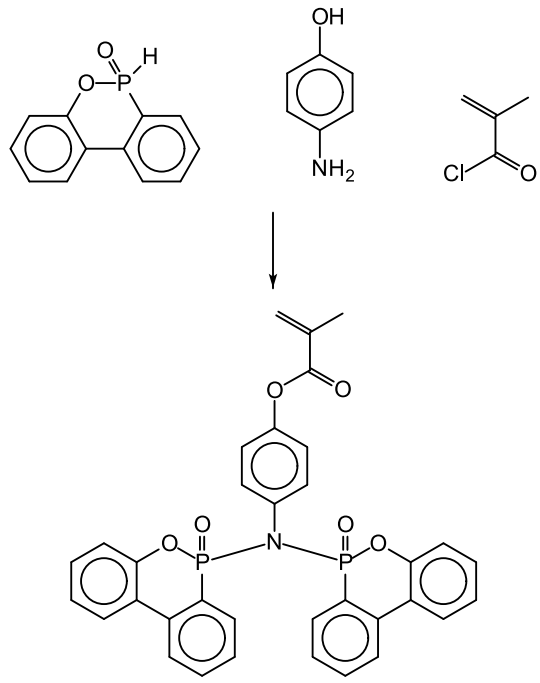

Figure 1.41 Synthesis of bis-9,10-dihydro-9-oxa-10-phosphaphenanthrene-10-oxide methacrylate (142).

retardant. Also, the residual char of the epoxy resin increased greatly.

With the incorporation of 4% of this material, the LOI value was enhanced to 31.1% and an UL-94 V-0 rating was achieved. In addition, the mechanical strength of the epoxy resin was improved (142).

1.9.5 Bio-Based Polyphosphonate and Modified Graphene Oxide

Superior flame retardant PLA composites were prepared using a bio-based polyphosphonate and a poly(ethylene imine)-modified graphene oxide as a flame retardant. The structure of this material is shown in Figure 1.42.

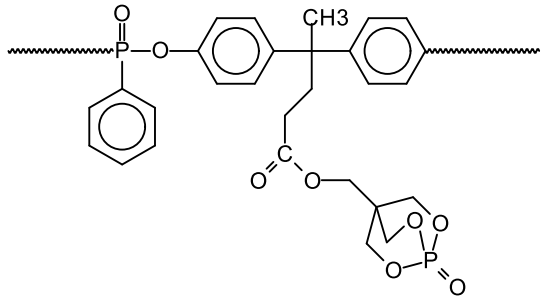

Figure 1.42 Structure of bio-based polyphosphonate (143).

With 2.4% of bio-based polyphosphonate and 0.6% of poly(ethylene imine)-modified graphene oxide in the polymer matrix, the prepared PLA composites can achieve the UL-94 V-0 grade and a LOI value of 36.0 (143).

The analysis of the residual char and pyrolytic products showed that the conjunction of a gas-phase and condensed-phase mechanism contributes to the good flame retardant performance.

In addition, the tensile toughness of PLA was enhanced. The PLA composite with 2.1% bio-based polyphosphonate and 0.9% poly(ethylene imine)-modified graphene oxide displayed an elongation at break of 13.1% and maintained a tensile strength of 39.1 *MPa* (143).

1.9.6 Black Phosphorene Graphene Composite

Phosphorene is a two-dimensional material and allotrope of phosphorus (144). Phosphorene can be viewed as a single layer of black phosphorus, much in the same way that graphene is a single layer of graphite. Phosphorene is believed to be a strong competitor of graphene because, in contrast to graphene, phosphorene has a band gap (145). Phosphorene was first isolated in 2014 by a mechanical exfoliation process (144).

Black phosphorene has outstanding flame retardant properties, however, it causes the mechanical degradation of waterborne PU (146). In order to solve this problem, the graphene has been introduced to fabricate a black phosphorene/graphene composite material using a high-pressure nano-homogenizer machine.

The results of a structure characterization show that the black phosphorene/graphene composite material can distribute uniformly into the waterborne PU. The addition of black phosphorene/-graphene significantly improves the residues of waterborne PU in both TG analysis (5.64%) and cone calorimeter test (12.50%), which indicates that the black phosphorene/graphene can effectively restrict the degradation of waterborne PU under high temperature (146).

The cone calorimeter test indicates that black phosphorene/G/waterborne PU has a lower peak release rate decreased by 48.18% and a total heat release decreased by 38.63%, than that of the pure waterborne PU.

The Young's modulus of the black phosphorene/graphene/waterborne PU has an increase of seven times more than that of the black phosphorene/waterborne PU, which indicates that the addition of graphene can effectively improve the mechanical properties of black phosphorene/waterborne PU (146).

1.9.7 Waste Deoxyribonucleic Acid

Waste deoxyribonucleic acid from the fishing industry was used as a sustainable source of phosphorus and nitrogen to functionalize graphene nanomaterials (147).

Waste-derived deoxyribonucleic acid was employed as a green modifier in a ball milling process. This method is capable

of producing the deoxyribonucleic acid functionalized graphene nanoplatelets from graphite with a high production yield, high oxygen, nitrogen and phosphorus contents, and a high water dispersion concentration.

Exfoliated nanoplatelets were obtained that mostly consisted of layers with a thickness <9 *nm* and a lateral size of 300 *nm* to 600 *nm* with a Brunauer-Emmett-Teller specific surface area of around 80 $m^2 g^{-1}$.

The deoxyribonucleic acid functionalized graphene was found to be an efficient and sustainable flame retardant for a wide range of polymer matrices, including epoxy resin, poly(vinyl alcohol) (PVA), and PS nanocomposites (147).

A multilayer char residue consisting of a compact layer and a porous layer was found to be the dominant mechanism in fire extinguishing. The combination of deoxyribonucleic acid and graphene can result in manufacturing value-added green flame retardants from indirect reuse of fish waste, which can be suitable for high performance polymer nanocomposites (147).

1.9.8 Poly(ionic liquid) and Graphene

Graphene and poly(ionic liquid) modified poly(urethane) (PU) sponges were prepared (148).

As ionic liquid monomer, 1-vinyl-3-ethyl imidazolium tetrafluoroborate and as comonomer, *N*,*N*′-methylene bisacrylamide was used. These monomers were polymerized with the aid of 2,2´-azobisisobutyronitrile.

The materials were prepared by the direct dip coating of graphene and ionic liquid monomers onto a PU sponge followed by the polymerization of ionic liquid monomers (148). The polymerization of the ionic monomer is shown in Figure 1.43.

With a content of 1.5% graphene in the ionic liquid, the LOI of PU/poly(ionic liquid)/graphene was 26.1%, whereas the neat PU sponge showed an LOI of only 17.9%. The horizontal flame test results indicate that poly(ionic liquid)/graphene prevented horizontal flame spread and eliminated melt dripping.

In comparison to a neat PU sponge, the PHRR of PU/poly(ionic liquid)/graphene decreased about 22.0%. These improvements on flame retardancy might have been due to a hybrid flame retardant

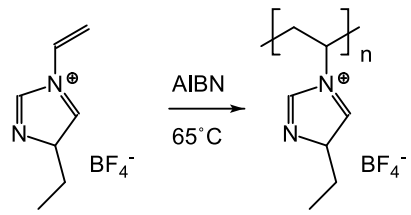

Figure 1.43 Polymerization of the ionic monomer (148).

originating from graphene, which acted as carbon source, and the poly(ionic liquid), which contained the flame retardant elements (148).

1.9.9 Copper Decorated Graphene

To explore the synergism and mechanism of diverse forms of copper decorated graphene on the improvement of the fireproof efficiency of an ammonium poly(phosphate)-based PA-cured epoxy resin, Cu(0) and Cu(II) decorated graphene hybrids were prepared through facile methods and used as synergists in epoxy resin/ammonium poly(phosphate) system (149).

Cu^{2+}-graphene oxide exhibits better synergistic effect with ammonium poly(phosphate) than Cu-reduced graphene oxide and CuO-graphene nanosheets on reducing heat release of epoxy resin.

This is because it is easier for Cu^{2+} than Cu and CuO to go through various oxidation states and intermediates, which catalyze epoxy resin/ammonium poly(phosphate) system rapid formation of protective char layer containing crosslinked junctions of organic phosphates and Cu(II) salts.

A CuO-graphene nanosheet exhibits better smoke suppression and harmful gases reduction in an epoxy resin/ammonium poly(phosphate) matrix, such as aliphatic hydrocarbons, aromatic compounds and CO, due to its better conversion of CO to CO_2 through a redox cycle (149).

1.9.9.1 Zeolitic Imidazolate Modified Graphene

A hybrid material of zeolitic imidazolate frameworks-8 (ZIF-8) loaded surface of graphene was synthesized (150). The ZIF-8 can be prepared as follows:

Preparation 1–11: First, 0.58 *g* of $Zn(NO_3)2 \times 6H_2O$ was dissolved in 100 *ml* methanol solution, and 1.30 *g* 2-methylimidazole was dissolved in 100 *ml* methanol solution. Then, the two kinds of these solutions were poured into a beaker, and the mixture was stirred by a magnetic stirrer for 2 *h*. Subsequently, the solution was washed 3 times by centrifugal washing and then washed once with deionized water. Finally, the product was placed in a vacuum freeze dryer for 4 *h*, and the ZIF-8 nanomaterial was obtained.

The ZIF-8 reduced graphene oxide was added into an epoxy resin, and the flame retardancy and the smoke suppression of these composites were studied. Compared with pure epoxy resin, the PHRR and the total heat release of the epoxy resin composites were reduced remarkably, and their LOI and UL-94 vertical burning rating were also improved. In addition, their smoke production rate and total smoke production were decreased drastically. The improved flame retardancy and smoke suppression were mainly attributed to the physical barrier effect of graphene (150).

In another study, zeolitic imidazolate frameworks were prepared and used for rigid poly(urethane) foams (RPUFs) (151). Here also, the combustion test results showed that the heat and smoke production of the composite containing zeolitic imidazolate frameworks were obviously reduced.

1.9.10 Lignin-Modified Carbon Nanotube Graphene

In order to reduce the fire hazards of lignocellulosic materials, thin films containing graphene nanoplatelets and multiwalled carbon nanotubes (MWCNTs) pre-adsorbed with alkali lignin were deposited by a Mayer rod process (152).

A Mayer rod is a metal bar with a wire wrapped around the outside that is used to draw a solution over a substrate surface (153). The diameter of the wire wrapped around the bar determines the thickness of the wet coating film.

Lightweight and highly flexible papers with increased gas impermeability were obtained by coating a protective layer of carbon nanomaterials in a randomly oriented and overlapped network structure (152).

The thermal and flammability properties of papers containing as low as 4% carbon nanomaterials exhibited a self-extinguishing behavior and yielded an up to 83.5% reduction in weight loss and an 87.7% reduction of burning area, compared to the blank papers. The maximum burning temperature, as measured by infrared pyrometry, decreased from 834°C to 705°C in the presence of flame retardants.

In addition, papers coated with composites of graphene nanoplatelets and MWCNTs pre-adsorbed with lignin showed an enhanced thermal stability and a superior fire resistance compared to samples treated with either component alone.

These flame retardant properties can be attributed to the synergistic effects between the graphene nanoplatelets, MWCNTs and lignin that enhance the physical barrier characteristics, the formation of char and the thermal management of the material (152).

1.9.11 κ-Carrageenan Flame Retardant Microspheres

Intumescent flame retardant microspheres were prepared by the technique of inverse emulsion polymerization (154). As carbon source κ-carrageenan was used, as acid source ammonium poly(phosphate) was used, with the use of κ-carrageenan as carbon source, and as gas source melamine. A benzoic acid functionalized graphene was synthesized as a synergist.

A *four-source flame retardant system* was constructed with κ-carrageenan and the benzoic acid functionalized graphene. This composition was blended with a waterborne epoxy resin to prepare flame retardant coatings.

The LOI values increased from 19.7% for the waterborne epoxy resin to 28.7% for the epoxy resin with 20% flame retardant. The LOI value reached 29.8% for an epoxy sample with 18% of the intumescent flame retardant and 2% benzoic acid functionalized graphene. Also, here the UL-94 test reached the V-0 level (154).

1.9.12 *Phenethyl-Bridged DOPO and Graphene Nanosheets*

A phenethyl-bridged DOPO derivative (DiDOPO) was combined with graphene nanosheets in an epoxy resin to improve its flame retardancy (155). The phenethyl-bridged DOPO is shown in Figure 1.44.

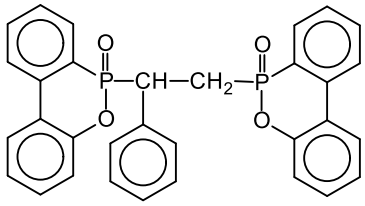

Figure 1.44 Phenethyl-bridged DOPO (155).

The DiDOPO and the graphene nanosheets were incorporated into an epoxy resin based on diglycidyl ether of bisphenol A and 2-ethyl-4-methyl-imidazole.

The introduction of only 1.5% DiDOPO and 1.5% graphene nanosheets in the epoxy resin increased the LOI from 21.8% to 32.2%, so an UL-94 V-0 rating was obtained. TG revealed that char yield rose in the presence of graphene nanosheets to form thermally stable carbonaceous char.

The evaluation of the flame retardant effect by cone calorimetry demonstrated that the graphene nanosheets improved the protective-barrier effect of fire residue of the flame-retarded epoxy resin (155).

1.9.13 *Graphene Nanoplatelets*

Graphene nanoplatelets were successfully prepared from graphite powder by simple and scalable thermal shock combined with ball milling methods (156).

In the first step, a thermal treatment of the graphite powder occurred. Typically, graphite powder was pretreated by being added to the mixture of 30% H_2O_2 and 98% H_2SO_4 in a ratio of 1:1.5 by volume at 20°C for 2 *h*. The solid was filtered and washed with distilled water to get a pH of 7.

The so obtained solid was dried at 80°C for 24 *h*. This solid was thermal shocked by using a microwave at 800 *W* for 60 *s*. The solid was subjected to the pretreatment and thermal shock once again by the same procedure described above to obtain the expanded graphite.

In the second step, the expanded graphite was ground by using NaCl salt as discussed in a study (157). A 5 *g* expanded graphite sample was mixed with NaCl salt in a molar ratio of 3:1. A planetary ball milling machine (Pulverisette 5) with ball to powder weight ratio of 20:1 was used to grind the obtained mixture with a rotational speed of 350 *rpm* for 2 *h* in argon inert gas medium. NaCl salt was removed from the obtained powder by distilled water using an ultrasonic bath. The final sample was centrifuged and dried at 80°C under vacuum to get the final sample.

Field-emission scanning electron microscopy experiments clearly show the exfoliation of expanded graphite to obtain graphene nanoplatelets with a monolayer or a few layers in its morphology. The exfoliation of material was further demonstrated with the increase of specific surface area by the Brunauer-Emmett-Teller (158) method.

The graphene nanoplatelets were combined with the conventional flame retardants aluminum trihydroxide and zinc borate to prepare a flame retardant PC plastic and chlorine-sulfonated PE rubber (156).

A mixture of graphene nanoplatelets, aluminum trihydroxide, and/or zinc borate was melt-compounded with a PC plastic or chlorine-sulfonated PE rubber in a Brabender closed mixing machine. The PC plastic or the chlorine-sulfonated PE rubber was melted in the first 4 *min* with a rotor speed of 50 *rpm* at 200°C (PC) and 85°C (chlorine-sulfonated PE). The above mixture with different percentages of graphene nanoplatelets, aluminum trihydroxide, and/or zinc borate was then added to the compound with PC plastic or chlorine-sulfonated PE rubber for 10 *min*. The compounded sample was hot-pressed in a Brabender molding machine at 210°C (PC) and 95°C (chlorine-sulfonated PE) for 7 *min* to obtain the sample.

The effectiveness of graphene nanoplatelets in combination with aluminum trihydroxide and/or zinc borate is shown in Table 1.9.

As can be seen from Table 1.9, the prepared composites showed an improvement of the flame resistance properties with V-0 level

Table 1.9 Effectiveness of graphene nanoplatelets (156).

Polymer	Filler	Content/[%]			LOI/[%]	UL-94
PC	–	0.0			21.1	V-2
PC	Graphite	5.0				V-2
PC	Gnps	5.0				V-1
PC		2.0				V-1
PC		1.5				V-0
PC		1.0				V-0
PC		0.5				V-2
PC	ATH	25.0				V-1
PC		20.0				V-2
PC		15.0				V-2
PC	ZB	15.0				V-1
PC		10.0				V-2
PC	Gnps-ATH	1.5	25.0		22.9	V-0
PC	Gnps-ZB	1.5	15.0		24.0	V-0
PC	Gnps-ATH-ZB	1.5	25.0	15.0	29.7	V-0
CSPE	CSPE	0.0			22.1	V-2
CSPE	Gnps	1.0				V-1
CSPE	ZB	15.0				V-1
CSPE	Gnps-ZB	1.0	15.0		23.1	V-0
CSPE	Gnps-ZB	1.5	15.0		28.6	V-0

PC:	Poly(carbonate)
CSPE:	Chlorine-sulfonated poly(ethylene)
Cnps:	Graphene nanoplatelets
ATH:	Aluminum trihydroxide
ZB:	Zinc borate

according to the UL-94 test method. Furthermore, the LOI value was higher than 27 (156).

1.9.13.1 Condensate and Graphene Nanoplatelets

A flame retardant composition has been described that contains graphene nanoplatelets and a condensation product of a sulfonated aromatic compound with formaldehyde and urea (159).

The condensation product of a sulfonated aromatic compound with formaldehyde, and optionally urea, is typically a polymer with a weight average molecular weight (M_w) up to 10 *kDalton*.

Such condensation products are usually commercially available, for example, under the brand name Setamol® WS from BASF AG.

A dispersion of the graphene nanoplatelets in water can be prepared with a process that consists of the expansion of intercalated graphite flakes having a lateral size 500 μm by exposing them to a temperature of at least 1300°C for a time of less than 1 *s* and it runs as follows (159):

1. The expanded graphite thus obtained is dispersed in water at a concentration in the range of 1% to 40% in the presence of a dispersing agent which is a condensation product of a sulfonated aromatic compound with formaldehyde in a weight-to-weight ratio from 1:15 to 4:1 of the weight of the graphite,
2. The water dispersion obtained in the first step is submitted to an ultrasound treatment with an energy level in the range of 100 to 2000 *W* for a time lasting between 1 *h* and 100 *h*.

1.9.13.2 Aluminated Graphene Nanoplatelets

Substantial amounts of aluminum can be incorporated into graphene nanoplatelets by ball milling graphite in the presence of solid aluminum beads (160). The nanoplatelets contain a considerable amount of aluminum of 30.9% and display a good dispersibility in various solvents, including water.

In the case of composite films from aqueous aluminated graphene nanoplatelets with PVA in a ratio of 1 to 4 it was shown that the aluminated graphene nanoplatelets serve as an outstanding flame re-

tardant that operates by both chemical (condensation) and physical (cooling and blocking) mechanisms (160).

1.9.14 Aerogels

An aerogel is a gel comprised of a microporous solid in which the dispersed phase is a gas (161). Aerogels exhibit versatile unique properties, such as an extremely high porosity, quite low apparent density, and a considerably high surface area, which enable them to be attractive materials for applications in chemical sensors, chemical adsorbents, catalytic carriers, and space exploration fields.

Poly(imide) (PI) composite aerogels with enhanced flame retardant performance have been fabricated with the addition of environmentally friendly flame retardant additives, i.e., graphene and montmorillonite, via an eco-friendly freeze-drying method followed by a thermal imidization process.

Due to the strong interaction between the two components, a graphene oxide/MMT hybrid can be synergistically dispersed in water, providing a good dispersibility in a PI matrix. So, such composite aerogels have enhanced mechanical, thermal and flame retardant properties (161).

1.9.14.1 Alumina Oxide Graphene Nanoflakes

Aluminum oxide (Al_2O_3) nanoflakes were decorated on the surface of graphene nanosheets by a hydrothermal method (162). The alumina nanoflake-coated graphene nanohybrids were incorporated into a PP matrix by a masterbatch-based melt mixing method.

The effects of alumina-graphene nanohybrid on the thermal stability and the combustion behavior of PP were investigated. More char residue is left for PP composite containing the alumina-graphene nanohybrid. The PHRR of pure PP is greatly decreased by this nanohybrid, with a reduction of 30.6%. So, the fire safety of PP is considerably enhanced (162).

1.9.14.2 Ternary Hybrid Graphene Nanoflakes

A ternary hybrid nanoflake based on graphene oxide, phenylphosphinic acid and a nano metal-organic framework (nano zeolitic

imidazolate frameworks) particles has been designed and synthesized via a simple two-step strategy (163). Phenylphosphinic acid is shown in Figure 1.45.

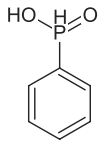

Figure 1.45 Phenylphosphinic acid.

The ternary hybrid nanoflake material shows a high thermal stability and a good compatibility with PLA matrix. When ternary hybrid nanoflakes are added to PLA, the tensile strength and toughness of the PLA-4 with 2.0% of ternary hybrid nanoflakes reach 44.1 *MPa* and 86.0 *MPa* compared with 30.0 *MPa* and 12.8 *MPa* of pure PLA owing to the good dispersion of ternary hybrid nanoflakes in PLA matrix and their reinforcing effects. The incorporation of ternary hybrid nanoflake also dramatically enhances the flame retardancy of PLA and the PHRR of PLA-4 with 2.0% of ternary hybrid nanoflake achieves about 316.2 $W\,g^{-1}$, which is decreased by 39.5% relative to 523.0 $W\,g^{-1}$ of pure PLA, respectively. The LOI of PLA-4 is 27.0%, increasing about 31.7% compared to 20.5% of pure PLA.

Meanwhile, the heat release rate and total heat release in the cone calorimeter test curves for the PLA nanocomposites have also been evidently reduced.

The TG-IR method was applied to characterize the pyrolysis gaseous products. The volatile components are suppressed due to the addition of ternary hybrid nanoflakes. The SEM, Raman spectroscopy and XPS results of the char residues show that a protective graphitized char layer plays a major role in improving the flame retardancy. This occurs mainly because of the catalytic and crosslinking effects of graphene oxide, nano zeolitic imidazolate frameworks and phenylphosphinic acid during combustion of the PLA nanocomposites (163).

1.9.15 Poly(etherimide) Membranes

Poly(ether imide) (PEI) membranes doped with different amounts (1% to 5%) of graphene oxide were prepared through a solution casting method (164). The effect of the incorporation of the graphene oxide on the mechanical and flame retardant properties was investigated by X-ray diffraction (XRD), FTIR, and SEM.

The results showed that the addition of 5% graphene oxide into the membranes caused a 30% improvement in the tensile strength and a significant increase in the glass transition temperature. The flame retardant properties were improved when the amount of graphene oxide in the PEI membrane was increased (164).

1.9.16 Chitosan-Graphene Coatings

The layer-by-layer technique can be adopted for the construction of multilayers encompassing chitosan and graphene oxide platelets that are capable of improving the flame retardant properties of open cell PU foams (165). The layer-by-layer assembly follows a linear growth regime as evaluated by infrared spectroscopy and yields a multilayer structure where graphene oxide platelets are embedded within a chitosan continuous matrix.

Three and six bi-layers can efficiently coat the complex 3D structure of the foam and substantially improve its flame retardant properties. Three bi-layers only add 10% to the original mass and can suppress the melt dripping during flammability and reduce both the peak of heat release rate by 54% and the total smoke released by 59% in forced combustion tests (165).

Unprecedented among other layer-by-layer assemblies employed for flame retardant purposes, the deposition of six bi-layers is capable of slowing down the release of combustible volatile to the limits of non-ignitability, thus preventing ignition in half of the specimens during cone calorimetry tests. This has been ascribed to the formation of a protective coating where the thermally stable char produced by chitosan serves as a continuous matrix embedding graphene oxide platelets, which control volatile release while mechanically sustaining the PU foam structure (165).

1.9.17 Polymeric Flame Retardant Functionalized Graphene

Fire hazards in polymer-based thermally conductive composites that are used in electronic equipment are a significant but often overlooked risk (166).

By incorporating a flame retardant functionalized graphene into polymer-based thermally conductive composites both their flame resistance and their thermal conductivity can be improved.

A flame retardant functionalized graphene was prepared by covalently grafting a poly(phosphoramide) oligomer onto the surface of graphene, which was then introduced *in situ* into epoxy resin/Al_2O_3 composites.

The incorporation of flame retardant functionalized graphene not only increased the thermal conduction paths by weakening the settlement of microparticles, but also reduced the interfacial thermal resistance by enhancing interfacial interactions, both of which resulted in an enhancement of the thermal conductivity of the ternary composites.

The resultant graphene composite exhibited a superior flame-retarding ability with dramatic decreases of the high PHRR of 53%, the total heat release of 37%, and the total smoke production of 57% when compared to a pure epoxy resin. In addition, a synergistic flame-retarding effect was found in the ternary composite.

The enhancement in the flame retardancy was mainly attributed to the catalytic charring effect of flame retardant functionalized graphene and the template effect of Al_2O_3, both of which resulted in the formation of a high strength, thermally stable protective layer in the condensed phase that is able to retard the permeation of heat and volatile degradation products during combustion, slow down the heat release rate and protect the underlying polymer (166).

1.9.18 Graphene Oxide Compositions

1.9.18.1 Synthesis of Graphene Oxide

A widely applied method for the synthesis of graphene oxide was developed by Hummers and Offeman in 1958 (Hummers method) (167).

Here, the oxidation of graphite was achieved by harsh treatment of one equal weight of graphite powders in a concentrated H_2SO_4

solution containing three equal weights of $KMnO_4$ and 0.5 equal weight of $NaNO_3$. The Hummers method has at least three important advantages over previous techniques (168):

1. The reaction can be completed within a few hours.
2. $KClO_3$ was replaced by $KMnO_4$ to improve the reaction safety, avoiding the evolution of explosive ClO_2.
3. The use of $NaNO_3$ instead of fuming HNO_3 eliminates the formation of acid fog.

However, the oxidation procedure releases toxic gasses, such as NO_2 and N_2O_4, and the residual Na^+ and NO^{3-} ions are difficult to remove from the wastewater formed in the course of synthesis.

Recently, the process of etching the basal planes of highly ordered pyrolytic graphite was studied with a hot mixture of H_2SO_4 and HNO_3 (169). Here, the graphene layers of highly ordered pyrolytic graphite were effectively cut and exfoliated after a long-term treatment.

An improved Hummers method without using $NaNO_3$ can produce graphene oxide nearly the same as that prepared by conventional Hummers method (168). This modification does not decrease the yield of product, eliminating the evolution of the toxic gases NO_2 or N_2O_4 and simplifying the disposal of wastewater because of the missing Na^+ and NO^{3-} ions.

Also, a method was developed of post-treating the wastewater collected from the systems of synthesizing and purifying graphene oxide. The content of Mn^{2+}ions in the purified wastewater was measured to be lower than the guideline value for drinking water (168).

Also, an improved $NaNO_3$-free Hummers method by partly replacing $KMnO_4$ with K_2FeO_4 and controlling the amount of concentrated sulfuric acid has been developed (170).

When compared to the existing $NaNO_3$-free Hummers methods, this improved routine greatly reduces the reactant consumption while keeping a high yield. The obtained graphene oxide was characterized by various techniques. The so derived graphene aerogel was demonstrated for use as high-performance supercapacitor electrodes. This improved synthesis shows good prospects for scalable production and applications of graphene oxide and its derivatives (170).

1.9.18.2 Phosphorus-Modified Graphene Oxide

Phosphorus acid (H_3PO_2) was used as reducing agent to prepare a phosphorus-modified graphene oxide. The preparation of phosphorus-modified graphene oxide runs as follows (171):

Preparation 1–12: First, 0.5 *g* of graphene oxide was mixed with 500 *ml* distilled water and ultrasonically treated for 1 *h*. Then the graphene oxide solution and 10.0 *g* of H_3PO_2 were mixed in a three-necked flask. The mixture was stirred for 24 *h* at 90°C. The mixture was centrifuged and washed with distilled water until a pH of 7 was reached. The precipitate after centrifugation was freeze-dried and a phosphorus-modified graphene oxide was obtained.

This material was added into an epoxy resin (EP) treated with ammonium poly(phosphate). As the curing reagent for the EP resin 1,3-cyclohexanediylbis(methenamine) was used (171).

Ammonium poly(phosphate) is a commercially available flame retardant that is always used for the flame retardancy of a polymer. With its good flame retardant properties, ammonium poly(phosphate) is used in flame retardant EP compositions (172–175).

The thermal stability, flame resistance, morphology of the residue char layer and impact fracture, and mechanical properties of the composites' materials were investigated (171).

The results of these tests showed that the filling of the phosphorus-modified graphene oxide can improve the mechanical properties of the EP composites. When the phosphorus-modified graphene oxide content of the EP composites system was 0.3%, the initial weight loss temperature was 311.7°C and the char yield was 19% at 600°C, the tensile strength was 49.3 *MPa* and the impact strength was 9.5 $kJ\ m^{-2}$. The LOI was 28.9 and the UL-94 test passed V-0 level. So, the phosphorus-modified graphene oxide had a good performance to enhance an ammonium poly(phosphate) flame retardant in an EP resin (171).

1.9.18.3 Organophosphate-Functionalized Graphene Oxide

A series of organophosphate-functionalized graphene oxide flame retardants could be synthesized by grafting flexible phosphate ester onto the surface of graphene oxide (176).

The obtained organophosphate-functionalized graphene oxide flame retardants were then incorporated into an amino resin to produce transparent fire retardant coatings for reducing the fire hazard of wood. The transparency analysis shows that the organophosphate-functionalized graphene oxide flame retardants endow the resulting coatings with a high degree of transparency even at relatively high graphene oxide contents due to the uniform dispersion and completely exfoliated states of graphene oxide in amino matrix.

The evaluation of combustion behavior revealed that the introduction of graphene oxide greatly reduces the weight loss, char index, flame spread rating, smoke production and heat release of the coatings concomitant with an increase in the insulation property (176).

1.9.18.4 Halloysite Nanotube Graphene Oxide Hybrid

Adding an environmentally friendly flame retardant to heat-resistant resins without deteriorating their outstanding thermal stability is an important research direction (177).

A unique hybrid consisting of graphene oxide and halloysite nanotubes was synthesized, and then a series of composites based on cyanate ester resin were fabricated.

Halloysite is an aluminosilicate clay mineral with the empirical formula $Al_2Si_2O_5(OH)_4$. It was first described in 1826 and named after the Belgian geologist Jean Baptiste d'Omalius d'Halloy (178). A halloysite nanotube is an eco-friendly and cheap clay nanotube that has a large aspect ratio and specific surface area as well as excellent heat resistance. It is stable up to 460°C (179).

The effects of graphene oxide/halloysite nanotubes on the heat resistance, flame retardancy, and smoke suppression of graphene oxide/halloysite nanotubes/cyanate ester composites were investigated (177). A graphene oxide/halloysite nanotubes/cyanate ester composite with 5.0% graphene oxide/halloysite nanotubes not only has about 15.1°C higher initial degradation temperature, but also shows 54.6% or 37.9% lower PHRR or maximum smoke density than the neat cyanate ester resin.

These results clearly demonstrate that graphene oxide/halloysite nanotubes is not the simple combination of graphene oxide and

halloysite nanotubes. Instead, it obviously shows positive synergistic effects in simultaneously improving the flame retardancy and thermal resistance of the cyanate ester resin. The improved flame retardancy could be attributed to condensed-phase mechanisms, including increasing char yield, building a dense char layer, and free-radical scavenging (177).

1.9.18.5 POSS-Functionalized Graphene Oxide

Functionalized graphene oxide sheets with improved dispersive and smoke-suppressive properties were synthesized by covalently grafting an octa(propyl glycidyl ether) polyhedral oligomeric silsesquioxane (POSS) on graphene oxide sheets with γ-aminopropyl triethoxy silane as a chemical bridge (180).

The good dispersion of the functionalized graphene oxide sheets in an epoxy resin matrix endowed the epoxy resin composites with a stable thermal resistance, enhanced tensile and smoke-suppressive properties.

Cone calorimeter tests indicated that the addition of only 0.7% functionalized graphene oxide sheets to epoxy resin composites reduced the peak of heat release rate, total heat release, and total smoke release by 49.7%, 34.3%, and 41.5%, respectively.

Two important effects that originated from functionalized graphene oxide promoted this improvement. The well-dispersed functionalized graphene oxide sheets exhibited a tortuous effect by lengthening the heat path and inhibiting heat diffusion in the epoxy resin matrix. Furthermore, the increase in char residue and the reduction in gas volatiles confirmed the barrier effect of functionalized graphene oxide sheets by forming protective char structures on the surface of the matrix, which restrained smoke release (180).

1.9.18.6 Aluminum Hypophosphite/Reduced Graphene Oxide

Aluminum hypophosphite (AHP)/reduced graphene oxide hybrid flame retardant with high thermal stability was successfully prepared by a one-step method consisting of the simultaneous reduction of graphene oxide and the deposition of AHP on graphene (181). The so-prepared sample was characterized by XRD, FTIR, SEM, transmission electron microscopy, XPS, and Raman spectroscopy.

The thermal decomposition of AHP may be as follows:

$$2Al(H_2PO_2)_3 \rightarrow Al_2(HPO_4)_3 + 3PH_3 \quad (1.1)$$

$$2Al(H_2PO_4)_3 \rightarrow Al_4(P_2O_7)_3 + 3H_2O \quad (1.2)$$

The material was used as a flame retardant for PBT (181). The flame retardancy of the composites was investigated by an LOI test, a UL-94 test, and cone calorimetry. The results of these tests showed that AHP/reduced graphene oxide exhibited an improved flame retardancy in comparison to bare AHP. The addition of AHP/reduced graphene oxide to PBT led to a significant reduction in the heat release rate and resulted in excellent anti-dripping properties for the composites (181).

1.9.18.7 Covalently Functionalized Graphene Oxide

A covalently functionalized graphene oxide was successfully prepared by grafting a phosphorus-containing flame retardant, 2-((6-oxidodibenzo[*c*,*e*][1,2]oxaphosphinin-6-yl)methoxy)acryloxyethylchlorophosphate (PACP), to graphene oxide (182). This compound is shown in Figure 1.46.

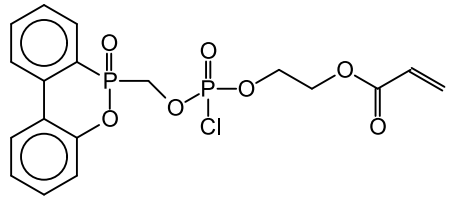

Figure 1.46 2-((6-Oxidodibenzo[*c*,*e*][1,2]oxaphosphinin-6-yl)methoxy)acryloxyethylchlorophosphate (182).

The functionalized graphene oxide demonstrated hydrophobicity and stability in polar solvents such as *N*,*N*-dimethylformamide. The reactive vinyl groups of PACP attached to the functionalized graphene oxide were further copolymerized with styrene to produce PS-functionalized graphene oxide nanocomposites.

The PS-functionalized graphene oxide samples showed an improved fire resistance, thermal behavior, and glass transition temperature in comparison with those of neat PS and PS-graphene oxide samples, due to the good dispersion of functionalized graphene oxide in PS, as well as the strong interfacial bonds between the functionalized graphene oxide and the matrix.

The evolution of volatile products from PS decomposition was significantly inhibited by the introduction of the functionalized graphene oxide. Furthermore, scanning electron microscopy (SEM) and FTIR and Raman spectroscopy were employed to investigate the char residue and to elaborate the mechanism of the flame retardance (182).

The presence of the functionalized graphene oxide in PS not only decreases gaseous volatiles and inhibits the combustion chain reactions in gas phase, but also serves as a physical barrier. Moreover, it reacts with the polymer molecule chains to catalyze the formation of char residue with an improved microstructure, exerting a flame retardant action in the condensed phase (182).

1.9.18.8 Functionalized Graphene Oxide

A functionalized graphene oxide was prepared from graphene oxide, boric acid and 3-aminopropyl triethoxy silane in an ethanol aqueous solution using ultrasonic agitation (183).

The structure was characterized by FTIR, XRD, TG, and elemental analysis. XRD is a powerful tool for the structure analysis of layered materials like graphene oxide. Graphene oxide has a strong and sharp diffraction peak at 2θ=11.0°, which corresponds to an interlayer distance of 8.04 Å. However, functionalized graphene oxide exhibits two intense peaks at 2θ=8.8° and 12.1°, indicating a change in d-spacing to 10.03 Å and 7.31 Å, respectively. The thermal degradation process of graphene oxide has two stages which correspond to the vaporization of water at about 100°C and the decomposition of the functional groups (−OH and −COOH) at about 220°C (184).

There are also two stages of the thermal decomposition process of functionalized graphene oxide, but it still has a difference comparison with graphene oxide (183). These are mainly divided into three aspects:

1. Functionalized graphene oxide showed a good thermal stability compared to graphene oxide before about 180°C, which was due to the decrease of water and unstable oxygen functional groups after graphene oxide functionalization.
2. A gradual weight loss above 180°C–220°C is observed in the TG curve of functionalized graphene oxide, predominantly due to decomposition of the Si–O–Si group and the B–O group in the functionalized graphene oxide.
3. The TG curve of functionalized graphene oxide is located above the graphene oxide after 220°C, which shows the higher thermal stability of functionalized graphene oxide at high temperature.

The functionalized graphene oxide was incorporated into the flame retardant PU system. Here, functionalized graphene oxide was used as a synergist and reinforcing agent. Expandable graphite and dimethyl methylphosphonate were used as flame retardants to improve its flame retardancy and mechanical properties. This was evidenced by the LOI, vertical burning test (UL-94) and a cone calorimeter test.

The LOI of flame retardant PU/functionalized graphene oxide composites reached 28.1% by the addition of 0.25 *phr* functionalized graphene oxide and 10 *phr* expandable graphite/dimethyl methylphosphonate. The UL-94 test reached a V-0 rating. The cone calorimeter test results revealed that the functionalized graphene oxide could significantly enhance flame retardant properties of flame retardant PU composites. The PHRR value of the flame retardant PU/functionalized graphene oxide was remarkably reduced by 32.9%. Also, the functionalized graphene oxide enhanced the mechanical properties of the rigid PU foam (183).

The thermal degradation of rigid PU samples was studied using TG and FTIR analysis (185). The activation energies (E_a) for the main stage of thermal degradation were obtained using the Kissinger equation (186).

The thermal degradation of RPUF specimens in air atmosphere can be divided into three steps (185). In pure RPUF curves, during the range of 110°C – 140°C, some mass loss occurs due to the volatilization of water vapor in the specimen.

The temperature range of the second degradation step was within

the range of 240°C – 450°C, which is mainly attributed to monomer precursors such as PU polyols and isocyanates. Subsequently, the isocyanate dimerizes to form carbodiimide, accompanied by the evolution of volatile compounds such as CO_2, CO, alcohols, amines, and aldehydes. The temperature range of the third degradation step was 450°C – 700°C, which is mainly due to the degradation of substituted urea that is formed due to the reaction of carbodiimide with alcohol or water vapors (187).

It was found that the functionalized graphene oxide can considerably increase the thermal stability and decrease the flammability of a rigid PU. Furthermore, the E_a of the composite reached 191 $kJ\ mol^{-1}$, which was 61 $kJ\ mol^{-1}$ higher than that of the pure rigid PU with 130 $kJ\ mol^{-1}$ (185).

1.9.18.9 Eco-friendly Epoxy/Multilayer Graphene Oxide Composites

Eco-friendly flame retardants have been prepared (188). Multilayer graphene nanosheets were used as the starting material for the preparation of graphene nanosheets oxide. Using the –OH and –COOH functional groups of multilayer graphene oxide for the hydrolytic condensation of tetraethoxysilane, the tetraethoxysilane was grafted onto the graphene oxide to form a Si-graphene oxide. Subsequently, *p*-aminophenol was grafted onto Si-graphene oxide. These materials were reacted with EP to form the desired composites.

The char yield for a pure epoxy was found to be 15.6%. With a content of this flame retardant of 10% in the epoxy resin, the char yield increased to 25%. The LOI for a pure epoxy was found to be 19%. With a content of this flame retardant of 10% in the epoxy resin, the char LOI increased to 26% (188).

1.9.18.10 Dual-Functionalized Graphene Oxide

Poly(siloxane) foam is a foam material with an outstanding performance. However, the LOI of pure poly(siloxane) foam is only 22.0%, which can be attributed to combustible materials (189).

Graphene oxide was functionalized with hexachlorocyclotriphosphazene, c.f. Figure 1.13, and 3-aminopropyl triethoxy silane. The introduction of the functionalized graphene oxide into the

poly(siloxane) foam matrix has significantly improved the dispersion and the flame retardant properties of the poly(siloxane) foam composite. The char residue of poly(siloxane) foam with a content of 1.0% functionalized graphene oxide is 43.04%, which is considerably higher than that of the pure poly(siloxane) foam, which is only 23.18% (189).

Furthermore, the T_{max} of poly(siloxane) foam with 5.0% functionalized graphene oxide content has increased from 585.9°C to 668.8°C. The results of a cone calorimetry test indicated that modification with functionalized graphene oxide prolongs the combustion of poly(siloxane) foam composites. The LOI value of poly(siloxane) foam with 5.0% functionalized graphene oxide content increased from 22.0% to 27.6%. In addition, the PHRR, total heat release, and total smoke production of poly(siloxane) foam with 5.0% functionalized graphene oxide content were decreased by 49.2%, 14.5%, and 62.2% relative to those of a neat poly(siloxane) foam.

These results arise from the barrier effect of the graphene oxide, the condensed-phase as well as gas-phase mechanisms of hexachlorocyclotriphosphazene, and the bonding effect of 3-aminopropyl triethoxy silane (189).

1.9.18.11 Poly(ether ether ketone)-Grafted Graphene Oxide

The interface of EP and graphene oxide was tailored using a hydroxylated poly(ether ether ketone) (HPEEK) (190). The resultant modification (HPEEK-*g*-graphene oxide) improved the interfacial adhesion between the EP and the carbon fiber in the laminates.

This tailoring strategy resulted in an improved tensile strength with respect to epoxy/carbon fiber laminates by 8%, improved modulus by 10%, and an improved storage modulus by 26%.

To check the challenges involved with a primary agglomeration, the composite formulation was subjected to mechanical stirring coupled with bath sonication throughout the mixing process. The improved structural properties in epoxy/carbon fiber laminates were attributed to HPEEK-*g*-graphene oxide *interconnects*, which provided the necessary reinforcement owing to a better interfacial adhesion with the carbon fiber mat, as inferred from the fracture surface morphology assessed using SEM (190).

In addition, the epoxy laminates containing HPEEK-*g*-graphene oxide also showed flame retardant properties along with good thermal stability.

Also, the electromagnetic interference shielding capability of the modified laminates was evaluated in the frequency range of 12 *GHz* – 18 *GHz*. The laminates exhibited a shielding effectiveness of −50 *dB* (190).

1.9.18.12 Mesoporous Zinc Ferrite Decorated Graphene Oxide

A mesoporous zinc ferrite decorated graphene oxide nanohybrid was prepared through a one-step solvothermal method (191).

It was tested to reduce the fire hazards of an epoxy resin. The results of the study showed that the LOI value of the epoxy resin filled with 3% mesoporous zinc ferrite decorated graphene oxide is 27.2. This is much higher than that of the neat epoxy resin (22.1) (191).

In comparison with the neat epoxy resin, the PHRR, total smoke release, and the peak CO productive rate of the mesoporous zinc ferrite decorated graphene oxide/epoxy resin nanocomposite are reduced by 39.57%, 32.56%, and 58.80%, respectively.

This behavior was attributed to the synergistic flame retardant effect between graphene oxide and mesoporous zinc ferrite. Graphene oxide can act as the physical barrier to block the release of combustible gases and the transfer of heat energy and oxygen, while mesoporous zinc ferrite can catalyze the crosslinking of macromolecules and promote the char formation of epoxy resin and absorb the inflammable gases and the produced heat (191).

1.9.18.13 Modified Graphene Oxide

Branch-Like Graphene Oxide. A ternary thermal interface material with an epoxy resin matrix, silver nanowires, and a small amount of flame retardant functionalized graphene (GP-DOPO) were fabricated (192). A polymer was used as the backbone and flame retardant molecule as the branch was used to functionalize reduced graphene oxide.

This increases the compatibility of the reduced graphene oxide in the matrix, and the resulted GP-DOPO was then *in-situ* introduced

into epoxy/silver nanowire composites. The incorporation of 2/5 GP-DOPO can increase the thermal conductivity to 1.413 $W\,(mK)^{-1}$ at a very low silver nanowire loading of 4 *vol*%.

This improvement in the thermal conductivity was obtained due to the synergetic effect of the silver nanowire and GP-DOPO, i.e., the improving dispersion and bridging effect for silver nanowires by adding GP-DOPO (192).

A strong catalytic charring effect of the epoxy matrix was observed, which formed a robust protective char layer by combining the silver nanowire and the graphene network (192).

Phosphazene Modified Graphene Oxide. To improve its dispersion and flame retardant efficiency, graphene oxide was dually modified with a polymeric flame retardant and a nanomaterial with the ability of a catalytic carbonation (193).

Via the reactions between oxygen functional groups in graphene oxide and the P–Cl groups in hexachlorocyclotriphosphazene, c.f. Figure 1.13, the phosphazene-based flame retardant is grafted onto the graphene oxide. Due to the strong affinity of Ni^{2+} with the NH_2 groups in this phosphazene flame retardant, the decoration of $Ni(OH)_2$ nanosheets on the graphene is facilitated.

A good dispersion and exfoliation state of graphene in a PP matrix was observed (193). Thus, the incorporation of functionalized graphene oxide results in the reduction of PHRR and total heat release and smoke release of PP during the combustion.

Functionalized Reduced Graphene Oxide. The use of reduced graphene oxide in a high-temperature oxidization environment is limited by its poor thermal oxidation and fire resistance. Phosphorus and nitrogen co-doped reduced graphene oxide with high oxidation and fire resistance was prepared by a hydrothermal and microwave treatment (194).

Furthermore, its thermal oxidation decomposition kinetics and mechanisms were analyzed. The composition presents an increment of 162°C in the decomposition temperature relative to undoped reduced graphene oxide, and excellent fire resistance with only a ~20% mass loss after burning (194).

A flame retardant containing phosphorus, nitrogen and silicon elements was used to functionalize reduced graphene oxide. The wrapped flame retardant chains induced the improvement in the dispersion and compatibility of reduced graphene oxide in an epoxy matrix (195).

The mechanical, thermal and flame retardant properties of the epoxy-based composites were significantly improved by adding the flame retardant functionalized reduced graphene oxide.

The PHRR was reduced by 34%, the total heat release was reduced by 14% and the total smoke production was reduced by 30% compared to the neat resin (195).

Boron Modified Graphene Oxide. An azo-boron modified reduced graphene oxide intercalated by sodium metaborate for use as flame retardant, smoke and toxic fume suppression and tensile strength enhancement of PLA nanocomposites was tested (196).

The reduced graphene oxide-azo-boron/sodium metaborate hybrid was prepared by aryl grafting of azo-boron on graphene oxide followed by *in-situ* reduction/intercalation with sodium borohydride/sodium metaborate.

Then, the reduced graphene oxide-azo-boron/sodium metaborate hybrid was incorporated into PLA, and the properties were examined. A cone calorimeter test demonstrated an improved flame retardant performance by substantial reductions in PHRR ~76.5%, total heat release ~76.9%, total smoke release ~55.6%, peak CO production ~25.9% and peak CO_2 production by ~78.6%. A V-0 rating was attained in the UL-94 test with a higher LOI value of 31.2%. Considerable reductions in pyrolysis products, mainly hydrocarbons, CO, CO_2, and carbonyl compounds, were observed.

The tensile strength and Young's modulus were improved by 49.1% and 34.9% respectively. The flame retardant mechanism of the reduced graphene oxide-azo-boron/sodium metaborate/PLA nanocomposites is based primarily on the glassy charring effect of the B–OH groups in azo-boron and the inherent lamellar blocking effect of reduced graphene oxide (196).

Dopamine-Graphene Oxide PLA Nanocomposites. A DOPO functionalized graphene oxide was used to improve the flame retar-

dancy of PLA nanocomposites (197). The nanocomposites showed an excellent flame resistance at a loading of 6% flame retardant. UL-94 testing reached a V-0 rating, the PHRR decreased by 24.0% and the total heat release decreased by 43.0%. Moreover, the smoke production rate decreased by 46% and the total smoke release decreased by 83%.

The incorporation of DOPO functionalized graphene oxide can effectively reduce the evaporation of a flammable gaseous product into the gas phase through quenching free radicals. Also, the nanocomposites showed good mechanical properties when flame retardant is added (197).

Poly(dopamine)-Graphene Oxide Nanocoatings. A highly effective flame retardant nanocoating was developed by conducting the oxidative polymerization of a dopamine monomer within an aqueous liquid crystalline graphene oxide scaffold coating (198). Dopamine is shown in Figure 1.47.

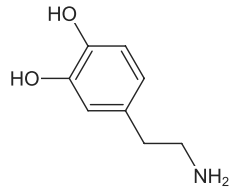

Figure 1.47 Dopamine.

Due to its high water content, the liquid crystalline scaffold coating approach facilitated the fast transport and polymerization of dopamine precursors into poly(dopamine) within the water swollen interlayer galleries.

Uniform and periodically stacked (14.5 Å*d*-spacing) poly(dopamine)/graphene oxide nanocoatings could be universally applied on different surfaces, including macroporous flexible PU foam and flat substrates such as silicon wafers (198).

To evaluate the flame retardant performance of the nanocoatings, a cone calorimeter was used with the standard testing protocol ASTM E1354 (199).

A poly(dopamine)/graphene oxide coated PU foam exhibited a highly efficient flame retardant performance reflected by a 65% reduction in PHRR at a 5% poly(dopamine)/graphene oxide loading in an 80 *nm* thick coating.

The poly(dopamine)/graphene oxide coating did not substantially affect the mechanical properties. In addition, the poly(dopamine)/graphene oxide coatings were stable in water due to the intrinsic adhesion capability of poly(dopamine) and the transformation of graphene oxide to the more hydrophobic reduced graphene oxide form. Since poly(dopamine) is produced from dopamine, a molecule prevalent in nature, these findings suggest that significant opportunities exist for new polymeric flame retardants derived from other natural catechols (198).

1.10 Flame Retardant Fillers

1.10.1 Mineral Fillers

The application of mineral fillers as flame retardant materials has been presented in a monograph (200). The use of fire retardant additives containing halogens is losing its popularity. So, there is a need for other systems.

The major materials that are used are alumina trihydrate or magnesium hydroxide, which account for more than 50% of the worldwide sale of flame retardants. It has been shown that such halogen-free compounds may give enhanced fire retardancy to polymeric materials when used in low levels, alone, or in synergistic mixtures. The corresponding fire performance depends on the dispersion of the mineral filler, with micrometer-scale dispersion leading to the best performances.

The application of mineral fillers with particular emphasis on action mechanisms, new materials including textiles, toxicology and hazards has been discussed (200).

1.10.2 Melamine Phosphate Compounds

Flame retardant fillers for PI-based adhesive compositions consist of melamine poly(phosphate) and melamine pyrophosphate. This

type of filler improves the flame retardancy of the material. The usage in PI-based adhesive compositions has been described (201).

Melamine poly(phosphate) is preferable for high temperature conditions. In contrast, melamine pyrophosphate exhibits the loss of water at temperatures above 300°C. This may cause blisters to form in flexible circuit laminates.

Other useful flame retardant fillers for PI-based adhesive compositions are summarized in Table 1.10.

Table 1.10 Flame retardant fillers (201).

Compound Class
Ammonium poly(phosphate)
Polyphosphoric acid amide
Ammonium polyphosphoric acid amide
Melamine poly(phosphate) (Melapur® 200)
Melamine poly(phosphate) acid
Melamine-modified ammonium poly(phosphate)
Melamine-modified polyphosphoric acid amide
Melamine-modified ammonium poly(phosphate)
Melamine-modified carbamyl poly(phosphate)
Carbamyl poly(phosphate)

1.11 Admixed Additives

In thermoplastic resins, the flame retardants are usually admixed, but not chemically bound onto the polymeric backbone. A wide variety of flame retardants are available for thermoplastics. Although halogen-based flame retardants are still heavily used, they are increasingly being replaced by non-halogen-containing flame retardants for environmental and health reasons.

Examples of halogenated flame retardants are shown in Table 1.11.

The synthesis of hexabromocyclododecane is shown in Figure 1.48. Hexabromocyclododecane is obtained by the trimerization of 1,3-butadiene followed by bromination. It is the most important flame retardant for foamed PS. In addition, sulfonic salt-based flame retardants are shown in Table 1.12.

Table 1.11 Halogenated flame retardants (202).

Compound
Hexabromocyclododecane
Bis(2,6-Dibromophenyl)methane
1,1-Bis-(4-iodophenyl)ethane
2,6-Bis(4,6-dichloronaphthyl)propane
2,2-Bis(2,6-dichlorophenyl)pentane
Bis(4-Hydroxy-2,6-dichloro-3-methoxyphenyl)methane
2,2-Bis(3-bromo-4-hydroxyphenyl)propane
2,2´-Dichlorobiphenyl
Polybrominated 1,4-diphenoxybenzene
2,4´-Dibromobiphenyl
2,4´-Dichlorobiphenyl
Decabromodiphenyl oxide

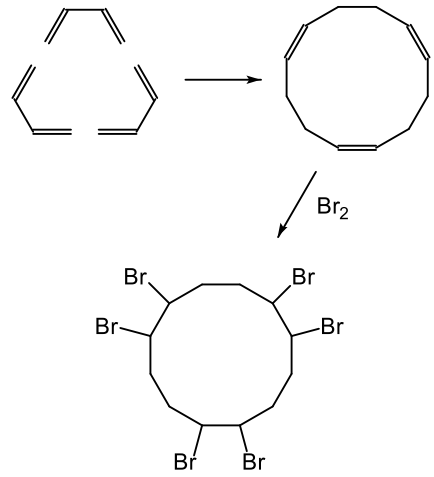

Figure 1.48 Synthesis of hexabromocyclododecane.

Table 1.12 Sulfonic salt flame retardants (202).

Compound	Remark
Potassium perfluorobutane sulfonate	Rimar salt
Potassium perfluorooctane sulfonate	
Tetraethylammonium perfluorohexane sulfonate	
Potassium diphenylsulfone sulfonate	

Organic phosphate compounds may be aromatic-based phosphates. Examples are shown in Table 1.13.

Table 1.13 Organic phosphate compounds (202).

Compound
Diphenyl pentaerythritol diphosphate
Phenyl bis(dodecyl) phosphate
Phenyl bis(neopentyl) phosphate
Phenyl bis(3,5,5´-trimethylhexyl) phosphate
Ethyl diphenyl phosphate, 2-Ethylhexyl di(*p*-tolyl) phosphate
Bis(2-ethylhexyl)-*p*-tolyl phosphate
Tritolyl phosphate
Bis(2-ethylhexyl)phenyl phosphate
Tri(nonylphenyl) phosphate
Bis(dodecyl)-*p*-tolyl phosphate
Dibutyl phenyl phosphate
2-Chloroethyl diphenyl phosphate
p-Tolyl bis(2,5,5´-trimethylhexyl) phosphate
2-Ethylhexyl diphenyl phosphate
Triphenyl phosphate
Tricresyl phosphate
Isopropylated triphenyl phosphate

A phosphorus-nitrogen synergism is seen in the flame retardant action. Therefore, flame retardant compounds containing phosphorus-nitrogen bonds have been developed. Examples are shown in Table 1.14.

Table 1.14 Nitrogen-phosphate compounds (202).

Compound
Phosphonitrilic chloride
Phosphoric acid amides
Phosphonic acid amides
Phosphinic acid amides
Tris(aziridinyl) phosphine oxide

Inorganic salts are likewise active as flame retardants. Examples are shown in Table 1.15.

Table 1.15 Inorganic salts (202, 203).

Compound	Remark
$CaCO_3$	Acts as diluent, lowers the combustible portion
$BaCO_3$	Inert filler
$Mg(OH)_2$	Breaks down endothermically
$Al(OH)_3$	Breaks down endothermically
KBF_4	(204)
Na_3AlF_6	(205)

1.11.1 Phosphorus-Based Flame Retardant Fillers

1.11.1.1 Ammonium Poly(phosphate)

Ammonium poly(phosphate) and inorganic fillers were used for improving flame retardancy and mechanical performance of recycled poly(ethylene terephthalate) (PET) (206). Recycled PET was compounded with 5% to 10% of talc and glass bead using a twin screw extruder. Then these materials were injection molded with 2% ammonium poly(phosphate).

The effects of filler contents and ammonium poly(phosphate) on the properties and flame retardancy of recycled PET composites were investigated (206). The incorporation of talc and glass bead as well as the addition of ammonium poly(phosphate) significantly improved tensile and flexural modulus of recycled PET composites.

SEM micrographs indicated a good distribution of talc, while the glass bead was agglomerated on the recycled PET matrix. The flame retardant property of neat recycled PET and the recycled PET composites revealed a V-2 of UL-94 flammability rating (206).

The composites were less dripping because of the synergistic effect of adding talc and glass bead with ammonium poly(phosphate). From the results of TG, larger contents of residual char and lower values of the activation energy were responsible for enhancing the flame retardancy in the recycled PET composites (206).

1.11.1.2 Ammonium Poly(phosphate), Boron Phosphate, Triphenyl Phosphate

The flame resistance and toughness of PLA were improved with the addition of a low amount of flame retardant fillers and plasticizer

simultaneously. Poly(ethylene glycol) (PEG) was used as plasticizer for PLA (207).

Ammonium poly(phosphate), boron phosphate, and triphenyl phosphate were used as flame retardant additives. Among these flame retardant additives, boron phosphate was synthesized from its raw materials by using a microwave heating technique (207).

Mechanical tests showed that the highest tensile strength, impact strength, and elongation at break values were obtained with the addition of ammonium poly(phosphate) and triphenyl phosphate into PLA/PEG matrix. SEM of the composites showed that the more homogeneous filler distribution in the matrix was observed for the triphenyl phosphate-containing composite. The best flame retardancy performance was also provided by triphenyl phosphate in comparison to the other flame retardant additives in the plasticized PLA-based composites (207).

1.11.2 Thermal Conductive Fillers

Poly(amide) (PA) 6 composites with an improved flame retardancy and improved thermal conductivity have been prepared with different thermal conductive fillers, such as aluminum nitride and boron nitride, in a PA 6 matrix with aluminum diethylphosphinate as a flame retardant (208).

The properties of the resultant halogen-free flame retardant and the thermal conductive PA 6 were investigated. It was found that the thermal conductivity of this composite increased with the amount of thermal conductive fillers. The thermal conductive fillers exerted a positive effect for flame retardant PA 6. Composites with the thickness of 1.6 *mm* successfully passed a UL-94 V-0 rating with an LOI of more than 29% with a loading of aluminum nitride and boron nitride of 30%.

The morphological structures of the char residues revealed that the thermal conductive fillers formed a highly integrated char layer surface (without holes) during the combustion process, as compared to that of the flame retardant PA 6/aluminum diethylphosphinate composites (208).

1.11.3 Organo-Modified Bentonites

Flame retardant organo-modified bentonites based on nitrogen-containing compounds were synthesized via an ion exchange process starting from pristine bentonite with acidified 6-(4-butylphenyl)-1,3,5-triazine-2,4-diamine and 11-amino-*N*-(pyridine-2yl)undecanamide (209). These compounds are shown in Figure 1.49.

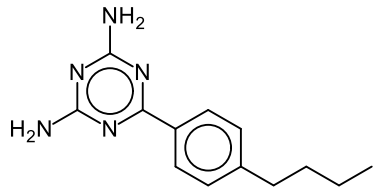

6-(4-Butylphenyl)-1,3,5-triazine-2,4-diamine

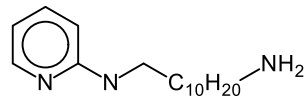

11-Amino-N-(pyridine-2yl)undecanamide

Figure 1.49 Nitrogen-containing compounds.

The amount of nitrogen-rich organic modifier in the so obtained organoclays was found to be around 0.4 $mmol\ g^{-1}$ for both samples. The effect of these additives on a commercial EP was studied, in which nanocomposites containing 3% and 5% of the nanofillers were prepared by solventless addition to the epoxy resin formulation.

The thermomechanical properties of all the produced samples were measured and they were slightly improved or practically unaffected. A decrease of 17% in the peak heat release rate was obtained with a 3% loading level with 11-amino-*N*-(pyridine-2yl)undecanamide containing bentonites (209).

1.11.4 Nanofillers

Recently developed fillers as flame retardants for polymer nanocomposite applications have been discussed in a monograph (210). Also,

flame retardant nanocomposites containing nanofillers have been described in a chapter of a monograph (211).

1.11.4.1 Poly(dimethylsiloxane)

The flame retardancy of poly(dimethylsiloxane) with different nanofillers was studied (212). The fire property of a poly(dimethylsiloxane) composite varies because of the shape, size, density, and chemical nature of nanofillers.

Carbon and bismuth oxide nanofillers were used in a poly(dimethylsiloxane) composite. Carbon from biochar (carbonized bamboo) and a carbon by-product (carbon soot) were selected. For a comparative study of the nanofillers, standard commercial multiwall carbon nanotubes (functionalized, graphitized and pristine) as nanofillers were selected (212).

Nanofillers in poly(dimethylsiloxane) positively affect their fire retardant properties such as total smoke release, PHRR, and time to ignition. Charring and surface ceramization are the main reasons for such an improvement. Nanofillers in poly(dimethylsiloxane) may affect the thermal mobility of polymer chains, which can directly affect the time to ignition.

So, the addition of pristine multiwall carbon nanotubes and bismuth oxide nanoparticles as filler in poly(dimethylsiloxane) composite improves the fire retardant properties (212).

1.12 Bound Additives

Bound additives are bonded into the backbone or as side chains into the polymer. This type of flame retardant is prevalent in thermosetting resins. Examples are shown in Table 1.16.

Table 1.16 Bound additives.

Compound
Tetrabromobisphenol A
Chlorendic anhydride
Tetrabromo phthalic anhydride

Some bound additives are shown in Figure 1.50.

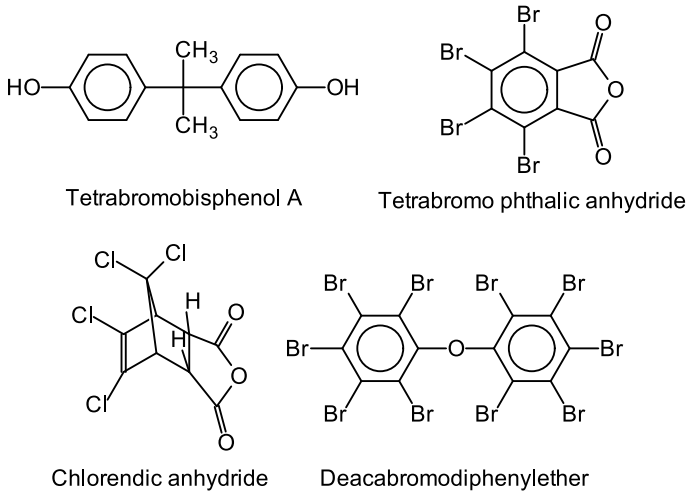

Figure 1.50 Some bound additives.

1.12.1 Vinyl Ester Resin Monomer

A novel bio-based and flame retardant UV-curable vinyl ester resin monomer, the diglycidyl ester of maleinized dipentene modified with dibutylphosphate and methacrylic anhydride was synthesized from industrial dipentene via Diels-Alder reaction, glycidylation, epoxy ring-opening reaction, and esterification (213). This compound is shown in Figure 1.51.

1.12.2 Flame Retardant and Ester Curing Agents

Compounds have been described which can concurrently function as a flame retardant and an active ester curing agent for thermosetting resins (214). These compounds are phosphorus-containing aromatic polyesters. When they are used as curing agents, it is possible to reduce the formation of undesirable hydroxyl groups during the curing reaction.

As reactive phosphorus-containing compound, DOPO, or a hydroquinone modified DOPO, 10-(2′,5′-dihydroxyphenyl)-9,10-dihydro-9-oxa-10-phosphaphenanthrene-10-oxide (DOPO-HQ) can be used. DOPO-HQ is shown in Figure 1.52.

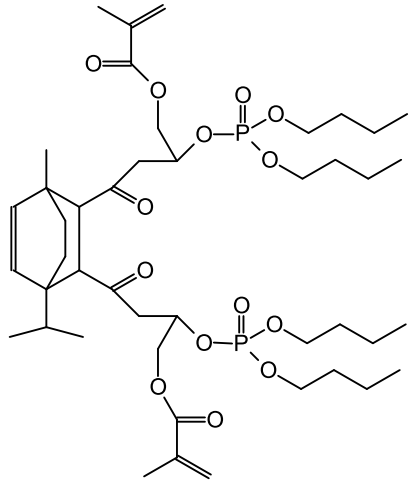

Figure 1.51 Bicyclo[2.2.2]oct-5-ene-2,3-dicarboxylic acid, 1-methyl-4-(1-methylethyl)-2,3-bis[2-[[bis(pentyloxy)phosphinyl]oxy]-3-[(2-methyl-1-oxo-2-propen-1-yl)oxy]propyl] ester (213).

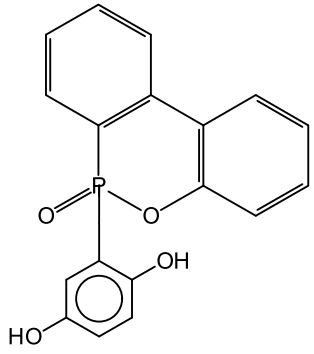

Figure 1.52 10-(2′,5′-dihydroxyphenyl)-9,10-Dihydro-9-oxa-10-phosphaphenanthrene-10-oxide.

A method of making an active ester curing agent can consist of the esterification of the DOPO-HQ with phthalic acid and acetic anhydride to produce oligomers. The synthesis of several other related compounds has been detailed (214), such as an oligomeric DOPO-HQ malonyl ester, an oligomeric DOPO-HQ terephthaloyl ester, and an oligomeric DOPO-HQ isophthaloyl ester. The compounds are intended to be used for epoxy resins (214).

1.12.3 DOPO Dicyandiamide

Resins for carbon fiber prepreg materials must be synthesized with a curing agent (hardener) and treated with other processes (215). Because DOPO can provide flame retardant characteristics to resins, a halogen-free flame retardant carbon fiber prepreg material can also be obtained using a DOPO-containing curing agent. Dicyandiamide can be connected with DOPO.

According to previous preparation methods disclosed in publications (216–218), the dicyandiamide must be heated at 120°C until it is completely molten. However, dicyandiamide has a high melting point of about 209.5°C. So, it is difficult to use a conventional apparatus to synthesize DOPO-dicyandiamide. To overcome the problem that curing agents such as DOPO-dicyandiamide are difficult to synthesize successfully, a novel flame retardant hardener has been fabricated by attaching the phosphorus-containing group of DOPO to a carbon of dicyandiamide (215). The samples that were synthesized are shown in Figure 1.53.

1.12.4 Mixed Flame Retardants

A flame retardant resin composition has been described which contains a sulfur-containing flame retardant, a phosphorus-containing flame retardant and/or a nitrogen-containing flame retardant, and a halogen-free epoxy resin (219). Here, the sulfur-containing flame retardant, phosphorus-containing flame retardant and nitrogen-containing flame retardant in the flame retardant resin composition play a synergistic effect.

The preferred materials for such a composition are collected in Table 1.17 and some compounds are shown in Figure 1.54.

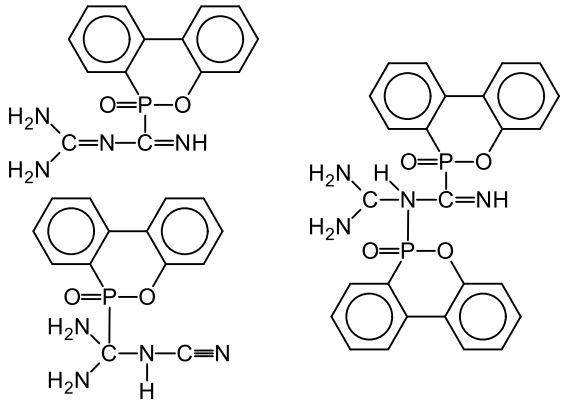

Figure 1.53 DOPO-dicyandiamide compounds (215).

Table 1.17 Compounds for flame retardant resin composition (219).

Sulfur-containing compounds
p-Benzenedithiol 4,4′-Diaminodiphenyl disulfide
Phosphorus-containing compounds
DOPO etherified bisphenol A DOPO modified epoxy resin Tris(2,6-dimethylphenyl)phosphine Tetra-(2,6-dimethylphenyl) resorcinol bisphosphate Resorcinol tetraphenyl diphosphate Triphenyl phosphate Bisphenol A bis(diphenyl phosphate) Phosphonitrile flame retardant 10-(2,5-Dihydroxyphenyl)-10-hydro-9-oxa-10-phosphaphenanthrene-10-oxide 10-(2,5-Dihydroxynaphthyl)-10-hydro-9-oxa-10-phosphaphenanthrene-10-oxide 9,10-Dihydro-9-oxa-10-phosphaphenanthrene-10-oxide (DOPO)
Nitrogen-containing compounds
Biurea Melamine Melamine phosphate

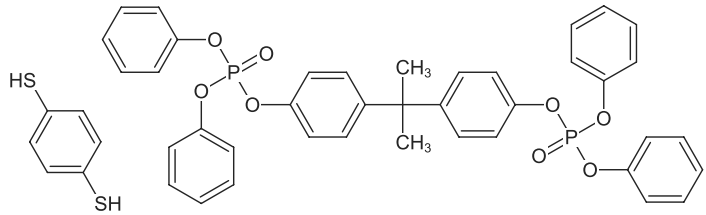

p-Benzenedithiol Bisphenol A bis(diphenyl phosphate)

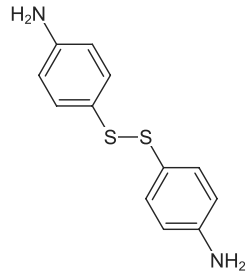

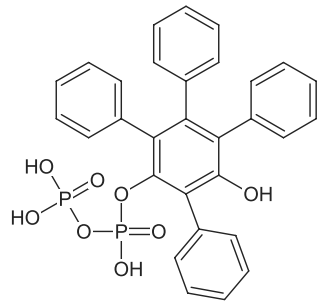

4,4′-Diaminodiphenyl disulfide Resorcinol tetraphenyl diphosphate

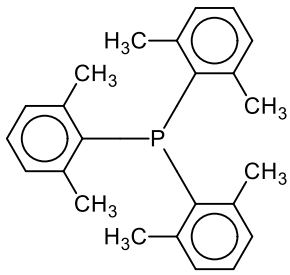

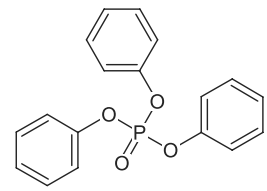

Tris(2,6-dimethylphenyl)phosphine Triphenyl phosphate

Figure 1.54 Compounds for flame retardant resin composition.

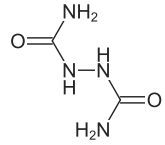

Figure 1.54 (cont) Biurea.

References

1. ASTM, Standard test method for measuring the minimum oxygen concentration to support candle-like combustion of plastics (oxygen index), ASTM Standard, Book of Standards, Vol. 08.01 2863-08, ASTM International, West Conshohocken, PA, 2008.
2. Kunststoffe - Bestimmung des Brennverhaltens durch den Sauerstoff-Index - Teil 2: Prüfung bei Umgebungstemperatur, DIN Standard DIN EN ISO 4589-2, DIN, Berlin, 2006.
3. M.W. Ranney, *Fire resistant and flame retardant polymers*, Chemical technology review, Noyes Data Corp., 1974.
4. A.R. Horrocks and D. Price, eds., *Fire Retardant Materials*, CRC Press, Boca Raton, 2001.
5. A.F. Grand and C.A. Wilkie, eds., *Fire Retardancy of Polymeric Materials*, Marcel Dekker, New York, 2000.
6. Y. Hu and X. Wang, eds., *Flame Retardant Polymeric Materials: A Handbook*, Series in Materials Science and Engineering, CRC Press, Boca Raton, London, New York, 2020.
7. Å. Bergman, A. Rydén, R.J. Law, J. de Boer, A. Covaci, M. Alaee, L. Birnbaum, M. Petreas, M. Rose, S. Sakai, N. Van den Eede, and I. van der Veen, *Environment International*, Vol. 49, p. 57, 2012.
8. M.D. Gold, A. Blum, and B.N. Ames, *Science*, Vol. 200, p. 785, 1978.
9. G. Menges, E. Haberstroh, W. Michaeli, and E. Schmachtenberg, *Werkstoffkunde Kunststoffe*, Hanser Publishers, München, 5th edition, 2002.
10. G. Menges, E. Haberstroh, W. Michaeli, and E. Schmachtenberg, *Werkstoffkunde Kunststoffe*, Vol. 2620 of *Sammlung Göschen*. Hanser Publishers, München, 6th edition, 2011.
11. S.M. Lomakin and G.E. Zaikov, *Modern Polymer Flame Retardancy*, New Concepts in Polymer Science, Taylor & Francis, 2003.
12. A. Blum, M.D. Gold, B.N. Ames, F.R. Jones, E.A. Hett, R.C. Dougherty, E.C. Horning, I. Dzidic, D.I. Carroll, R.N. Stillwell, and J.P. Thenot, *Science*, Vol. 201, p. 1020, 1978.
13. WHO/IPCS, *Environmental Health Criteria*, Vol. 192, p. 133, 1997. World Health Organization.
14. A.M.C.M. Pijnenburg, J.W. Everts, J. de Boer, and J.P. Boon, Polybrominated biphenyl and diphenylether flame retardants: Analysis, toxicity, and environmental occurrence, in G.W. Ware and F.A. Gunther, eds., *Reviews of Environmental Contamination and Toxicology: Continuation of Residue Reviews*, pp. 1–26. Springer New York, New York, 1995.
15. J. de Boer, K. de Boer, and J.P. Boon, Polybrominated biphenyls and diphenylethers, in O. Hutzinger and J. Paasivirta, eds., *Anthropogenic Compounds*, Vol. 3K of *The Handbook of Environmental Chemistry Book*

Series, chapter 3, pp. 61–96. Springer Berlin Heidelberg, Berlin, Heidelberg, 2000.
16. C.A. de Wit, *Chemosphere*, Vol. 46, p. 583, 2002.
17. R.J. Law, M. Alaee, C.R. Allchin, J.P. Boon, M. Lebeuf, P. Lepom, and G.A. Stern, *Environment International*, Vol. 29, p. 757, 2003. The State-of-Science and Trends of BFRs in the Environment.
18. L.S. Birnbaum and D.F. Staskal, *Environmental Health Perspectives*, Vol. 112, p. 9, 2004.
19. K. D'Silva, A. Fernandes, and M. Rose, *Critical Reviews in Environmental Science and Technology*, Vol. 34, p. 141, 2004.
20. EFSA Panel on Contaminants in the Food Chain (CONTAM), *EFSA Journal*, Vol. 8, p. 1789, 2010.
21. EFSA Panel on Contaminants in the Food Chain (CONTAM), *EFSA Journal*, Vol. 9, p. 2156, 2011.
22. EFSA Panel on Contaminants in the Food Chain (CONTAM), *EFSA Journal*, Vol. 9, p. 2296, 2011.
23. EFSA Panel on Contaminants in the Food Chain (CONTAM), *EFSA Journal*, Vol. 9, p. 2477, 2011.
24. EFSA Panel on Contaminants in the Food Chain (CONTAM), *EFSA Journal*, Vol. 10, p. 2634, 2012.
25. E. Eljarrat and D. Barceló, *Brominated Flame Retardants*, Springer, Berlin Heidelberg New York, 2011.
26. A. Covaci, A.C. Gerecke, R.J. Law, S. Voorspoels, M. Kohler, N.V. Heeb, H. Leslie, C.R. Allchin, and J. de Boer, *Environmental Science & Technology*, Vol. 40, p. 3679, 2006.
27. A. Covaci, S. Harrad, M.A.-E. Abdallah, N. Ali, R.J. Law, D. Herzke, and C.A. de Wit, *Environment International*, Vol. 37, p. 532, 2011.
28. R.J. Law, C.R. Allchin, J. de Boer, A. Covaci, D. Herzke, P. Lepom, S. Morris, J. Tronczynski, and C.A. de Wit, *Chemosphere*, Vol. 64, p. 187, 2006. Brominated Flame Retardants (BFRs) in the Environment.
29. R.J. Law, D. Herzke, S. Harrad, S. Morris, P. Bersuder, and C.R. Allchin, *Chemosphere*, Vol. 73, p. 223, 2008. Brominated Flame Retardants (BFRs).
30. I. van der Veen and J. de Boer, *Chemosphere*, Vol. 88, p. 1119, 2012.
31. E. Sverko, G.T. Tomy, E.J. Reiner, Y.-F. Li, B.E. McCarry, J.A. Arnot, R.J. Law, and R.A. Hites, *Environmental Science & Technology*, Vol. 45, p. 5088, 2011.
32. H. Yin, F.D. Sypaseuth, M. Schubert, R. Schoch, M. Bastian, and B. Schartel, *Polymers for Advanced Technologies*, Vol. 30, p. 187, 2019.
33. G.J. van Esch, *Chlorendic Acid and Anhydride*, Vol. 17 of *Environmental Health Criteria*, World Health Organization, Geneva, 1996, [electronic:] http://www.inchem.org/documents/ehc/ehc/ehc185.htm.
34. E. Hoh, L. Zhu, and R.A. Hites, *Environmental Science & Technology*, Vol. 40 4, p. 1184, 2006.

35. P. Wang, Q. Zhang, H. Zhang, T. Wang, H. Sun, S. Zheng, Y. Li, Y. Liang, and G. Jiang, *Environment International*, Vol. 88, p. 206, 2016.
36. Q. Xian, S. Siddique, T. Li, Y. lai Feng, L. Takser, and J. Zhu, *Environment International*, Vol. 37, p. 1273, 2011.
37. C. Brasseur, C. Pirard, B. L'homme, E. De Pauw, and J.-F. Focant, *Rapid Communications in Mass Spectrometry*, Vol. 30, p. 2545, 2016.
38. J. Dou, Y. Jin, Y. Li, B. Wu, and M. Li, *Chemosphere*, Vol. 135, p. 462, 2015.
39. H.M. Stapleton, S. Klosterhaus, A. Keller, P.L. Ferguson, S. van Bergen, E. Cooper, T.F. Webster, and A. Blum, *Environmental Science & Technology*, Vol. 45, p. 5323, 2011.
40. E. Tung, S. Ahmed, V. Peshdary, and E. Atlas, *PLoS ONE*, Vol. 12, p. e0175855, 04 2017.
41. G.J. van Esch, *Brominated Diphenyl Ethers*, Vol. 162 of *Environmental Health Criteria*, World Health Organization, Geneva, 1994, [electronic:] http://www.inchem.org/documents/ehc/ehc/ehc162.htm.
42. M. Altarawneh and B.Z. Dlugogorski, *Environmental Science & Technology*, Vol. 48, p. 14335, 2014.
43. F. Zhan, H. Zhang, R. Cao, Y. Fan, P. Xu, and J. Chen, *Environmental Science & Technology*, Vol. 53, p. 185, 2019.
44. EFSA Panel on Contaminants in the Food Chain, *EFSA Journal*, Vol. 10, p. 2908, 2012.
45. J. Guo, W.A. Stubbings, K. Romanak, L.V. Nguyen, L. Jantunen, L. Melymuk, V. Arrandale, M.L. Diamond, and M. Venier, *Environmental Science & Technology*, Vol. 52, p. 3599, 2018.
46. S.V. Levchik and E.D. Weil, *Journal of Fire Sciences*, Vol. 24, p. 345, 2006.
47. Z. Chen, P. Xiao, J. Zhang, W. Tian, R. Jia, H. Nawaz, K. Jin, and J. Zhang, *Chemical Engineering Journal*, Vol. 379, p. 122270, 2020.
48. M. Katayama, M. Ito, and Y. Otsuka, Polycarbonate resin composition containing block copolymer, US Patent 6 316 579, assigned to Daicel Corp., November 13, 2001.
49. J.R. Campbell and J.J. Talley, Flameproofed nylon molding compositions, US Patent 5 973 041, assigned to SABIC Innovative Plastics IP BV, September 26, 1999.
50. J.A. Cella, J.R. Campbell, and P.E. Howson, Method for preparing sterically hindered phosphoramidates, US Patent 6 291 700, assigned to General Electric Company (Schenectady, NY), September 18, 2001.
51. J.A. Cella, Method for preparing sterically hindered phosphoramidates, WO Patent 2 001 062 766, assigned to General Electric Company, August 30, 2001.

52. J. Cheol, K. Hoon, and S. Joo, Oligomeric phosphoric acid ester morpholide compound and flame retardant thermoplastic resin composition containing the same, EP Patent 1 209 163, assigned to Cheil Industries Inc., January 25, 2006.
53. K. Maruyama and R. Motoshige, Flame retardant thermoplastic resin composition, EP Patent 0 728 811, assigned to Mitsubishi Chemical Corp, August 28, 1996.
54. Y. Nakacho, T. Yabuhara, Y. Tada, and Y. Nishioka, Crosslinked phenoxyphosphazene compounds, flame retardants, flame-retardant resin compositions, and moldings of flame-retardant resins, US Patent 6 596 893, assigned to Otsuka Chemical Co., Ltd. (Osaka, JP), July 22, 2003.
55. J.T. Wertz, B.M. Kobilka, J.T. Porter, and J. Kuczynski, Flame-retardant microcapsule containing cyclic phosphazene, US Patent 10 253 166, assigned to International Business Machines Corp., April 7, 2019.
56. E. Çakmakçi and M.V. Kahraman, Boron/phosphorous-containing photocurable coatings, in A. Tiwari and A. Polykarpov, eds., *Photocured Materials*, RSC Smart Materials, chapter 9, pp. 150–187. Royal Society of Chemistry, 2014.
57. S.G. Cook, Boron-containing compositions, US Patent 8 623 423, assigned to U.S. Borax, Inc. (Greenwood Village, CO), January 7, 2014.
58. M. Dogan and S.M. Unlu, *Polymer Degradation and Stability*, Vol. 99, p. 12, 2014.
59. S. Tang, L. Qian, Y. Qiu, and Y. Dong, *Polymers for Advanced Technologies*, Vol. 29, p. 641, 2018.
60. Q. Tai, L. Song, H. Feng, Y. Tao, R.K.K. Yuen, and Y. Hu, *Journal of Polymer Research*, Vol. 19, p. 9763, 2012.
61. L. Ai, L. Yang, J. Hu, S. Chen, J. Zeng, and P. Liu, *Polymer Engineering & Science*, Vol. 60, p. 414, 2020.
62. L. Ai, S. Chen, J. Zeng, L. Yang, and P. Liu, *ACS Omega*, Vol. 4, p. 3314, 2019.
63. S.M. Unlu, S.D. Dogan, and M. Dogan, *Polymers for Advanced Technologies*, Vol. 25, p. 769, 2014.
64. S. Yang, Q. Zhang, and Y. Hu, *Polymer Degradation and Stability*, Vol. 133, p. 358, 2016.
65. K. Zhao, W. Xu, L. Song, B. Wang, H. Feng, and Y. Hu, *Polymers for Advanced Technologies*, Vol. 23, p. 894, 2012.
66. J. Xiao, H. Peng, F. Wang, X. Liu, Y. Wang, J. Feng, and J.W. Hao, Relationship between acidity of boron phosphate and its catalytic flame retardancy for epoxy composites, in *1st Asia-Oceania Symposium on Fire Safety Materials Science and Engineering*, pp. 64–65, Suzhou, China, 2015. University of Science and Technology of China, Hefei.

67. Y.-Y. Li, Y.-L. Wang, X.-M. Yang, X. Liu, Y.-G. Yang, and J.-W. Hao, *Journal of Thermal Analysis and Calorimetry*, Vol. 129, p. 1481, 2017.
68. C. Martín, J.C. Ronda, and V. Cádiz, *Polymer Degradation and Stability*, Vol. 91, p. 747, 2006.
69. C. Martín, J.C. Ronda, and V. Cádiz, *Journal of Polymer Science Part A: Polymer Chemistry*, Vol. 44, p. 3503, 2006.
70. A. Lang, J. Knizek, H. Nöth, S. Schur, and M. Thomann, *Zeitschrift für anorganische und allgemeine Chemie*, Vol. 623, p. 901, 1997.
71. C. Martín, J.C. Ronda, and V. Cádiz, *Journal of Polymer Science Part A: Polymer Chemistry*, Vol. 44, p. 1701, 2006.
72. G. Saischek, K. Wegleitner, F. Heu, and R. Wohlmuth, Spirocyclic boron compounds, a process for their manufacture and their use as a flame-retardant additive, US Patent 4 265 664, assigned to Chemie Linz Aktiengesellschaft (Linz, AT), May 5, 1981.
73. T. Zhang, W. Liu, M. Wang, P. Liu, Y. Pan, and D. Liu, *High Performance Polymers*, Vol. 29, p. 513, 2017.
74. S. Chen, L. Ai, T. Zhang, P. Liu, W. Liu, Y. Pan, and D. Liu, *Arabian Journal of Chemistry*, Vol. 13, p. 2982, 2020.
75. Q. Zhang, Z. Li, X. Li, L. Yu, Z. Zhang, and Z. Wu, *Chemical Engineering Journal*, Vol. 356, p. 680, 2019.
76. C. Tian, L. Yuan, G. Liang, and A. Gu, *Journal of Materials Science*, Vol. 54, p. 7651, 2019.
77. Y. Feng, L. Yuan, G. Liang, and A. Gu, *Polymers for Advanced Technologies*, Vol. 30, p. 2340, 2019.
78. D. Wang, X. Mu, W. Cai, L. Song, C. Ma, and Y. Hu, *Composites Part A: Applied Science and Manufacturing*, Vol. 109, p. 546, 2018.
79. S. Qiu, Y. Hou, W. Xing, C. Ma, X. Zhou, L. Liu, Y. Kan, R.K. Yuen, and Y. Hu, *Chemical Engineering Journal*, Vol. 349, p. 223, 2018.
80. W. Cai, X. Mu, Y. Pan, W. Guo, J. Wang, B. Yuan, X. Feng, Q. Tai, and Y. Hu, *Polymers for Advanced Technologies*, Vol. 29, p. 2545, 2018.
81. L. Wang, L. Zhang, A. Fischer, Y. Zhong, D. Drummer, and W. Wu, *Journal of Polymer Engineering*, Vol. 38, p. 767, 2018.
82. X. Qiu, Z. Li, X. Li, L. Yu, and Z. Zhang, *Journal of Applied Polymer Science*, Vol. 136, p. 47839, 2019.
83. Q. Zhang, Z. Li, X. Li, L. Yu, and Z. Wu, *Materials Research Express*, Vol. 5, p. 095019, aug 2018.
84. Q. Zhang, Z. Li, X. Li, L. Yu, Z. Zhang, and Z. Wu, *Nano*, Vol. 14, p. 1950063, 2019.
85. H. Liu, Y. Du, S. Lei, and Z. Liu, *Textile Research Journal*, Vol. 0, p. 0040517519871260, 2019.
86. B. Tawiah, B. Yu, W.Y. Cheung, S.Y. Chan, W. Yang, and B. Fei, *Polymer Degradation and Stability*, Vol. 152, p. 64, 2018.
87. B. Tawiah, B. Yu, W. Yang, R.K.K. Yuen, and B. Fei, *Polymers for Advanced Technologies*, Vol. 30, p. 2207, 2019.

88. P. Sheth, S. Mestry, D. Dave, and S. Mhaske, *Journal of Coatings Technology and Research*, Vol. 17, p. 231, 2020.
89. L. Ai, S. Chen, J. Zeng, P. Liu, W. Liu, Y. Pan, and D. Liu, *Polymer Degradation and Stability*, Vol. 155, p. 250, 2018.
90. V. Benin, S. Durganala, and A.B. Morgan, *J. Mater. Chem.*, Vol. 22, p. 1180, 2012.
91. V. Benin, B. Gardelle, and A.B. Morgan, *Polymer Degradation and Stability*, Vol. 106, p. 108, 2014. Special Issue Based on the 14th European meeting on Fire Retardancy and Protection of Materials, held at Ecole Nationale Supérieure de Chimie de Lille (U. Lille-1), France, July 2013.
92. T. Zhang, W. Liu, M. Wang, P. Liu, Y. Pan, and D. Liu, *Polymer Degradation and Stability*, Vol. 130, p. 257, 2016.
93. X. Liu, Y. Zhou, H. Peng, and J. Hao, *Polymer Degradation and Stability*, Vol. 119, p. 242, 2015.
94. W. Guo, X. Wang, C.S.R. Gangireddy, J. Wang, Y. Pan, W. Xing, L. Song, and Y. Hu, *Composites Part A: Applied Science and Manufacturing*, Vol. 116, p. 13, 2019.
95. L. Wang, M. Sánchez-Soto, J. Fan, Z.-P. Xia, and Y. Liu, *Polymers for Advanced Technologies*, Vol. 30, p. 1807, 2019.
96. S. Hamdani, C. Longuet, D. Perrin, J.-M. Lopez-Cuesta, and F. Ganachaud, *Polymer Degradation and Stability*, Vol. 94, p. 465, April 2009.
97. M.N. Prabhakar, A.U.R. Shah, and J.-I. Song, *Polymer*, Vol. 37, p. 40, 2015.
98. X. Chen and C. Jiao, *Fire Safety Journal*, Vol. 44, p. 1010, 2009.
99. C.M. Jiao and X.L. Chen, *Polymer-Plastics Technology and Engineering*, Vol. 48, p. 665, 2009.
100. X. Chen, C. Jiao, and J. Zhang, *Journal of Thermal Analysis and Calorimetry*, Vol. 104, p. 1037, 2011.
101. J. Jiang, Y. Wang, Z. Luo, T. Qi, Y. Qiao, M. Zou, and B. Wang, *Polymers*, Vol. 11, p. 1155, Jul 2019.
102. L. Ding, R. Song, and B. Li, *Journal of Applied Polymer Science*, Vol. 126, p. 1489, 2012.
103. J.L. Zhuo, J. Dong, C.M. Jiao, and X.L. Chen, *Plastics, Rubber and Composites*, Vol. 42, p. 239, 2013.
104. X. Chen, W. Song, J. Liu, C. Jiao, and Y. Qian, *Journal of Thermal Analysis and Calorimetry*, Vol. 120, p. 1819, 2015.
105. W. Chen, Y. Liu, C. Xu, Y. Liu, and Q. Wang, *RSC Advances*, Vol. 7, p. 39786, 2017.
106. Z.-S. Li, J.-G. Liu, T. Song, D.-X. Shen, and S.-Y. Yang, *Journal of Applied Polymer Science*, Vol. 131, p. 1, 2014.
107. S. Hamdani, C. Longuet, J.-M. Lopez-Cuesta, and F. Ganachaud, *Polymer Degradation and Stability*, Vol. 95, p. 1911, 2010.

108. S. Hamdani-Devarennes, C. Longuet, R. Sonnier, F. Ganachaud, and J.-M. Lopez-Cuesta, *Polymer Degradation and Stability*, Vol. 98, p. 2021, 2013.
109. X. Lai, C. Yin, H. Li, and X. Zeng, *Journal of Applied Polymer Science*, Vol. 132, p. 1, 2015.
110. X. Li, Z. Yang, J. Yao, and Y. Zhang, *Journal of Macromolecular Science, Part B*, Vol. 54, p. 1282, 2015.
111. X. Chen, M. Li, J. Zhuo, C. Ma, and C. Jiao, *Journal of Thermal Analysis and Calorimetry*, Vol. 123, p. 439, 2016.
112. C. Jiao, J. Zhuo, and X. Chen, *Plastics, Rubber and Composites*, Vol. 42, p. 374, 2013.
113. J. Qi, Q. Wen, J. Zhu, and T. He, *Journal of Thermal Analysis and Calorimetry*, Vol. 137, p. 1549, 2019.
114. J. Qi, Q. Wen, and J. Zhu, *Materials Letters*, Vol. 249, p. 62, 2019.
115. H. Wang and B. Li, *Polymers for Advanced Technologies*, Vol. 21, p. 691, 2010.
116. X. Chen, J. Zhuo, W. Song, C. Jiao, Y. Qian, and S. Li, *Polymers for Advanced Technologies*, Vol. 25, p. 1530, 2014.
117. J. Han, G. Liang, A. Gu, J. Ye, Z. Zhang, and L. Yuan, *J. Mater. Chem. A*, Vol. 1, p. 2169, 2013.
118. B. Yuan, A. Fan, M. Yang, X. Chen, Y. Hu, C. Bao, S. Jiang, Y. Niu, Y. Zhang, S. He, and H. Dai, *Polymer Degradation and Stability*, Vol. 143, p. 42, 2017.
119. G. Yuan, B. Yang, Y. Chen, and Y. Jia, *RSC Advances*, Vol. 8, p. 36286, 2018.
120. S.-B. Deng, W. Liao, J.-C. Yang, Z.-J. Cao, and Y.-Z. Wang, *Industrial & Engineering Chemistry Research*, Vol. 55, p. 7239, 2016.
121. J. Zhang, E. Fleury, Y. Chen, and M.A. Brook, *RSC Adv.*, Vol. 5, p. 103907, 2015.
122. W. Wang, M. Zammarano, J.R. Shields, E.D. Knowlton, I. Kim, J.A. Gales, M.S. Hoehler, and J. Li, *Construction and Building Materials*, Vol. 189, p. 448, 2018.
123. M.Y. Wang, A.R. Horrocks, S. Horrocks, M.E. Hall, J.S. Pearson, and S. Clegg, *Journal of Fire Sciences*, Vol. 18, p. 265, 2000.
124. British Standard, British standard methods for methods of test for flammability of textile fabrics when subjected to a small igniting flame applied to the face or bottom edge of vertically oriented specimens, British Standard BS 5438, British Standards Institution, London, 1989. Inactive at 2020.
125. L. Karlsson, A. Lundgren, J. Jungqvist, and T. Hjertberg, *Fire and Materials*, Vol. 35, p. 443, 2011.
126. J.-W. Jiang, *Frontiers of Physics*, Vol. 10, p. 287, 2015.
127. H. Pan, Q. Shen, Z. Zhang, B. Yu, and Y. Lu, *Journal of Materials Science*, Vol. 53, p. 9340, 2018.

128. K. Zhou, W. Yang, G. Tang, B. Wang, S. Jiang, Y. Hu, and Z. Gui, *RSC Adv.*, Vol. 3, p. 25030, 2013.
129. Wikipedia contributors, Graphene — wikipedia, the free encyclopedia, https://en.wikipedia.org/w/index.php?title=Graphene&oldid=939792839, 2020. [Online; accessed 12-February-2020].
130. B. Sang, Z.-W. Li, X.-H. Li, L.-G. Yu, and Z.-J. Zhang, *Journal of Materials Science*, Vol. 51, p. 8271, 2016.
131. G. Malucelli, *Curr. Graphene Sci.*, Vol. 2, p. 27, 2018.
132. P. Govindaraj, B. Fox, P. Aitchison, and N. Hameed, *Industrial & Engineering Chemistry Research*, Vol. 58, p. 17106, 2019.
133. V. Dhinakaran, M. Lavanya, K. Vigneswari, M. Ravichandran, and M. Vijayakumar, *Materials Today: Proceedings*, 2020.
134. B. Yuan, Y. Sun, X. Chen, Y. Shi, H. Dai, and S. He, *Composites Part A: Applied Science and Manufacturing*, Vol. 109, p. 345, 2018.
135. S. Pei and H.-M. Cheng, *Carbon*, Vol. 50, p. 3210, 2012. Festschrift dedicated to Peter A. Thrower, Editor-in-Chief, 1972 - 2012.
136. X. Wang, B. Bi, J. Liu, S. Yang, L. Zhou, L. Lu, Y. Wang, F. Xu, and R. Huang, *Journal of Applied Polymer Science*, Vol. 135, p. 46361, 2018.
137. L. Li, X. Liu, X. Shao, L. Jiang, K. Huang, and S. Zhao, *Composites Part A: Applied Science and Manufacturing*, Vol. 129, p. 105715, 2020.
138. W. Cai, X. Feng, B. Wang, W. Hu, B. Yuan, N. Hong, and Y. Hu, *Chemical Engineering Journal*, Vol. 316, p. 514, 2017.
139. K. Parvez, Z.-S. Wu, R. Li, X. Liu, R. Graf, X. Feng, and K. Müllen, *Journal of the American Chemical Society*, Vol. 136, p. 6083, 2014.
140. H. Ma, L. Zhao, J. Liu, J. Wang, and J. Xu, *Polymer Composites*, Vol. 35, p. 2187, 2014.
141. W. Chen, Y. Liu, P. Liu, C. Xu, Y. Liu, and Q. Wang, *Scientific Reports*, Vol. 7, p. 8759, 2017.
142. M. Li, H. Zhang, W. Wu, M. Li, Y. Xu, G. Chen, and L. Dai, *Polymers*, Vol. 11, p. 241, February 2019.
143. J. Jing, Y. Zhang, X. Tang, X. Li, M. Peng, and Z. Fang, *RSC Advances*, Vol. 8, p. 4304, 2018.
144. Wikipedia contributors, Phosphorene — Wikipedia, the free encyclopedia, https://en.wikipedia.org/w/index.php?title=Phosphorene&oldid=939802534, 2020. [Online; accessed 15-February-2020].
145. A. Carvalho, M. Wang, X. Zhu, A.S. Rodin, H. Su, and A.H. Castro Neto, *Nature Reviews Materials*, Vol. 1, p. 16061, 2016.
146. X. Ren, Y. Mei, P. Lian, D. Xie, W. Deng, Y. Wen, and Y. Luo, *Polymers*, Vol. 11, p. 193, January 2019.
147. O. Zabihi, M. Ahmadi, Q. Li, M.R.G. Ferdowsi, R. Mahmoodi, E.N. Kalali, D.-Y. Wang, and M. Naebe, *Journal of Cleaner Production*, Vol. 247, p. 119150, 2020.
148. H. Wei, Z. Zhu, H. Sun, P. Mu, W. Liang, and A. Li, *Journal of Applied Polymer Science*, Vol. 134, p. 45477, 2017.

149. T.-P. Ye, S.-F. Liao, Y. Zhang, M.-J. Chen, Y. Xiao, X.-Y. Liu, Z.-G. Liu, and D.-Y. Wang, *Composites Part B: Engineering*, Vol. 175, p. 107189, 2019.
150. B. Xu, W. Xu, G. Wang, L. Liu, and J. Xu, *Polymers for Advanced Technologies*, Vol. 29, p. 1733, 2018.
151. J. Cheng, D. Ma, S. Li, W. Qu, and D. Wang, *Polymers*, Vol. 12, p. 347, February 2020.
152. K. Song, I. Ganguly, I. Eastin, and A. Dichiara, *International Journal of Molecular Sciences*, Vol. 18, p. 2368, November 2017.
153. J. Wang, M. Liang, Y. Fang, T. Qiu, J. Zhang, and L. Zhi, *Advanced Materials*, Vol. 24, p. 2874, 2012.
154. N. Wang, H. Teng, F. Yang, J. You, J. Zhang, and D. Wang, *Polymers*, Vol. 11, p. 1708, October 2019.
155. W. Yan, M.-Q. Zhang, J. Yu, S.-Q. Nie, D.-Q. Zhang, and S.-H. Qin, *Chinese Journal of Polymer Science*, Vol. 37, p. 79, 2019.
156. V.Q. Tran, H.T. Doan, N.T. Nguyen, and C.V. Do, *Journal of Chemistry*, Vol. 2019, 2019.
157. B. Alinejad and K. Mahmoodi, *Functional Materials Letters*, Vol. 10, p. 1750047, 2017.
158. S. Brunauer, P.H. Emmett, and E. Teller, *Journal of the American Chemical Society*, Vol. 60, p. 309, 1938.
159. G. Cesareo, M.R. Parrini, and L.G. Rizzi, Flame retardant composition comprising graphene nanoplatelets, US Patent 9 909 015, assigned to Directa Plus S.p.A. (Lomazzo, IT), March 6, 2018.
160. I.-Y. Jeon, S.-H. Shin, H.-J. Choi, S.-Y. Yu, S.-M. Jung, and J.-B. Baek, *Carbon*, Vol. 116, p. 77, 2017.
161. L. Zuo, W. Fan, Y. Zhang, L. Zhang, W. Gao, Y. Huang, and T. Liu, *Composites Science and Technology*, Vol. 139, p. 57, 2017.
162. B. Yuan, G. Chen, Y. Zou, S. Shang, Y. Sun, B. Yu, S. He, and X. Chen, *Polymers for Advanced Technologies*, Vol. 30, p. 2153, 2019.
163. M. Zhang, X. Ding, Y. Zhan, Y. Wang, and X. Wang, *Journal of Hazardous Materials*, Vol. 384, p. 121260, 2020.
164. V. Lopez, A. Paton-Carrero, A. Romero, J.L. Valverde, and L. Sanchez-Silva, *Polymer-Plastics Technology and Materials*, Vol. 58, p. 1170, 2019.
165. L. Maddalena, F. Carosio, J. Gomez, G. Saracco, and A. Fina, *Polymer Degradation and Stability*, Vol. 152, p. 1, 2018.
166. Y. Feng, J. Hu, Y. Xue, C. He, X. Zhou, X. Xie, Y. Ye, and Y.-W. Mai, *J. Mater. Chem. A*, Vol. 5, p. 13544, 2017.
167. W.S. Hummers and R.E. Offeman, *Journal of the American Chemical Society*, Vol. 80, p. 1339, 1958.
168. J. Chen, B. Yao, C. Li, and G. Shi, *Carbon*, Vol. 64, p. 225, 2013.
169. Y.-R. Shin, S.-M. Jung, I.-Y. Jeon, and J.-B. Baek, *Carbon*, Vol. 52, p. 493, 2013.

170. H. Yu, B. Zhang, C. Bulin, R. Li, and R. Xing, *Scientific Reports*, Vol. 6, p. 36143, 2016.
171. J. Long, B. Liang, and Z. Wang, *Plastics, Rubber and Composites*, Vol. 0, p. 1, 2020.
172. L. Song, K. Wu, Y. Wang, Z. Wang, and Y. Hu, *Journal of Macromolecular Science, Part A*, Vol. 46, p. 290, 2009.
173. Q. Hongqiang, W. Weihong, H. Jianwei, S. Jianhong, and X. Jianzhong, *Journal of Macromolecular Science, Part B*, Vol. 53, p. 278, 2014.
174. L. Liu, X. Chen, and C. Jiao, *Iranian Polymer Journal*, Vol. 24, p. 337, 2015.
175. M.-J. Chen, X. Wang, X.-L. Li, X.-Y. Liu, L. Zhong, H.-Z. Wang, and Z.-G. Liu, *RSC Advances*, Vol. 7, p. 35619, 2017.
176. L. Yan, Z. Xu, and N. Deng, *Polymer Degradation and Stability*, Vol. 172, p. 109064, 2020.
177. Z. Zhang, W. Xu, L. Yuan, Q. Guan, G. Liang, and A. Gu, *Journal of Applied Polymer Science*, Vol. 135, p. 46587, 2018.
178. Wikipedia contributors, Halloysite — Wikipedia, the free encyclopedia, https://en.wikipedia.org/w/index.php?title=Halloysite&oldid=939452440, 2020. [Online; accessed 16-February-2020].
179. B. Zhong, J. Lin, M. Liu, Z. Jia, Y. Luo, D. Jia, and F. Liu, *Polymer Degradation and Stability*, Vol. 141, p. 19, 2017.
180. L. Qu, Y. Sui, C. Zhang, P. Li, X. Dai, B. Xu, and D. Fang, *European Polymer Journal*, Vol. 122, p. 109383, 2020.
181. Y. Qi, W. Wu, X. Liu, H. Qu, and J. Xu, *Fire and Materials*, Vol. 41, p. 195, 2017.
182. K. Dai, S. Sun, W. Xu, Y. Song, Z. Deng, and X. Qian, *RSC Advances*, Vol. 8, p. 24993, 2018.
183. M. Gao, J. Li, and X. Zhou, *Polymer Composites*, Vol. 40, p. E1274, 2019.
184. D.-D. Zhang, S.-Z. Zu, and B.-H. Han, *Carbon*, Vol. 47, p. 2993, 2009.
185. X. Chen, J. Li, and M. Gao, *Polymers*, Vol. 11, p. 78, January 2019.
186. H.E. Kissinger, *Analytical Chemistry*, Vol. 29, p. 1702, 1957.
187. L. Verdolotti, M. Lavorgna, E.D. Maio, and S. Iannace, *Polymer Degradation and Stability*, Vol. 98, p. 64, 2013.
188. M.-H. Chen, C.-Y. Ke, and C.-L. Chiang, *Journal of Composites Science*, Vol. 2, p. 18, Mar 2018.
189. T. Xu, C. Zhang, P. Li, X. Dai, L. Qu, Y. Sui, J. Gu, and Y. Dou, *New J. Chem.*, Vol. 42, p. 13873, 2018.
190. P. Katti, K.V. Kundan, S. Kumar, and S. Bose, *ACS Omega*, Vol. 3, p. 17487, 2018.
191. C. Yang, Z. Li, L. Yu, X. Li, and Z. Zhang, *Industrial & Engineering Chemistry Research*, Vol. 56, p. 7720, 2017.
192. Y. Feng, X. Li, X. Zhao, Y. Ye, X. Zhou, H. Liu, C. Liu, and X. Xie, *ACS Applied Materials & Interfaces*, Vol. 10, p. 21628, 2018.

193. B. Yuan, Y. Hu, X. Chen, Y. Shi, Y. Niu, Y. Zhang, S. He, and H. Dai, *Composites Part A: Applied Science and Manufacturing*, Vol. 100, p. 106, 2017.
194. Y. Feng, B. Wang, X. Li, Y. Ye, J. Ma, C. Liu, X. Zhou, and X. Xie, *Carbon*, Vol. 146, p. 650, 2019.
195. Y. Feng, C. He, Y. Wen, Y. Ye, X. Zhou, X. Xie, and Y.-W. Mai, *Composites Part A: Applied Science and Manufacturing*, Vol. 103, p. 74, 2017.
196. B. Tawiah, B. Yu, R.K. Yuen, Y. Hu, R. Wei, J.H. Xin, and B. Fei, *Carbon*, Vol. 150, p. 8, 2019.
197. X. Shi, X. Peng, J. Zhu, G. Lin, and T. Kuang, *Journal of Colloid and Interface Science*, Vol. 524, p. 267, 2018.
198. H. Kim, D.W. Kim, V. Vasagar, H. Ha, S. Nazarenko, and C.J. Ellison, *Advanced Functional Materials*, Vol. 28, p. 1803172, 2018.
199. Standard test method for heat and visible smoke release rates for materials and products using an oxygen consumption calorimeter, ASTM Standard E1354-17, ASTM International, West Conshohocken, PA, 2017. https://www.astm.org/Standards/E1354.htm.
200. P.R. Hornsby, M. Le Bras, R. Rothon, S. Bourbigot, K. Takeda, S. Duquesne, C. Pelegris, C. Jama, T. Kashiwagi, and C. Wilkie, *Fire Retardancy of Polymers: New Applications of Mineral Fillers*, Royal Society of Chemistry, 2007.
201. T.E. Dueber, M.W. West, B.C. Auman, and R.V. Kasowski, Polyimide based adhesive compositions useful in flexible circuit applications, and compositions and methods relating thereto, US Patent 7 220 490, assigned to E. I. du Pont de Nemours and Company (Wilmington, DE), May 22, 2007.
202. N. Agarwal, Thermoplastic polycarbonate compositions, articles made therefrom and method of manufacture, US Patent 7 498 401, assigned to SABIC Innovative Plastics IP B.V. (Bergen op Zoom, NL), March 3, 2009.
203. K. Ueno, Flame retardant and smoke suppressed polymeric composition and electric wire having sheath made from such composition, US Patent 5 059 651, assigned to Sumitomo Electric Industries, Ltd. (Osaka, JP), October 22, 1991.
204. M.A. Kasem and H.R. Richards, *Ind. Eng. Chem. Prod. Res. Dev.*, Vol. 11, p. 114, June 1972.
205. S.R. Kim, Y.J. Choi, and J.S. Song, Flame retardant polymer resin composition having improved heat distortion temperature and mechanical properties, US Patent 5 864 004, assigned to Samyang Corporation (Seoul, KR), January 26, 1999.
206. S. Thumsorn, T. Negoro, W. Thodsaratpreeyakul, H. Inoya, M. Okoshi, and H. Hamada, *Polymers for Advanced Technologies*, Vol. 28, p. 979, 2017.

207. F. Yemisci, S. Yesil, and A. Aytac, *Fire and Materials*, Vol. 41, p. 964, 2017.
208. F. Wang, W. Shi, Y. Mai, and B. Liao, *Materials*, Vol. 12, p. 4114, December 2019.
209. T. Benelli, L. Mazzocchetti, E. D'Angelo, M. Lanzi, F. Saraga, L. Sambri, M.C. Franchini, and L. Giorgini, *Polymer Engineering & Science*, Vol. 57, p. 621, 2017.
210. S.S. Ray and M. Kuruma, *Halogen-Free Flame-Retardant Polymers: Next-generation Fillers for Polymer Nanocomposite Applications*, Vol. 294, Springer Nature, 2020.
211. H. Kim, J.-W. Park, H.-J. Kim, and P. Di Sia, Flame retardant nanocomposites containing nano-fillers, in P. Di Sia, ed., *Science and Applications of Tailored Nanostructures*, pp. 1–28. One Central Press Cheshire, UK, 2017.
212. P. Jagdale, S. Salimpour, M.H. Islam, F. Cuttica, F.C.R. Hernandez, A. Tagliaferro, and A. Frache, *Journal of Nanoscience and Nanotechnology*, Vol. 18, p. 1468, 2018.
213. W. Mao, S. Li, M. Li, X. Yang, J. Song, M. Wang, J. Xia, and K. Huang, *Journal of Applied Polymer Science*, Vol. 133, p. 44084, 2016.
214. A. Piotrowski, J. Zilberman, S.V. Levchik, M. Zhang, E. Gluz, and K.A. Suryadevara, Active ester curing agent compound for thermosetting resins, flame retardant composition comprising same, and articles made therefrom, US Patent 10 500 823, assigned to ICL-IP America Inc. (Tarrytown, NY, US) , December 10, 2019.
215. C.-M. Wu, L.-L. Huang, S.-K. Lee, et al., *Sensors and Materials*, Vol. 28, p. 477, 2016.
216. C.-S. Wang, J.-Y. Shie, and C.-S. Lin, Phosphorus group containing flame retardant hardener, advanced epoxy resins and cured epoxy resins thereof, TW Patent 593 526, assigned to Wangsuen Su Jen, June 21, 2004.
217. C.-S. Wang, J.-Y. Shieh, and C.H. Lin, Phosphorus-containing flame-retardant hardeners, epoxy resins, advanced epoxy resins and cured epoxy resins, US Patent Application 20 050 004 339, assigned to Chun-Shan Wang, January 6, 2005.
218. M. Rakotomalala, S. Wagner, and M. Döring, *Materials*, Vol. 3, p. 4300, August 2010.
219. Q. Pan, Flame-retardant resin composition, thermosetting resin composition, flame-retardant engineering plastic and composite metal substrate, US Patent Application 20 180 022 898, assigned to Guangdong Guangshan New Material Co. Ltd., January 25, 2018.